# Wind-packing of snow: How do wind crusts form?

PAR

## Christian Gabriel SOMMER

ÉCOLE POLYTECHNIQUE
FÉDÉRALE DE LAUSANNE

Suisse
2018

# Acknowledgments

The making of this PhD thesis was supported by many people. I would like to thank my thesis director Michi Lehning and my co-director Charles Fierz. They guided me through the project, provided input and ideas during regular meetings, helped design the wind tunnel and the experiments, helped with the data analysis and provided feedback for manuscripts and presentations. Charles Fierz wrote the project proposal together with Stefan Horender and in doing so, they laid a solid foundation on which all of my work was based. I very much enjoyed working with Michi and Charles and I am very grateful to them.

The SLF workshop and electronics lab is highly acknowledged for working out the detailed design and building the wind tunnel. They also provided support over the years and helped to update and modify the wind tunnel before each winter. This PhD thesis would certainly not have been possible without them.

I would also like to thank the SLF wind tunnel team, Philip Crivelli and Enrico Paterna, for their help with experiments and helpful discussions. Their company certainly made the many hours in the often very cold wind tunnel more enjoyable.

Finally, I would like to thank all my friends and colleagues at SLF for a great time in Davos, at the office as well as out in the mountains.

Davos, July 25, 2018

# Abstract

Wind-packing of snow is the process responsible for the formation of wind slabs and wind crusts. These are hard layers of well-sintered snow often found in the snowpack in mountains as well as in polar regions. Wind-packing affects the local mass balance, the avalanche danger and how the snow cover interacts with the atmosphere. Yet, it is a poorly understood process. Many ideas about what wind-packing actually is have been proposed in the literature but there is almost no quantitative information about the involved physical processes available.

In this thesis, we present quantitative results from wind tunnel and field experiments on wind-packing. A closed-circuit wind tunnel simulating an infinite fetch was specifically designed and built for this purpose. Experiments were performed with natural snow that was collected on a pair of wooden trays. The hardness of the snow and how it changed during experiments was measured with a SnowMicroPen. Meteorological parameters such as wind speed, air temperature, etc. were also measured. In the literature, there is conflicting information about the necessity of drifting snow for wind-packing. The wind tunnel experiments showed that drifting snow is a necessary but not sufficient condition for wind-packing. We observed no hardening during experiments without drifting snow, but not all drifting snow events lead to the formation of a wind crust. The spatial variability of the hardness of wind-influenced snow was high and this appeared to be related to the dynamics of erosion and deposition.

To analyze the influence of these processes in more detail and quantitatively, a Microsoft Kinect sensor was added to the wind tunnel. This instrument measures the snow depth in the main test section with a high spatial and temporal resolution. These measurements showed that wind-packing only occurs through the deposition of snow. If drifting snow causes the snow to be eroded, there is no hardening effect on the remaining snow. Furthermore, the Kinect data allowed to explain about 50% of the observed variability of the hardness of wind-packed snow with only two parameters. Most important was the wind exposure. The snow became harder in more wind-exposed positions compared to wind-sheltered areas. We used the parameter Sx to characterize how wind-exposed a certain position is based on the upstream snow surface. A wind-sheltered position has a high Sx value and a wind-exposed position has a negative Sx value. To increase the range of Sx values, some experiments were performed with an artificial obstacle in the main test section, which created highly wind-sheltered positions. Sx alone explained almost 40% of the variability. The second parameter was the deposition rate. We found a negative correlation of -0.4 between the deposition rate and the snow hardness. Wind-packing is more efficient at creating a hard layer if the snow is deposited slowly. The effect of other parameters, such as wind speed, air humidity or initial density of the snow on the hardness was studied. However, there was either no robust trend

in our data or the addition to the multilinear regression did not significantly increase the explanatory power of the model. This does not necessarily mean that these parameters are not relevant for wind-packing.

The analysis of a wind-packing event that was observed in Antarctica provided a valuable validation of the wind tunnel results. Similar measurements to those in the wind tunnel were performed in Antarctica. The result that no wind-packing occurs without drifting was confirmed. However, no significant correlation was found between Sx and the hardness change. This is most likely due to the available data not having a high enough temporal resolution. In addition, it was observed how drifting snow forms barchan dunes. One dune was surveyed in detail and it was found that the hardness was high at all positions on the dune.

The wind tunnel and polar field experiments provided quantitative information and new insights about wind-packing of snow and under what conditions it occurs. However, the question about which physical processes are most important could not yet be fully answered.

# Zusammenfassung

Durch den Einfluss von Wind können sich an der Schneeoberfläche Winddeckel oder Windkrusten bilden. Das sind harte Schichten aus verdichtetem und gesintertem Schnee. Solche Schichten kommen in der Schneedecke in Bergregionen und auch in polaren Gebieten vor. Sie beeinflussen die lokale Massenbilanz, die Lawinengefahr und den Austausch zwischen der Schneedecke und der Atmosphäre. Trotzdem gibt es zum Prozess der Schneeverdichtung durch den Wind (im Folgenden Winddeckelbildung) noch viele offene Fragen. In der Literatur finden sich viele Ideen darüber welche physikalischen Prozesse bei der Entstehung von Windkrusten ablaufen aber es gibt kaum quantitative Informationen dazu.

In dieser Dissertation werden quantitative Resultate von Windkanal- und Feldexperimenten präsentiert. Um die Winddeckelbildung zu untersuchen wurde ein spezieller Windkanal mit einem geschlossenen Kreislauf entwickelt und gebaut. Für die Experimente liess man natürlichen Schnee sich auf zwei Holzbrettern ablagern. Die Schneehärte wurde mit einem SnowMicroPen gemessen. Ausserdem wurden im Windkanal meteorologische Parameter wie Windgeschwindigkeit, Lufttemperatur, etc. gemessen. In der Literatur gibt es widersprüchliche Angaben über die Notwendigkeit von Schneeverfrachtung für die Entstehung von Windkrusten. Die Windkanalexperimente haben gezeigt, dass Schneeverfrachtung eine notwendige aber nicht hinreichende Voraussetzung ist. Es gab keine Verhärtung des Schnees während Experimenten ohne Verfrachtung aber nicht jede Periode mit Schneeverfrachtung führte zur Entstehung einer Windkruste. Die räumliche Variabilität der Härte von wind-beeinflusstem Schnee war gross und dies schien mit der Dynamik von Erosion und Ablagerung von Schnee zusammenzuhängen.

Um den Einfluss dieser Prozesse detailliert und quantitativ zu untersuchen wurde ein Microsoft Kinect Sensor im Windkanal installiert. Dieses Messgerät misst die Schneehöhe in der Testsektion mit grosser räumlicher und zeitlicher Auflösung. Diese Messungen haben gezeigt, dass die Winddeckelbildung nur stattfindet wenn Schnee abgelagert wird. Führt Schneeverfrachtung zur Erosion von Schnee wird der zurückbleibende Schnee dabei nicht härter. Des Weiteren konnte mit den Kinect Daten etwa 50% der gemessenen Variabilität der Schneehärte mit nur zwei Parametern erklärt werden. Am wichtigsten war dabei die Windausgesetztheit. In windausgesetzten Positionen wurde der Schnee mehr verhärtet als in windgeschützten Bereichen. Der Parameter Sx wurde benutzt um zu beschreiben wie windausgesetzt eine bestimmte Position ist. Die Berechnung basiert dabei darauf wie die Schneeoberfläche im Luv aussieht. Ein hoher Sx Wert bedeutet, dass die Position windgeschützt ist, während dem Wind ausgesetzte Stellen negative Sx Werte aufweisen. Um den Bereich der Sx Werte zu vergrössern wurden Experimente mit einem künstlichen Hindernis im Testbereich durchgeführt. Dies führt zu stark windgeschützten Stellen hinter dem Hindernis. Sx alleine konnte fast 40% der Variabilität erklären. Der

zweite Parameter ist die Ablagerungsrate. Es gibt eine negative Korrelation von -0.4 zwischen der Ablagerungsrate und der Schneehärte. Die Winddeckelbildung verhärtet den Schnee mehr wenn dieser langsam abgelagert wird. Der Effekt von anderen Parametern wie Windgeschwindigkeit, Luftfeuchte oder Anfangsschneedichte wurde ebenfalls untersucht. Allerdings gab es in unseren Daten für diese Parameter keine robuste Tendenz oder das Bestimmtheitsmass des Models erhöhte sich beim Hinzufügen zur linearen Regression nicht signifikant. Dies heisst aber nicht, dass diese Parameter gar nicht relevant für die Winddeckelbildung sind.

Die Auswertung eines Verfrachtungsereignisses, das in der Antarktis beobachtet wurde, ermöglichte die Windkanalexperimente zu validieren. In der Antarktis wurden ähnliche Messungen wie im Windkanal durchgeführt. Das Resultat, dass die Winddeckelbildung ohne Verfrachtung nicht stattfindet, konnte bestätigt werden. Allerdings gab es zwischen Sx und der Veränderung der Schneehärte keine signifikante Korrelation. Dies hängt wahrscheinlich damit zusammen, dass die zeitliche Auflösung der vorhandenen Daten zu gering ist. Des weiteren wurde beobachtet wie Schneeverfrachtung Sicheldünen bildete. Eine Düne wurde genau vermessen und dabei stellte sich heraus, dass der Schnee überall auf der Düne sehr hart war.

Durch die Windkanal- und Feldexperimente konnten quantitative Informationen gesammelt und neue Erkenntnisse über die Verdichtung von Schnee durch Wind gewonnen werden. Es wurde zudem klarer unter welchen Bedingungen die Verhärtung stattfindet. Allerdings konnte die Frage, welche physikalischen Prozesse wichtig sind, noch nicht abschliessend beantwortet werden.

**Stichwörter:** Schnee, Härte, Windharsch, Winddeckel, Windkruste, Schneeverfrachtung, Erosion, Ablagerung, Windexponiertheit, Antarktis, Sicheldüne

# Contents

# List of Figures

# List of Tables

# 1. Introduction

Snow covers a significant part of the globe's surface either continuously or seasonally (Robinson and Estilow, 2012). To name just a few of the snow's effects: The presence or absence of snow impacts the climate partly due to the drastically higher albedo compared to the snow-free ground (e.g. Armstrong and Brun, 2008). The seasonal snow cover stores most of the winter's solid precipitation, releases it as water in spring and summer and is therefore highly relevant for the hydrological cycle (e.g. Barnett et al., 2005). In mountainous regions, winter tourism destinations rely on snow to generate a large part of their income (e.g. Rixen et al., 2011). At the same time, snow avalanches are a major natural hazard in these areas (e.g. Smith, 2013).

Snow influenced by wind often constitutes an important part of the snowpack. For example, wind redistributes the snow, it is eroded in one place and redeposited in another leading to highly variable snow depths. Wind also changes the microstructure of snow. Wind-affected snow is often denser than fresh snow, has different grain shapes and sizes and in some conditions it is also harder. Snow hardened by wind is generally called wind-packed snow and the formation process is called wind-packing. The latest edition of the international classification for seasonal snow on the ground (Fierz et al., 2009) describes wind-packed snow as "small, broken or abraded, closely-packed and well-sintered particles."

Having a different microstructure, wind-packed snow at the surface of the snowpack impacts the interaction between the snow cover and the atmosphere. Wind-packing changes the snow's specific surface area which leads to a different albedo and affects the exchange of chemical species with the atmosphere. Wind-packing is furthermore closely related to the formation of depositional and erosional surface features such as dunes and zastrugi (Filhol and Sturm, 2015). Especially in polar regions, new snow gets reorganized into such features by wind and is hardened at the same time. Wind-packing therefore links precipitation to the permanent deposition of the snow and thus affects the surface mass balance (Groot Zwaaftink et al., 2013). In mountainous terrain, wind-packing is relevant for the avalanche hazard. Wind-packed snow is an ideal slab and it may release as a slab avalanche if there is a weak layer below it (Schweizer et al., 2003).

Qualitative descriptions of wind-hardened surface layers are abundant, especially in polar research literature (e.g. Alley, 1988; Benson, 1967; Kotlyakov, 1966; Schytt, 1958). Several studies also address the formation of such layers. However, most of them remain qualitative and many different physical processes of what "wind-packing" actually is, are proposed.

Seligman (1936) performed extensive field observations in the Alps and also conducted some experiments. He defines "wind-packing as a special form of firnification accelerated by a wet wind." For him, the main process is condensation of water vapor among the

snow grains. He mentions an effect today called ventilation which may increase the vapor flux through the snow. Snow ventilation is the air flux through the pore space of the snowpack induced by wind (Bartlett and Lehning, 2011). Seligman (1936) found that the air humidity must be higher than 85% for wind-packing to take place. A dry wind would sublimate the bonds between the grains and therefore loosen the snow.

Seligman (1936) differentiates between wind slab and wind crust. According to him, a slab would be formed when drifting snow is deposited in a sheltered area during a wet wind event. A slab is therefore a new layer and may be quite thick. A crust, on the other hand, could be formed with or without drifting snow and would usually form in wind-exposed areas. A crust is the hardened part of an already deposited layer, is usually quite thin and very hard. The grains in both types of wind-packed snow are rounded due to metamorphism. The grains in a slab are more rounded than in a crust because they were already rounded in the saltation layer (Seligman, 1936).

There is no conclusive definition of what a "wind slab" or a "wind crust" is. Seligman (1936)'s definition is given above. Fierz et al. (2009) define wind crust as a "thin, irregular layer" which is "hard but usually breakable" and wind slab as "thicker, often dense layers, usually found on lee slopes." For Colbeck (1991) a wind slab is a layer of wind-hardened snow tens of cm thick, whereas a wind crust is thin (tens of millimeters), very hard and formed during high wind events. For Alley (1988) and Kotlyakov (1966), a wind crust is a thin (1 mm), hard layer formed during periods of strong winds combined with a low availability of drifting particles. Clifton et al. (2006) define wind slabs as being formed by snow deposition on lee slopes during snow storms. In contrast, a wind crust would form if significant drifting only takes place after a snowfall. For most authors, the main difference between slab and crust seems to be their thickness and hardness. A slab is thick and (relatively) soft and a crust is thin and hard. Seligman (1936) is the only one to mention different formation processes.[1] In polar research literature, a third type of surface is frequently mentioned. It is sometimes described as a "glazed surface" and sometimes specifically called "wind glaze" (Gow, 1965; Jones, 1983). However, it is unclear if such surfaces should be considered as wind-packed snow. Gow (1965) suggests that glazed surfaces may originate as sun crusts which subsequently become polished or glazed by prolonged exposure to wind.

Benson (1967), Kotlyakov (1966) and Schytt (1958) agree with Seligman (1936) that the hardness increase during wind-packing is mainly due to an increased vapor flux which accelerates sintering of the snow. According to Seligman (1936) part of this moisture comes from the humid air and part from the grains themselves (sublimation and redeposition). According to Benson (1967) most of the vapor comes from layers deeper within the snowpack. The upward vapor flux is caused by a temperature gradient and part of the vapor is then deposited in the surface layers. He also mentions ventilation, which would increase the vapor transfer rate. Schytt (1958) agrees with Benson (1967) on the

---

[1] In the following chapters, we almost exclusively use the term wind crust. This is mainly because the hard layers in the wind tunnel were never thicker than a few centimeters and not because of a specific formation process. Basically, "wind crust", "wind-packed snow" and also "wind-hardened snow" are used interchangeably.

origin of the moisture but for him it is high wind speeds at the surface, which "cause an outflow of air from the firn and snow", that are responsible for the vapor flux. With this formulation, Schytt (1958) may also describe ventilation. According to Kotlyakov (1966) the moisture is deposited directly from the cold, humid air onto the surface.

Kotlyakov (1966) was the first to also mention another process: the mechanical fragmentation of snow crystals by the wind. These smaller particles are then packed close upon deposition and create a denser layer. Adams et al. (2008) studied the evolution of fragmented particles under the microscope. They found that these particles were very small and presented sharp edges. They were therefore subject to rapid metamorphism and sintering due to locally high vapor pressures. They observed rapid bond growth and also the formation of new contact points through dendritic growth on particles. Several other authors, although not all independently of each other, mention mechanical fragmentation and rounding followed by rapid sintering of the small grains as the main process in wind-packing (Alley, 1988; Colbeck, 1991; Endo and Fujiwara, 1973; Fierz et al., 2009; Kozak et al., 2003). According to Guyomarc'h and Mérindol (1998), wind creates small particles in two ways. First, by fragmentation due to collisions between the snow grains themselves and with the ground and second, due to sublimation while the grains are airborne. Sato et al. (2008) performed wind tunnel experiments on the collision of sieved snowflakes with the surface. They found that above a wind speed threshold, the snowflakes break up upon collision and are either deposited at the impact point or, if the wind speed is high enough, are entrained in the flow. In that case they would then be deposited later, once the saltation layer reaches saturation.

Some other ideas appear in the literature but not as frequently as the processes described above. Domine et al. (2009) suggest that ventilation may also, in addition to increasing the vapor flux, deposit very small, fragmented grains within the snowpack down to several centimeters. These particles would increase the density of the snow and create new contact points between the original grains and therefore increase the hardness. According to Domine et al. (2009), the very high specific surface area (SSA) of these fragmented grains would increase the average SSA of the affected layer. The SSA of snow is the ratio of surface area per volume (or mass) of ice and is an important microstructural parameter. The SSA generally decreases due to metamorphism (Fierz et al., 2009). Clifton et al. (2006) also suggest that small particles are deposited into the snowpack but do not say how or how deep. Furthermore, they also mention turbulent eddies whose dynamic pressure may further pack deposited snow together. Endo and Fujiwara (1973) and in part also Kotlyakov (1966) see a combination of mechanical fragmentation followed by packing through "the pressure of the flying fragments and the moving air" as the main process. We assume that "pressure of the moving air" refers to the dynamic pressure of the flow and "pressure of the flying fragments" to the impact pressure when saltating particles hit the surface. Jones (1983) mentions yet another process, namely frictional heat dissipated from the drifting particles which would cause some melting at the surface and form a 1 mm thick "wind glaze" at the surface. He also observed a 30 cm "wind crust" below the "wind glaze" and attributed its formation to ventilation and sintering.

In summary, the following processes are proposed in the literature:

- Mechanical fragmentation (combined with rounding by friction and sublimation) followed by sintering

- Ventilation leading to increased vapor transfer rates

- Ventilation leading to deposition of very small, fragmented particles within the snowpack

- Condensation of vapor from the humid air and the snow in the surface layer

- A temperature gradient in the snowpack leading to a vapor flux from lower layers and condensation in the surface layer

- Packing by dynamic pressure of wind

- Packing due to the impact forces of drifting particles

- Friction leading to melt and refreeze at the surface

Some studies present evidence or arguments against some of these processes. There is debate about the importance of ventilation. Sokratov and Sato (2000) observed an indirect effect down to tens of centimeters below the surface while Bartlett and Lehning (2011) concluded that ventilation has a very limited effect in a shallow layer below the surface. Often the induced flows may not even penetrate the bulk snowpack but be limited to the roughness elements, such as dunes. Groot Zwaaftink et al. (2013) argue that the high humidity in the saltation layer does not have a large effect because the air in the snowpack is close to saturation as well. They point out that the latent heat flux at the surface is generally small. Based on that, it would be expected that vapor condensation from the air onto the surface is negligible. It must be kept in mind, however, that Groot Zwaaftink et al. (2013) made their observations on the Antarctic Plateau, where the temperature is extremely low. This leads to a low absolute humidity and therefore small latent heat fluxes. A potential upward vapor flux due to a temperature gradient in the snowpack is unrelated to wind above the surface as was already pointed out by Benson (1967). It makes therefore no sense to consider this process when studying wind-packing. Seligman (1936) states that the effect of wind pressure is negligible because the pressure variations at the low wind speeds, at which wind-packing takes place, are very small. In fact, the dynamic pressure of a 10 m s$^{-1}$ wind is about 60 Pa. This corresponds to an overburden pressure of about 6 cm of snow with a density of 100 kg m$^{-3}$. This is far from enough to pack snow into a dense, hard layer. Seligman (1936) dismisses friction leading to melt and refreeze mostly because he observed wind crusts to form without drifting snow. He admits that friction may round grains during the formation of wind slab. Melt and refreeze can also be dismissed as a process in wind-packing because melt forms (Fierz et al., 2009) are easily distinguishable and usually do not appear in layers of wind-packed snow.

The literature also contains some information on the conditions that are necessary for wind-packing and on the influence of meteorological parameters on wind-packed snow. According to Seligman (1936) the only real condition is that the wind has a relative humidity above about 85%. This appears to be a rather qualitative observation. Because, according to him, a crust can form without drifting, he gives no lower limit on the wind speed, but he observed that the wind-packed snow is harder, the longer and stronger the wind blew. Several polar studies observed that the density of the surface snow increases with wind speed and air temperature and decreases with accumulation rate (Craven and Allison, 1998; Endo and Fujiwara, 1973; Kotlyakov, 1966; Sugiyama et al., 2012). In snow cover models, the density of freshly fallen snow is modeled as a function of wind speed and air temperature (Crocus, Vionnet et al. (2012)), Snowpack additionally includes air humidity and the snow surface temperature (Lehning et al., 2002). Schmucki et al. (2014) propose another parametrization for Snowpack based on air temperature, air humidity and wind speed. Snowpack and Crocus also provide routines for further compaction during drifting snow events (Brun et al., 1997).

In summary, the following variables may influence wind-packing:

- Air humidity

- Wind speed

- Air temperature

- Accumulation rate

As can be seen, many different physical processes and influencing parameters have been proposed. However, it remains unclear which processes are actually acting during wind-packing, which ones are more important than others and how that and the properties of the resulting crust or slab depend on the meteorological variables. Furthermore, most of the information outlined above is qualitative or speculative. The only experiments to study wind-packing specifically were performed by Seligman (1936). He blew air through a column of snow in a simple wind tunnel. Using water or calcium chloride he achieved relative humidities as high as 85% or as low as 60%. His results showed that a dry wind evaporates some of the snow and does not lead to the formation of a slab or crust while a humid wind "coalesces or cakes it [the snow] with icing-up of the particles". This shows that the humidity has to be high enough for wind-packing to take place. However, blowing air through the snow instead of over its surface is not very realistic. For example, the effect of drifting snow, which is necessary for the mechanical fragmentation of snow particles, cannot be tested with such a setup. Sato et al. (2008) studied the breakup of snowflakes in the wind tunnel and Adams et al. (2008) studied the bonding process between such mechanically fragmented grains. These studies provide valuable insight but only into parts of the possible formation process of slabs or crusts. As mentioned above, snow cover models such as Crocus or Snowpack include parameterized routines to simulate wind-packing. However, the implemented formulations appear to be mostly based on "educated guesses" about what wind-packing is and how it affects the snow.

This is simply due to a lack of corresponding measurements and physical understanding of wind-packing.

There is, therefore, a need for realistic wind tunnel experiments on wind-packing to gain quantitative information about this process. The main goal of this dissertation is to determine which processes are dominant in the formation of wind-packed snow and how the meteorological conditions affect the importance of the processes and the properties of wind-packed snow. New insights into the physics of wind-packing will improve our understanding of the surface mass balance and the formation of surface features especially in polar areas, but also in mountainous regions. The data and physical understanding gained through the experiments will also help to improve snow cover models, either through improved parameterization or, if possible, even through a physical model of wind-packing. Better snow cover models will, in turn, improve e.g. climate change simulations or the avalanche danger forecast.

The following three main chapters of this thesis correspond to two published journal articles and one still in the revision process. Chapter 2 introduces the wind tunnel and presents results showing that drifting snow is a necessary condition for wind-packing. Chapter 3 explores the influence of erosion and deposition on wind-packing and chapter 4 presents a wind-packing event observed in Antarctica. An overall conclusion and an outlook follow in chapters 5 and 6. Some other studies, that were done but not published elsewhere, are described in the appendix.

# 2. Wind tunnel experiments: saltation is necessary for wind-packing

## Authors

Christian G. Sommer[1,2], Michael Lehning[1,2], Charles Fierz[1]
[1]WSL Institute for Snow and Avalanche Research SLF, Davos, Switzerland
[2]CRYOS, School of Architecture, Civil and Environmental Engineering, EPFL, Lausanne, Switzerland

## Abstract

Wind-packed snow in the form of slabs or crusts is an important part of alpine and polar snow covers. Yet, the formation process of such layers is poorly understood. For example, it remains unclear whether drifting snow is necessary for wind-packing or not. A better understanding of wind-packing could improve snow cover models and avalanche danger forecasts and contribute to the assessment of mass balances in polar regions. We designed a closed-circuit, obround wind tunnel to study the process of wind crust formation. A SnowMicroPen was used to measure how the hardness of the snow evolved. The results show that no crust forms without saltation. Drifting snow is a necessary but not sufficient condition for wind-packing. The dynamics of erosion and deposition appear to be equally important.

## 2.1. Introduction

Wind-packing is the process of snow hardening under the influence of wind. Snow covers in alpine and polar regions often contain the resulting wind slabs or wind crusts. Such layers are relevant for the avalanche danger in alpine areas and they affect the interaction between the snow cover and the atmosphere. In polar regions, wind-packing influences the mass balance, as new snow is often only immobilized through hardening (Groot Zwaaftink et al., 2013).

Many studies describe wind-packed snow qualitatively (e.g. Alley, 1988; Benson, 1967; Schytt, 1958). However, it remains unclear how these layers form. Many processes have been proposed but real evidence is scarce. Some authors focus on humidity and see wind-packing as "firnification accelerated by a wet wind" (Seligman, 1936). According to Benson (1967), Schytt (1958) and Seligman (1936) the wind leads to an increased vapour flux which causes rapid sintering of the snow. The only condition is that the air humidity must be above 85% because a dry wind would sublimate some of the snow and therefore loosen it (Seligman, 1936). There is debate about whether the extra humidity is deposited directly from the humid air or whether some of the snow is sublimated and redeposited within the snowpack. Several authors see the mechanical fragmentation of snow crystals by the wind and their subsequent sintering as the main process behind wind packing (Alley, 1988; Colbeck, 1991; Endo and Fujiwara, 1973; Fierz et al., 2009; Guyomarc'h and Mérindol, 1998; Kotlyakov, 1966; Kozak et al., 2003). This process can only happen in a saltation layer, where snow particles collide with each other and with the surface. This is in contrast to the "accelerated firnification", which could also happen without drifting snow.

This paper aims at answering the question whether saltation is a prerequisite for wind-packing or not by observing the formation of wind crusts in a wind tunnel. The gained insight could be useful to improve the implementation of wind-packing in snow cover models. This would in turn improve stability assessments and avalanche danger forecasts.

## 2.2. Methods

### 2.2.1. Wind tunnel

A straight, open-circuit, boundary-layer wind tunnel has been in operation at SLF since 2001 (e.g. Clifton et al., 2006; Walter et al., 2014; Paterna et al., 2016; Crivelli et al., 2016). However, this facility is not suited to investigate wind-packing. In an open-circuit wind tunnel, any drifting particles are ejected within seconds. There is not enough time for mechanical fragmentation and subsequent sintering. We need a closed-circuit configuration or ideally an infinite fetch. An annular or obround wind tunnel is a way to achieve that. There already are some closed-circuit wind tunnels adapted for cryospheric studies, such as the Cryospheric Environment Simulator (CES) in Shinjo, Japan (Sato et al., 2001) or the Jules Verne wind tunnel at the Centre Scientifique et Technique du Bâtiment (CSTB) in Nantes, France (Naaim-Bouvet et al., 2002). But these facilities use snow tables of a limited size and can therefore not mimic an infinite fetch. Annular wind

tunnels of various sizes have been built at the University of Heidelberg to investigate air-sea gas transfer under different water surface conditions (e.g. Münnich et al., 1978; Jähne, 1980; Schmundt et al., 1995; Krall, 2013). The idea of simulating an infinite fetch with such a shape is therefore not new.
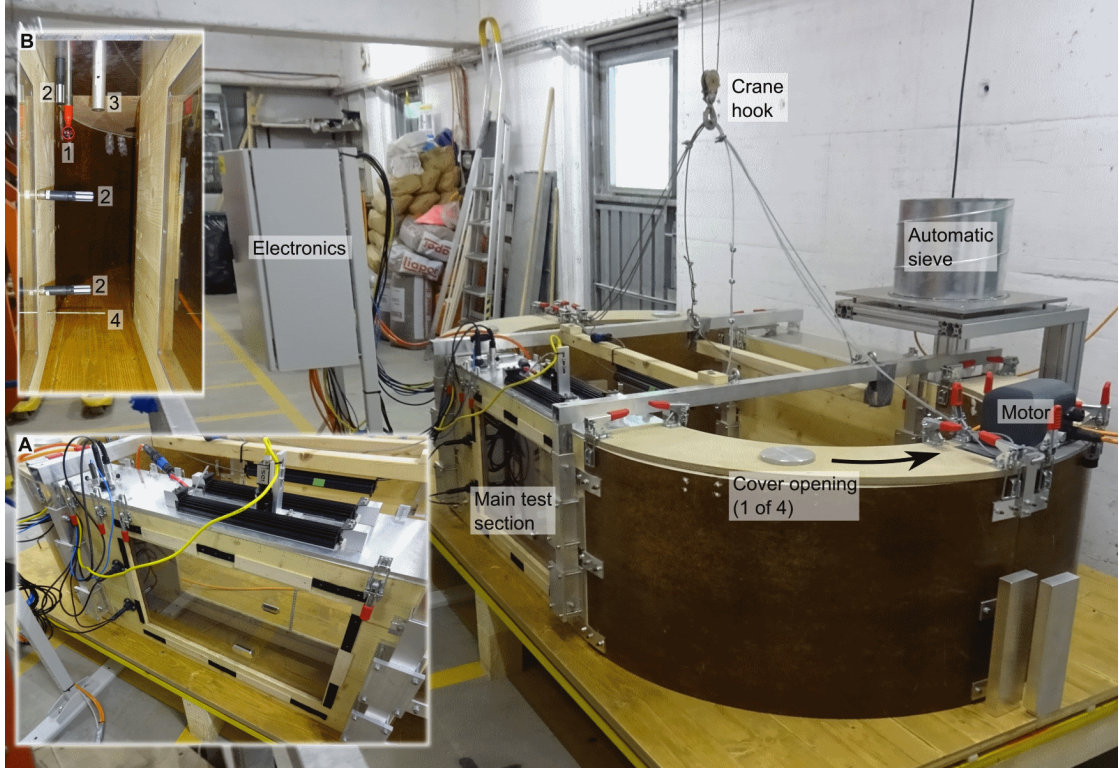


**Figure 2.1.:** The wind tunnel on its 1.5 m wide and 2.5 m long platform. It is located in the same building as the straight wind tunnel. The arrow indicates the direction of the airflow. The cover openings allow a basic control over the temperature and humidity in the wind tunnel. Insert (A) shows the main test section with the camera above the windows and the sensors to the left. Insert (B) shows the sensors listed in Table 2.1 at the upstream end of the main test section. 1: MiniAir, 2: Rotronic, 3: SI-131, 4: Pt100. The snow surface is usually between the Pt100 and the bottom Rotronic sensor. The Pt100 is inserted after lowering the tunnel onto the snow.

Our new wind tunnel has an obround shape as can be seen in Fig. 2.1. The two straight sections provide additional space for measurements as compared to an annular design and are not subject to centrifugal effects like the curved parts. The wind tunnel has an overall length of 2.2 m and a width of 1.2 m. The channel is 20 cm wide and 50 cm high. The airflow is created by a model-aircraft propeller driven by an electric motor. Free stream wind speed of up to 8 m s$^{-1}$ can be reached. A vibrating sieve can be used to simulate snowfall. This is useful to obtain drifting snow at wind speeds below the actual saltation threshold.

Before each experiment, 10 to 30 cm of fresh snow are collected on a pair of wooden trays outside the building (Fig. 2.2A). The wind tunnel, which is open at the bottom, is lifted by crane and the trays are arranged underneath it (Fig. 2.2B). Finally the wind tunnel is lowered into the snow cover (Fig. 2.2C). As a result, we have a continuous cover of almost undisturbed, natural snow in the wind tunnel. Each experiment consisted usually of several wind periods. Different measurements were performed before and after each one. Wind periods were often 30 min or one hour long but could be as short as a few minutes or as long as several hours.



**Figure 2.2:** Operation of the wind tunnel. (A): Snow is collected on trays and (B) arranged below the wind tunnel. (C): Then, the wind tunnel is lowered into the snow. (D): The SnowMicroPen (SMP) during a measurement. The SMP is the main instrument.

The flow quality in this wind tunnel cannot be compared to standards of wind tunnels used for aerodynamic testing. The high curvature, the narrow channel, the use of a propeller as a wind source and the unsteady snow surface make for a chaotic flow. It is therefore not possible to make quantitative statements about the interaction of the flow with saltating particles for example. However, we are certain that this facility is adapted to test whether drifting snow is necessary for wind-packing or not. More details about the design and flow characteristics of the wind tunnel can be found in the Appendix.

### 2.2.2. Instrumentation

The instrumentation in the wind tunnel is located in the second straight section downstream of the motor, called the main test section (Fig. 2.1). The measured parameters are wind speed, air humidity, air temperature, snow surface temperature and snow temperature. Air humidity and air temperature are measured at three heights. Table 2.1

lists the used sensors. The data are acquired at 5 Hz with LabVIEW through National Instruments CompactDAQ hardware. In addition to the automatic measurements, a mm scale was used to manually measure the snow height in the test section. Unfortunately, this measurement was only reliable while the snow surface was flat, which was usually only the case before experiments or during experiments without drifting snow.

**Table 2.1.:** Installed sensors and measured parameters.

| Sensor | Parameter |
| --- | --- |
| MiniAir60 (Schildknecht) | Wind speed |
| HC2-S (Rotronic) (3x) | Air humidity |
| | Air temperature |
| SI-131 (Apogee) | Snow surface temperature |
| Pt100 (Mösch AG) | Snow temperature |

A SnowMicroPen (SMP, Fig. 2.2D) is used to measure the most important properties of a slab/crust, namely its hardness and thickness. The SMP is a high-resolution constant-speed penetrometer (Schneebeli and Johnson, 1998; Proksch et al., 2015). The SMP measures penetration resistance, which is directly related to hardness. We are mainly interested in the evolution of the hardness at the surface.

For some experiments, an industrial camera looking down vertically at the surface was used. We attempted to use it to detect drifting snow events by correlating sequences of images. This was not completely reliable. Wind periods with drifting snow were subsequently identified by eye. The camera images were used to create time lapse videos of the experiments. These were helpful to see what happened at the snow surface.

### 2.2.3. Postprocessing

The goal of the postprocessing of the SMP measurements (SMPs) is to reduce each force profile to a representative number. That way, large numbers of SMPs can be analysed using statistical methods. First, the location of the snow surface in the profile is determined. An automatic algorithm based on a threshold relative to the force signal in the air applied to a smoothed signal works well. Then, a linear trend is fitted to the signal in the air and subtracted from the force profile. The linear trend always had a negative slope on the order of $10^{-6}$ N mm$^{-1}$ and an offset of about 48 mN. These values are related to the signal amplifier in the SMP and are within the expected range.

To find a representative number for an SMP, we attempted to determine the depth down to which the wind had affected each measurement by comparing the current SMP with the initial measurements. Then, a statistic could be calculated for the signal between the snow surface and this affected depth. Finding this depth was obvious in many cases but sometimes the natural variability of the snowpack, snow settling or other reasons prevented a precise determination. Therefore, the representative number is now defined as the 90% quantile of the force signal in the 10 mm below the snow surface. The

advantage of using a high quantile as a representative statistic is that thin crusts can still be detected. If the mean or median were considered they would be averaged out by the unaffected, soft snow below the crust. However, the single number looses descriptive power with respect to the crust if the quantile is too high. For example, if the force signal in the complete snowpack is used, only quantiles higher than 99% were able detect thin crusts. Considering only the snow close to the surface has another advantage. The hardness of the initial snowpack usually increased with increasing penetration depth. As a result, the overall quantiles characterized the snow close to the bottom. A subsequently formed crust at the surface could therefore only be detected if it was harder than the initial snow at the bottom and this was not always the case. The surface quantiles easily detect such changes. The 90% quantile of the force signal in the topmost centimeter of snow is henceforth referred to as "SMP hardness".

## 2.3. Results

In the winters 2015/16 and 2016/17 a total of over 1000 SMP measurements were acquired during 38 experiments. The data are publicly available on Envidat (Sommer et al., 2017a). Fig. 2.3 shows the SMP hardness of all initial SMPs. Usually, four measurements were taken before the beginning of each experiment. Fig. 2.3 shows the spread of the initial conditions. The fresh snow was usually only a few hours and at most about a day old. But depending on the temperature and the wind speed during the snowfall, the initial SMP hardness varied by a factor of three. The standard deviation of initial SMP hardnesses of a single experiment is on average four times lower than the standard deviation of all 148 initial SMP hardnesses (1.9 mN and 7.3 mN). Each snow cover is therefore fairly homogeneous and the variability in Fig. 2.3 is mainly due to the different snow covers in each experiment. The density of the initial snow was usually measured close to the snow surface and close to the bottom with a 3 cm high box density cutter. The initial density varied between 30 kg m$^{-3}$ and 94 kg m$^{-3}$ at the top and between 38 kg m$^{-3}$ and 124 kg m$^{-3}$ at the bottom. The correlation between the initial surface densities and the mean initial SMP hardnesses is 0.64.
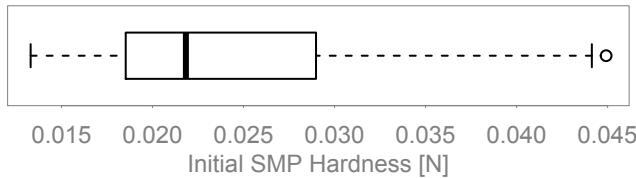


**Figure 2.3:** SMP hardness of 148 initial SMPs showing the variability in the initial conditions.

As a result of the initial variability between the experiments, the following plots will not show absolute SMP hardness but SMP hardness change. The main difficulty with SMP measurements is that only one measurement can be acquired at a specific location. Two measurements must be at least 3 cm apart. At a closer distance, the hole of the first penetration would influence the next measurement. Looking at SMP hardness change is therefore only meaningful if the snow cover was homogeneous at a scale of at least

3 cm before the change happened. As mentioned above, the initial snow cover is quite homogeneous for every experiment. Therefore, changes between the current and the initial conditions can always be calculated. SMP measurements acquired at the same time in different positions showed that wind without saltation has a homogeneous effect on the snow cover. For these experiments, we can therefore assume that the snow cover remains homogeneous and it is possible to look at changes in SMP hardness over single wind periods. The effect of saltation, on the other hand, was strongly heterogeneous. As a result, changes between the current and the initial conditions must generally be used for experiments with drifting snow. A SMP hardness change was calculated by averaging the SMP hardness of the SMPs in the reference group (e.g. the initial SMPs) and subtracting this mean from the SMP hardness of the subsequent measurements.



**Figure 2.4:** Comparison of the overall SMP hardness change between SMPs acquired after wind periods with and without drifting snow
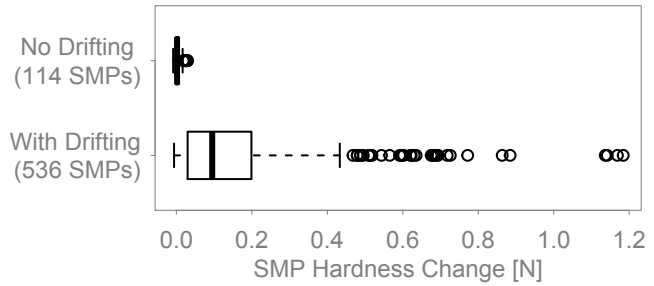
Figure 2.4 shows the change in SMP hardness between the initial SMPs and the subsequent measurements grouped by whether there had been saltation or not. For the "No Drifting" SMPs, there had not been any drifting snow in any previous wind period and for the "With Drifting" SMPs there had been drifting snow at least during the last wind period before the measurement. The "No Drifting" group of 114 SMPs has a small variability around a median SMP hardness increase of 2 mN. There are some outliers where the SMP hardness increased by up to 30 mN. The 536 SMPs in the "With Drifting" group have SMP hardness increases up to 1.18 N. The median change, however, is only 95 mN and for many measurements the change was negligible. A SMP hardness of 1 N corresponds about to a hand hardness of "1 finger" (Fierz et al., 2009). A Kruskal-Wallis test confirms that the two groups are different with a p-value of the order $10^{-16}$.

Nine of the ten SMPs with the largest SMP hardness increase in the "No Drifting" group are from an experiment on 6 March 2017. Figure 2.5 shows averaged SMPs before and after this experiment, which consisted of a single wind period. The hardness increased in the complete snowpack and the snow surface settled by about 4 mm. There was no formation of a crust at the surface. This experiment was quite special because it was very warm. The air temperature was around 1 °C during the whole experiment and the snow temperature was about -1.5 °C at the beginning. Furthermore, the wind speed could be increased to 8 m s$^{-1}$ without initiating saltation. The observed hardening was achieved within 20 minutes. After that, the experiment was stopped because the snow temperature was reaching 0 °C. Similar combinations of decreases of snow depth and overall increases in hardness were also observed in other experiments, where the temperatures and the wind speed were lower but the duration of the wind periods was longer.
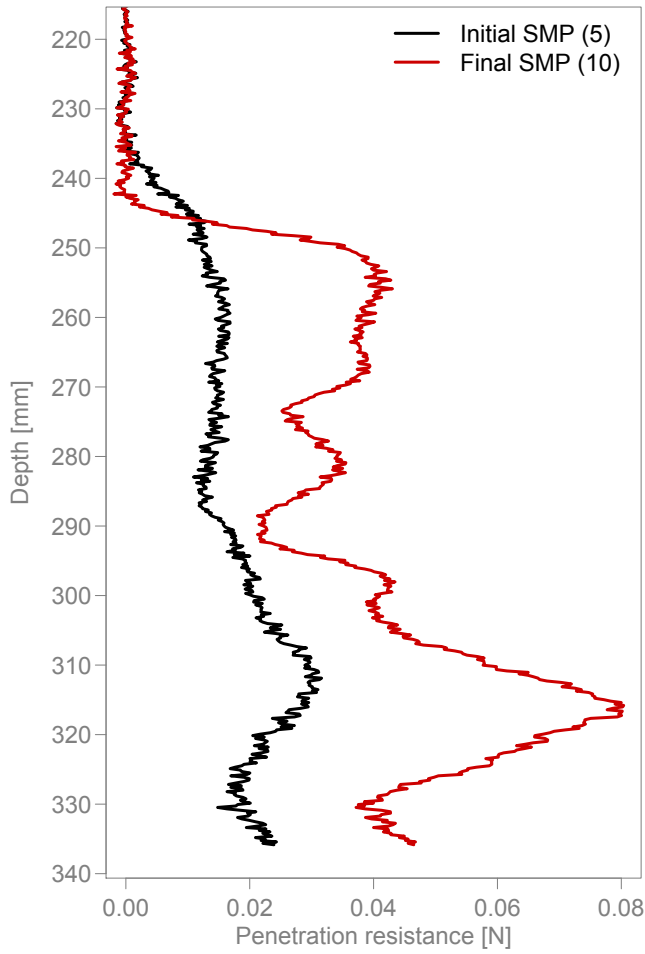
**Figure 2.5:** Averaged SMPs before and after an experiment without drifting on 6 March 2017. In 20 minutes, the snow hardness increased throughout the snowpack and the snow settled considerably. The parentheses in the legend contain the number of SMPs that were used for the average.

According to e.g. Seligman (1936) a humid wind is able to generate a wind crust without saltation. To reproduce such conditions, an insulated water bowl was placed in the wind tunnel (see Fig. 2.6) for some of the "No Drifting" experiments. This should saturate the air in the wind tunnel. The water was heated to about 20 °C and was usually replaced after it had cooled down to about 5 °C, which took about 30 min.



**Figure 2.6:** The water bowl was placed in the snow at the start of the main test section. The bowl was insulated with styrofoam.

Figure 2.7A compares groups of SMPs taken after wind periods with and without added water. Because only "No Drifting" SMPs are used here, the plot shows the SMP hardness change over single wind periods. The SMP hardness change without added water was, if anything, larger than with added water. The median was 3 mN for the "No Water" group and only 0.3 mN for the "With Water" group. The p-value of the Kruskal-Wallis test comparing the two groups is 0.005. The mean relative humidities during the wind periods in question are shown in Figure 2.7B. The added water did not have a large effect. The medians are almost equal and the Kruskal-Wallis test shows no significant difference (p-value of 0.29). However, the added water increased the minimum relative humidity from 80% to 90%.

During most experiments without drifting snow, additional SMPs were acquired outside the wind tunnel to test whether the wind has any influence at all. The snow in the obround area enclosed by the channel was used for these measurements. Fig. 2.8 shows
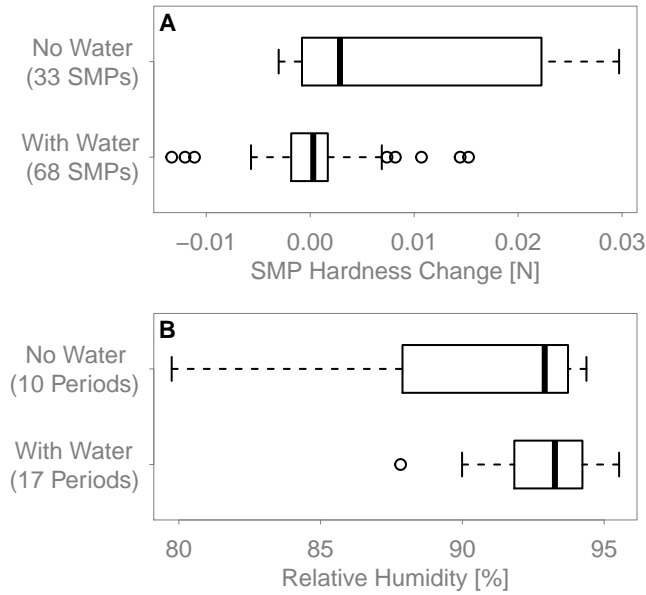
**Figure 2.7:** (A) Comparison of the SMP hardness change in wind periods with and without added water. (B) Comparison of the mean relative humidity during the same wind periods.
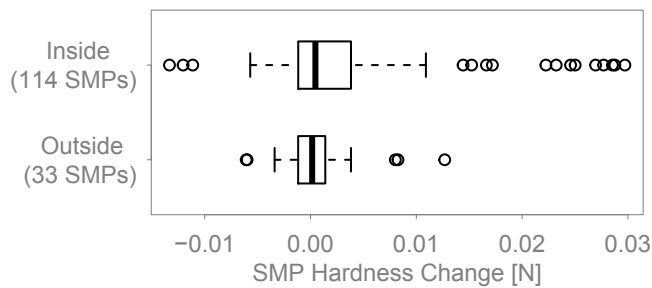


**Figure 2.8:** Comparison of the SMP hardness change in wind periods without drifting and the SMP hardness change measured outside the wind tunnel during the same time periods.

the comparison between the "No Drifting" SMPs acquired inside the wind tunnel and the corresponding SMPs taken outside the channel. The boxplots show changes over single wind periods. The median is 0.5 mN for the "Inside" SMPs and 0.2 mN for the "Outside" SMPs. The variability is smaller outside than inside. In particular, there are several outliers with higher SMP hardness changes in the "Inside" group (Fig. 2.5). The p-value of the Kruskal-Wallis test comparing the two groups is 0.1.



**Figure 2.9:** Three of the SMPs acquired during an experiment on 5 February 2016. SMP1 was acquired at the start of the experiment, SMP2 after the first wind period and SMP3 after the second wind period. Both periods were 15 min long, the wind speed was 5 m s$^{-1}$ and there was saltation during both periods. The short horizontal lines show the snow surfaces.
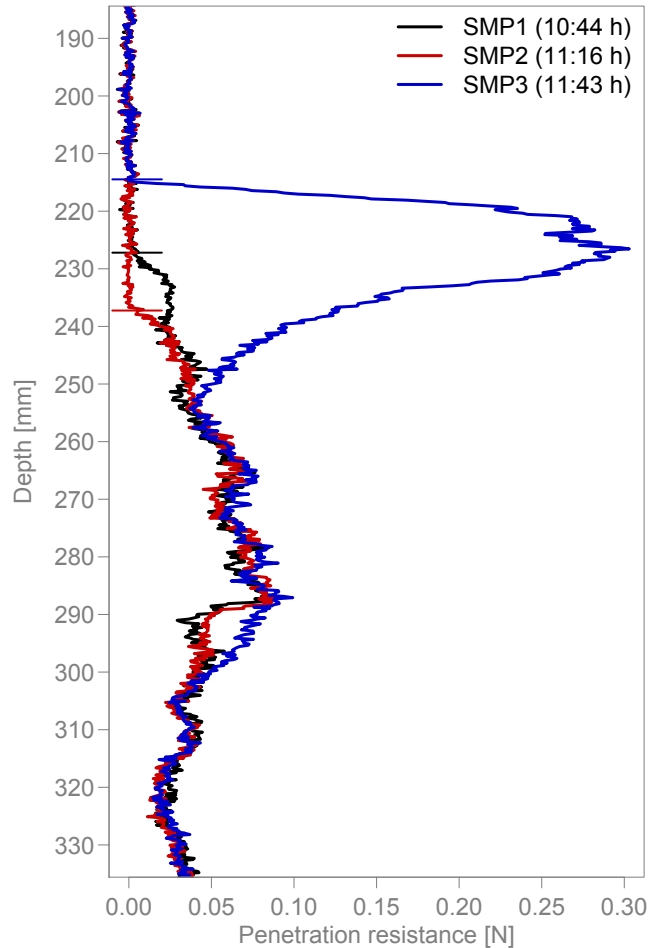
In Fig. 2.4, the striking feature about the "With drifting" boxplot is the large variability of the SMP hardness changes. Fig. 2.9 illustrates this with three SMP measurements from 5 February 2016. SMP1 is one of the initial SMPs. SMP2 was measured after a 15 min wind period at 5 m s$^{-1}$ with drifting snow and is very similar to SMP1 except that the snow depth decreased by 10 mm. After a second identical wind period, SMP3 was acquired. The snow depth increased by 14 mm and the SMP hardness increased to about 0.3 N. The example shows that similar conditions can have completely different results.

## 2.4. Discussion and Conclusions

The wind tunnel was designed to approximate an infinite fetch with regard to snow saltation. This worked quite well and it was possible to observe the formation of wind crusts. Nevertheless, the experimental setup could certainly be improved. The flow conditions are largely uncontrolled and unknown and this limits the insights that can be gained from this facility. No quantitative statements about the interaction of the flow and the mechanics of wind-packing can be made. Such experiments could perhaps be performed under controlled flow conditions in the facilities at the CSTB or CES mentioned in the introduction. The main constraint for the new wind tunnel was to have an infinite fetch, meaning a continuous and unobstructed cover of natural and undisturbed fresh snow. We do not think that this is possible to achieve in these other facilities. Therefore, while the possibilities of the new wind tunnel may be very limited, we believe it is adapted to gain knowledge about wind-packing in general and to test whether drifting snow is necessary for the formation of wind crusts in particular.

The boxplots in Fig. 2.4 clearly show that no wind crust forms without drifting snow. In some cases, wind without saltation still had a small hardening influence on the snow. An example of this is shown in Fig. 2.5. The hardness increased throughout the snowpack as opposed to only at the surface, the snow depth decreased and the final hardness resulting from this settling and slight compaction was still very low. These processes take place with or without wind but based on the comparison of the "Inside" and "Outside" SMPs in Fig. 2.8 we can assume that wind slightly accelerates them. "Wind-accelerated settling and compaction" sounds very similar to what Seligman (1936) describes as "firnification accelerated by a wet wind", which is how he defines "wind-packing". This definition is based on experiments where Seligman (1936) blew either dry or humid air through a column of snow. He noticed that after the passage of dry wind, the snow remained loose while wet wind led to coalescence of the snow. Seligman (1936) did not really measure the hardness of the resulting snow. Our results show that this process, if at all, hardens snow only slightly and/or slowly. Therefore, we propose to call this process wind-compaction instead of wind-packing.

The added water did not have the expected effect to enhance or accelerate "wind-compaction" or to lead to the actual formation of a wind crust. We also would have expected a larger influence of the added water on the humidity itself. It could be that the sensors become unreliable so close to saturation. It is also likely that the humidity was higher locally, e.g. close to the snow surface. The SMP hardness change with added water was in fact smaller than without added water (Fig. 2.7A). However, this result is most likely unrelated to the water. The correlation coefficient between the SMP hardness changes and the relative humidities of both groups shown in Fig. 2.7 is -0.37. The fact that the air humidity was always high could be the reason for this absence of correlation. Seligman (1936) gives a lower limit of 85% air humidity for "wind-compaction" to take place. The humidity in the wind tunnel was almost always above this limit (Fig. 2.7B). The increased hardening without water as compared to with water is most likely a result of a combination of factors such as temperature, wind

speed and wind period duration. We would expect wind-compaction to be more efficient at higher temperatures and higher wind speeds due to the increased heat transfer to the snowpack. There was one experiment without drifting snow and with added water where one measurement showed a SMP hardness increase only at the surface unlike the SMPs in Fig. 2.5. The SMP hardness increased by 20 mN. All other measurements in this experiment, however, showed no hardening. This could mean that the added water can, in some cases, have a local hardening effect on the surface but this measurement could also be attributed to natural variability. Overall, the conclusion remains that no wind crust forms without saltation.

The enormous variability in the "With Drifting" group in Fig. 2.4 needs explaining. Clearly, not all drifting snow events lead to the formation of a wind crust. Saltation is a necessary condition but it is not sufficient. During the experiment shown in Fig 2.9 some snow was eroded in the main test section during the first wind period. The SMPs acquired afterwards showed no hardening. During the second wind period, in contrast, snow was deposited in the main test section and the subsequent SMPs exhibited a crust at the surface. In this case, the two wind periods in question were short and at the beginning of the experiment. Therefore, it was easy to keep track by eye of where and when snow was eroded and deposited. This was usually not possible. The location of the snow surface in the SMPs can easily be determined but is a bad indicator of erosion or deposition. The wind tunnel, on which the SMP is placed for the measurements, may be oblique relative to the snow surface. In this case, the SMP snow surface location depends on the SMP position in the test section and would lead to wrong estimates of erosion or deposition. Furthermore, there may be a lot of erosion followed by a little deposition in the same wind period. In such cases, the change of the SMP snow surface location only indicates the overall erosion and cannot detect the deposition. The camera in the wind tunnel gives a qualitative idea of when and where snow is either eroded or deposited. The height information, however, is missing and the field of view is very limited. From the few SMP measurements where the erosion or deposition patterns were known, it appears that these processes are vital to understand when a wind crust forms. They could also explain the, sometimes very complicated, shapes of SMP force profiles. To analyze erosion and deposition quantitatively, the wind tunnel will be outfitted with a Microsoft Kinect sensor (Mankoff and Russo, 2013). This instrument is a low-cost 3D scanner and will provide snow depth information at a spatial resolution of less than a centimeter and at a sub-second temporal resolution.

The wind crusts in the wind tunnel reached hardnesses on the order of 1 N. This is significantly harder than the initial snow. However, compared to wind crusts in nature, which can reach a hardness of several Newtons, the snow in the wind tunnel remains relatively soft. This could be due to the relatively low wind speeds in the wind tunnel and the short duration of most experiments.

## Acknowledgments

## 2.5. Appendix: Design and characterization of the wind tunnel

### 2.5.1. Design of the wind tunnel

An infinite-fetch wind tunnel will obviously have a closed-circuit configuration. A typical closed-circuit wind tunnel has a well-defined test section and the circuit is closed with 90° turns with guide vanes, contractions and diffusers. The fan and flow conditioners, such as screens and honeycombs, occupy the complete cross section. (Mehta and Bradshaw, 1979). An infinite fetch cannot be achieved with such a setup. Snow saltation should be able to continue over the snow surface to approximate "infinite fetch" in this particular aspect. Therefore, the complete channel floor (and not just a test section) should be snow-covered and the saltation layer should be unobstructed. Therefore, the channel should have a constant cross section and smooth turns. An annular shape appears suitable. Furthermore, the drive system and potential flow conditioners cannot occupy the complete cross section. Due to the increased complexity, we decided not to consider a drive system with mobile flow boundaries (Schmundt et al., 1995; Krishnappan, 1993), but to move the fluid instead.

For a given application, there is an ideal type of fluid machinery (radial, axial, etc.). It is chosen based on the Cordier Diagram (Cordier, 1953; Bleier, 1998; Wright and Gerhart, 2009; Carolus, 2013). This diagram gives the efficiency of the machine as a function of two other non-dimensional numbers, the diameter number and the speed number. The two numbers depend on the pressure drop the machine has to overcome, the volume flow through the machine and either the diameter or the rotating speed. We thus have to estimate the pressure drop and the volume flow in the tunnel.

The pressure drop or head loss in a pipe or duct is mainly due to wall friction and can be estimated using the Darcy-Weisbach equation (Moody, 1944; Ward-Smith, 1980). The head loss depends on the pipe diameter, the pipe length, the mean velocity and a dimensionless friction factor, which can be found in the Moody Chart (Moody, 1944) or be calculated using, for example, the Churchill formula (Churchill, 1977). The friction factor depends on the Reynolds number and the surface roughness of the walls. All these relations are valid in a straight pipe with a circular cross section and must be adapted to our case of a strongly curved, rectangular duct. This was done based on the work by Hartnett et al. (1962) and Mori and Nakayama (1967). Ward-Smith (1980) gives typical ranges of the surface roughness for a variety of materials. The surface roughness of a

snow saltation layer was estimated based on Clifton et al. (2006), Fang and Sill (1992) and Tabler (1980).

The volume flow is estimated by choosing a free stream velocity and by assuming a velocity profile in the duct. In a turbulent duct flow, there is a large turbulent core flowing at the free stream velocity. According to Kleinstreuer (2010) this core occupies 92% of the cross section. The free stream velocity was chosen such that the flow should be able to transport most types of snow. Threshold friction velocities for snow transport vary between about 0.2 and 0.7 m s$^{-1}$ (Doorschot et al., 2004; Clifton et al., 2006). If there were a logarithmic profile, a velocity of 10 m s$^{-1}$ at a height of 0.5 m would lead to a friction velocity of about 0.5 m s$^{-1}$ over snow ($z_0 = 0.1$ mm, Clifton et al. (2006)). Centrifugal forces lead to a higher friction velocity in a curved duct than in a straight channel with a logarithmic profile and the same free stream velocity (Jähne, 1980). A free stream wind speed of 10 m s$^{-1}$ should therefore be sufficient. The remaining 8% of the cross section are assumed to have an average velocity of half the free stream velocity. The mean velocity used to estimate the volume flow is thus 9.6 m s$^{-1}$.

Originally, the wind tunnel was planned to be annular and to have a cross section of 50 by 60 cm (width × height) and an outer diameter of 3 m. In such a configuration, the volume flow is very high while the pressure drop is very low. This leads to a small diameter number and a high speed number. To use an industrial axial fan efficiently, its diameter would have to be larger than the width of the channel. This would have complicated the wind tunnel construction significantly. If the diameter is limited to the channel width, only two-bladed propellers can be operated efficiently in the domain in question (diameter number ≈ 0.5, speed number ≈ 20, Cordier (1953)). Propellers with a diameter of 50 cm would be custom-made and expensive. The width of the channel was therefore reduced to 18 cm. This allows to use a cheap propeller made for model aircraft rotating at up to 12000 rpm. The height of the duct was reduced to 50 cm (about 10 cm snow and 40 cm air) and the outer diameter was reduced to 1.2 m. With these dimensions, the estimates of pressure drop and volume flow are of the order of 50 Pa and 2000 m$^3$ h$^{-1}$. A propeller design tool was used to choose the correct propeller (http://www.mh-aerotools.de/airfoils/javaprop.htm). The theory behind this tool is called optimum propeller design (Glauert, 1935; Adkins and Liebeck, 1994). The propeller is driven by an electric motor (Maxon RE50, 200 Watts) via a toothed belt with a 2:1 reduction.

First experiments with the purely annular design confirmed that the curvature has a strong influence on the flow and on saltating particles. While drifting occurred across the whole width of the channel at moderate wind speeds (up to about 6 m s$^{-1}$), the centrifugal force became more dominant at higher speeds and most particles followed the outer wall. There was no excessive accumulation of snow at the outer wall, however. To locally eliminate the centrifugal effect and to increase the room available for measurements in general, two 1 m long straight sections were added. The initial experiments also showed important deposition and erosion features in the vicinity of the propeller coming from irregularities in the flow. To obtain a more uniform flow and to be closer to the ideal of an infinite fetch, a honeycomb was installed in the upper half of the cross section.

Unfortunately, it turned out that a considerable amount of snow is in suspension at this height and the honeycomb had to be removed again due to clogging.

### 2.5.2. Flow characteristics

The MiniAir (see Table 2.1) was used to measure the large-scale flow features in the main test section. This was done without snow to have a well-defined lower boundary. Nine vertical profiles were acquired at the locations shown in Fig. 2.10. The results are shown in Fig. 2.11. The lowest measurement point is at a height of 11 mm. It was acquired with the MiniAir touching the floor. The cylindrical measurement head of the MiniAir has a diameter of 22 mm. The wind speed was measured every two centimeters until the measurement head touched the ceiling. The wind speed close to the surface is almost constant across the width of the channel. The difference between the inner and outer profiles is less than 10%. Furthermore, the normalized wind speed is close to unity, which means that the reference wind speed gives a good indication of the flow close to the surface. The inner profiles exhibit a jet close to the lower boundary, i.e. the wind speed close to the floor is higher than a few centimeters above. The center and outer profiles are quite uniform across the height of the channel. An exception are the two drops in wind speed at 15 cm and 30 cm above the floor in the outer, upstream profile. These are the wakes of the bottom two Rotronic sensors. These wakes become weaker further downstream in the test section. Other than that, the profiles are quite similar over the length of the main test section. The boundary layer at the bottom appears to be very thin. The wind speed is already at its free-stream value at the lowest measurement point. This may be a result of the curvature and leads to high friction velocities at the snow surface.
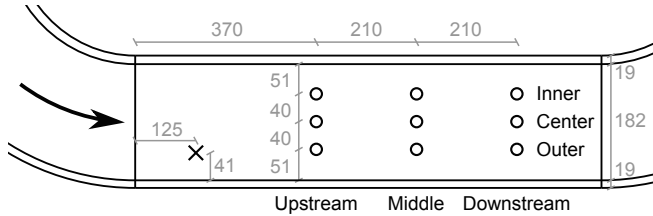


**Figure 2.10:** Locations of the wind profiles (○) in the main test section. The reference location of the MiniAir (✕) is 10 cm below the ceiling. The dimensions are given in mm. The sketch is not to scale.

### 2.5.3. Discussion

The idea behind the new wind tunnel was to simulate an infinite fetch. This could not be fully achieved. The snow surface did not remain uniform during drifting snow events. It appears that the propeller is the main cause for these irregularities. The use of a single wind source necessarily results in a flow which is not uniform. Simple simulations of the flow with ANSYS Fluent revealed that a jet forms behind the propeller which then bends downwards and reaches the surface a certain distance downstream. Furthermore, there is an area with low wind speeds below the propeller. In the annular as well as
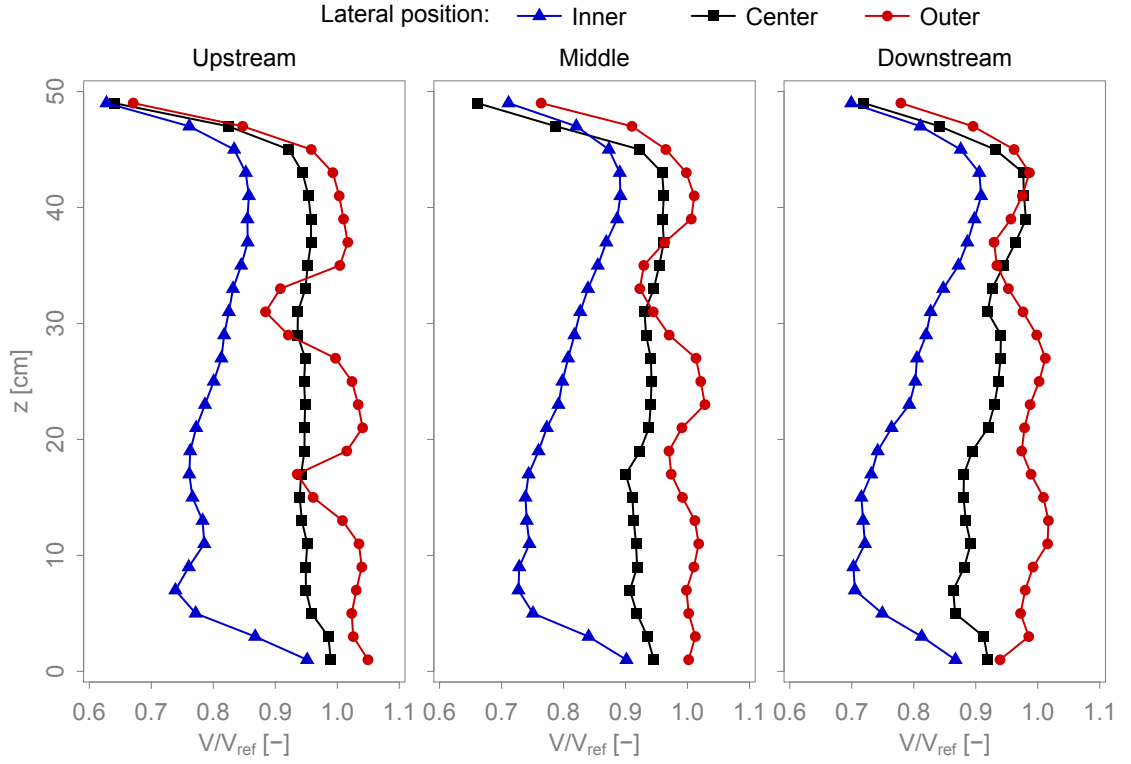
**Figure 2.11.:** Vertical profiles of normalized wind speed. $z$ is the height above the wooden floor. The reference wind speed $V_{ref}$ is the wind speed measured in the usual position of the MiniAir. $V_{ref}$ was $3 \text{ m s}^{-1}$. Fig. 2.10 shows the locations of these profiles.

in the obround wind tunnel, we always observed an accumulation below the propeller and strong erosion downstream of it. The simulations may not be very precise but the deposition/erosion patterns observed in the wind tunnel correspond well to the simulated jet and low-speed area. It must be concluded that a single propeller is not a suitable drive system to create an uniform flow in a closed-circuit wind tunnel. A more uniform flow could be achieved by moving the flow boundaries instead of the fluid, by either rotating the cover or both the channel and the cover (Schmundt et al., 1995; Krishnappan, 1993). This comes at a price of complexity and practicality and is only possible with a circular channel. As a consequence, we used the wind tunnel similarly to a normal closed-circuit facility with most of the measurements being performed in the main test section. In the beginning, the propeller was placed just downstream of the main test section to allow for a maximum of flow settling. During drifting snow events, however, the deposition below the propeller propagated into the main test section. This is why the motor/propeller was moved downstream to its current location. With the motor in the old position, the wind profiles were quite different. For example, the wind speed close to the surface of the inner profiles was 40% lower than that of the outer profiles. This corresponds to our observations that there was much more drifting snow in the outer half-width than close to the inner wall. It was fortunate that moving the motor to its current position also lead to a more uniform wind speed across the width of the channel, as shown in Fig. 2.11. The saltation intensity was fittingly observed to be much more uniform across the width of the channel. The wind profiles in Fig. 2.11 sustain the assumption made in the beginning, that there is a large core flowing at the free stream velocity. Despite this, the estimates made in the design phase were not entirely correct. For example, the measured free stream velocity never exceeded 8 m s$^{-1}$, whereas up to 10 m s$^{-1}$ were expected. However, we rarely experimented with wind speeds above 7 m s$^{-1}$ because the centrifugal effects simply became too strong. The wind profiles above snow may be different from those shown in Fig. 2.11, even though the shape of the profiles is expected to be similar as long as the snow surface is flat. But uneven erosion and deposition patterns will certainly modify the flow conditions. So, the flow is neither steady nor uniform as it would ideally be in an infinite-fetch wind tunnel. Furthermore, our knowledge of the existing flow is limited to the large-scale flow features in the main test section. Therefore, we cannot make quantitative statements concerning the flow's effects on individual snow grains. This wind tunnel is not adapted to measure onset of saltation for example. However, the focus of this facility is on the bed material, how it reacts and how its properties change under the influence of wind, and not on the flow itself.

# 3. Wind tunnel experiments: influence of erosion and deposition on wind-packing of new snow

## Authors

Christian G. Sommer[1,2], Michael Lehning[1,2], Charles Fierz[1]
[1]WSL Institute for Snow and Avalanche Research SLF, Davos, Switzerland
[2]CRYOS, School of Architecture, Civil and Environmental Engineering, EPFL, Lausanne, Switzerland

## Publication

## Abstract

Wind sometimes creates a hard, wind-packed layer at the surface of a snowpack. The formation of such wind crusts was observed during wind tunnel experiments with combined SnowMicroPen and Microsoft Kinect sensors. The former provides the hardness of new and wind-packed snow and the latter spatial snow depth data in the test section. Previous experiments had shown that saltation is necessary but not sufficient for wind-packing. The combination of hardness and snow depth data now allows to study the case with saltation in more detail. The Kinect data requires complex processing but with the appropriate corrections, snow depth changes can be measured with an accuracy of about 1 mm. The Kinect is therefore well suited to quantify erosion and deposition. We found that no hardening occurred during erosion and that a wind crust may or may not form when snow is deposited. Deposition is more efficient at hardening snow in wind-exposed than in wind-sheltered areas. The snow hardness increased more on the windward side of artificial obstacles placed in the wind tunnel. Similarly, the snow was harder in positions with a low Sx parameter. Sx describes how wind-sheltered (high Sx) or wind-exposed (low Sx) a position is and was calculated based on the Kinect data. The correlation between Sx and snow hardness was -0.63. We also found a negative correlation of -0.4 between the snow hardness and the deposition rate. Slowly deposited snow is harder

than a rapidly growing accumulation. Sx and the deposition rate together explain about half of the observed variability of snow hardness.

## 3.1. Introduction

Wind-packed snow in the form of thin, hard crusts or thicker slabs is relevant in both alpine and polar areas. In mountainous terrain, wind slabs affect the avalanche danger and wind-packed snow in general affects how the snow cover interacts with the atmosphere. Especially at high latitudes, wind-packing affects the mass balance. Permanent deposition of snow often only occurs when the snow is packed and hardened by wind (Groot Zwaaftink et al., 2013). Yet, it is still not clear how these wind-hardened layers form. There are many qualitative descriptions of wind-packed snow, especially in polar literature (e.g. Alley, 1988; Benson, 1967; Schytt, 1958) and many different formation processes such as e.g. deposition of humidity onto the surface, fragmentation of snow crystals or sintering have been proposed (e.g. Alley, 1988; Benson, 1967; Kotlyakov, 1966; Schytt, 1958; Seligman, 1936). Experimental evidence and quantitative information, however, are scarce.

In Sommer et al. (2017a), we presented a new wind tunnel specifically designed to study the formation of wind crusts. A SnowMicroPen (SMP) (Schneebeli and Johnson, 1998; Proksch et al., 2015) was used to measure changes in snow hardness. We showed that saltation is a necessary condition for wind-packing. No wind crust formed without drifting snow. However, saltation is not a sufficient condition. In many cases, wind with drifting snow did not lead to the formation of a crust or the resulting "crust" was still very soft. We suggested that spatial and temporal patterns of erosion and deposition may play a key role.

The available SMP data did not permit to test this hypothesis, however. Now, wind tunnel experiments were performed with an additional instrument, a Microsoft Kinect, allowing us to quantify erosion and deposition. Their influence on wind-packing is studied in this paper. The goal is to better understand why drifting snow forms a wind crust in some cases but not always.

In section 3.2, the wind tunnel and the main instruments are briefly introduced. The Kinect data acquisition and processing is described and the sensor is characterized with regard to its accuracy. Furthermore, the performed experiments and analyses are described. The combined SMP and Kinect results are presented in section 3.3. Discussion of the results and conclusions follow in sections 3.4 and 3.5.

## 3.2. Methods

### 3.2.1. Wind tunnel and main instruments

The wind tunnel consists of a closed-circuit channel with an obround shape. This setup allows to simulate an infinite fetch. The two half-circles are separated by 1 m long straight sections. The overall length is 2.2 m and the width 1.2 m. The channel itself is 50 cm high and 20 cm wide (Fig. 3.1A). An electric motor drives a model-aircraft propeller to create wind. The wind speed and other meteorological parameters are measured at the start of the main test section (Fig. 3.1A). The wind tunnel and the instrumentation is described in detail in Sommer et al. (2017a).

The SMP is the main instrument and is used to measure the hardness of snow on the ground. The SMP is a constant speed penetrometer measuring a profile of resisting force with a spatial resolution of 4 $\mu$m as the measuring tip is pushed into the snow. SMP measurements (SMPs) were acquired mostly in the main test section. The SMP can be positioned freely but most often SMP positions were chosen on a regular grid. In the cross-stream direction, SMPs were acquired in the center and 4 cm to each side. In the streamwise direction, the SMPs were 3 cm apart (see also Fig. 3.3F).

In winter 2016/2017, a Microsoft Kinect 2.0 (or v2, Pagliari and Pinto (2015)) was installed as an additional instrument. The Kinect is a motion sensing input device for the Microsoft Xbox gaming console. It is basically a low-cost 3D scanner. The Kinect was installed above the main test section (Fig. 3.1A) and it measures the evolution of snow depth in the entire straight section. The Kinect (Fig. 3.1B) computes depth by measuring the phase shift of the emitted, modulated infrared light. The depth camera has a resolution of 512x424 pixels and a field of view of 70x60°. The sensor, including accuracy considerations and comparisons to the Kinect 1.0, is described in Lachat et al. (2015), Pagliari and Pinto (2015) and Yang et al. (2015). Pagliari and Pinto (2015) attest an accuracy of about 1.5 cm and a precision (repeatability) of about 1 mm to the depth camera at ranges up to 4 m. Yang et al. (2015) reported an accuracy of below 2 mm over most of the field of view at a range of 1 m. In the center of the field of view, the same accuracy was observed at distances up to 3 m.



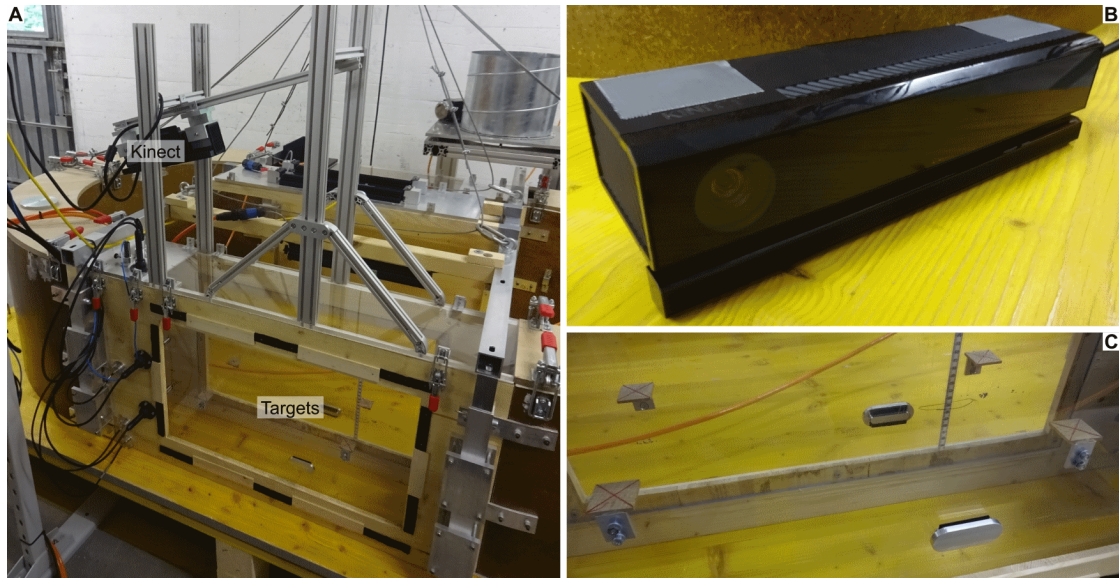**Figure 3.1.:** (A): The Kinect mounted obliquely above the main test section of the wind tunnel. The modular support allowed us to find the best possible position and orientation of the Kinect in situ. Details of the Kinect sensor (B) and of the four reference targets attached to the windows of the main test section (C). The channel in (A) is 20 cm wide and 50 cm high. The straight section is 1 m long.

The Kinect is mounted about 30 cm above the cover of the main test section at an oblique angle of about 17° (Fig. 3.1A). Ideally, the Kinect would be embedded in the cover and look straight down at the surface. The sensor is mounted above the cover because the minimum distance it can resolve is 50 cm. Furthermore, the emitted infrared light is reflected off the Plexiglas cover and leads to a blind spot in the depth image. The oblique mounting angle moves this blind spot from the center to the edge of the field of view. The exact mounting angle is measured before each experiments by taking 100 depth images of a flat surface in the main test section. The cover of the test section with the Kinect on it has to be removed for SMP measurements between the wind periods. Therefore, it cannot be excluded that the Kinect is in a slightly different position for each wind period. Such misalignments were on the order of millimeters but still reduce the accuracy of the snow depth measurements. To correct these errors, four rectangular reference targets were installed in the main test section (Fig. 3.1C). These fixed targets can be used to align the images of the different wind periods with each other. The eight corners of these targets pointing into the channel were used as reference points for the registration. During wind periods, depth images were acquired at a nominal rate of 5 Hz. The effective frame rate was only about 3.6 Hz on average due to the long ($\approx$ 10 m) USB cable even though an active cable was used.

### 3.2.2. Experiments

All experiments started with fresh snow collected on trays outside the building during snowfalls. The filled trays are placed underneath the wind tunnel while it is lifted by a crane. The wind tunnel, which is open at the bottom, is then lowered into the snow cover. The experiments therefore start with a continuous cover of natural and almost undisturbed new snow. The initial snow was usually a few hours old and had a density between 30 kg m$^{-3}$ and about 100 kg m$^{-3}$. Grain sizes and shapes varied with the meteorological conditions during the snowfalls.

Experiments consisted of one or several wind periods, before and after which, SMP measurements were performed. A typical wind period was about 30 minutes long but there were some as long as several hours or as short as a few minutes. Averaged over all SMPs, the cumulative duration of wind periods before an SMP was almost 3 hours. The median was 1 hour and 15 minutes, the maximum almost 21 hours and the minimum was less than 4 minutes. The wind speed was between 3 m s$^{-1}$ and 7 m s$^{-1}$ in most wind periods. Higher wind speeds would be possible but were not practical due to the increasing centrifugal effects in the turns. The air temperature in the wind tunnel varied between -9°C and 1°C.

Several experiments were performed with an obstacle in the test section. This allowed to force deposition of snow and to test the difference between wind-exposed and wind-sheltered deposition. Fig. 3.2 shows the obstacle at the beginning of an experiment. A 6 cm x 6 cm x 18 cm rectangular block of wood was pressed halfway into the snow such that a triangular obstacle with a height of about 4 cm remained.

**Figure 3.2:** The obstacle in the test section at the beginning of an experiment. The obstacle is a block of wood with a square 6x6 cm cross section.
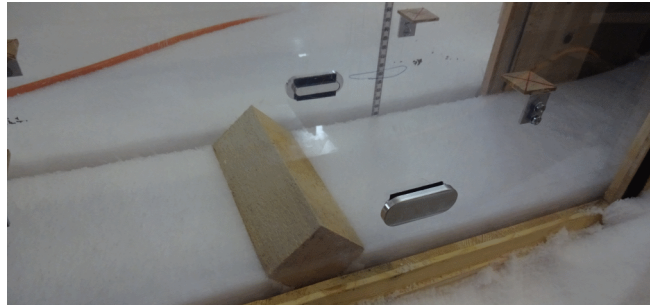
### 3.2.3. Data processing

The SMP data processing is described in Sommer et al. (2017a). In short, each force profile is reduced to a representative number called "SMP hardness" by calculating the 90% quantile of the force signal in the topmost centimeter of snow. Section 3 shows results using the SMP hardness as well as the full SMP profile.

The Kinect depth images are processed in Matlab. After aligning all raw depth images (Fig. 3.3A) to those of the first wind period to account for the variable Kinect position, they are transformed into 3D point clouds to simplify the further processing. The point clouds are rotated by the previously determined mounting angle (Fig. 3.3B). The point clouds are then cropped to contain only the snow surface (Fig. 3.3C). The corners are cut off because there, the four targets obstruct the view of the snow surface. Finally, the point clouds are filtered to remove isolated points, for example in SMP measurement holes (Fig. 3.3D), and transformed back to depth images with a resolution of 2 mm per pixel (Fig. 3.3E). Additionally, the average depth of each target is calculated at each time step and these target depths are saved for later use.

Some corrections are then applied to the processed depth images. The measured depth of the stationary targets usually varied by a few mm during experiments. These variations could be due to temperature variations of the Kinect's electronics. Furthermore, the measured depth always decreased by about 2 mm when a person was close to the window in the main test section. Apparently, the infrared signal measured by the Kinect is influenced by the body heat or the additional reflection. These errors were corrected using the target depths. The variations around the mean target depths was subtracted from the measured snow depth. The depth evolution was a little different for each target. Therefore, each pixel was corrected individually using a weighted average of the four targets based on the distances between the current pixel and the four targets. The accuracy and linearity of the Kinect were characterized by taking depth images of a flat surface in the main test section at nine different known heights above the floor (see also section 3.2.4). The height of the flat surface was increased by either 20 mm or 21 mm at each step. The characterization revealed a slight non-linearity of the measured depth that, in addition, depended on the position in the field of view. This non-linearity of the Kinect was corrected using the characterization images. The depth images of the flat surface were smoothed by applying a moving window filter that averaged the depths within radii of five pixels. A five pixel wide band was therefore
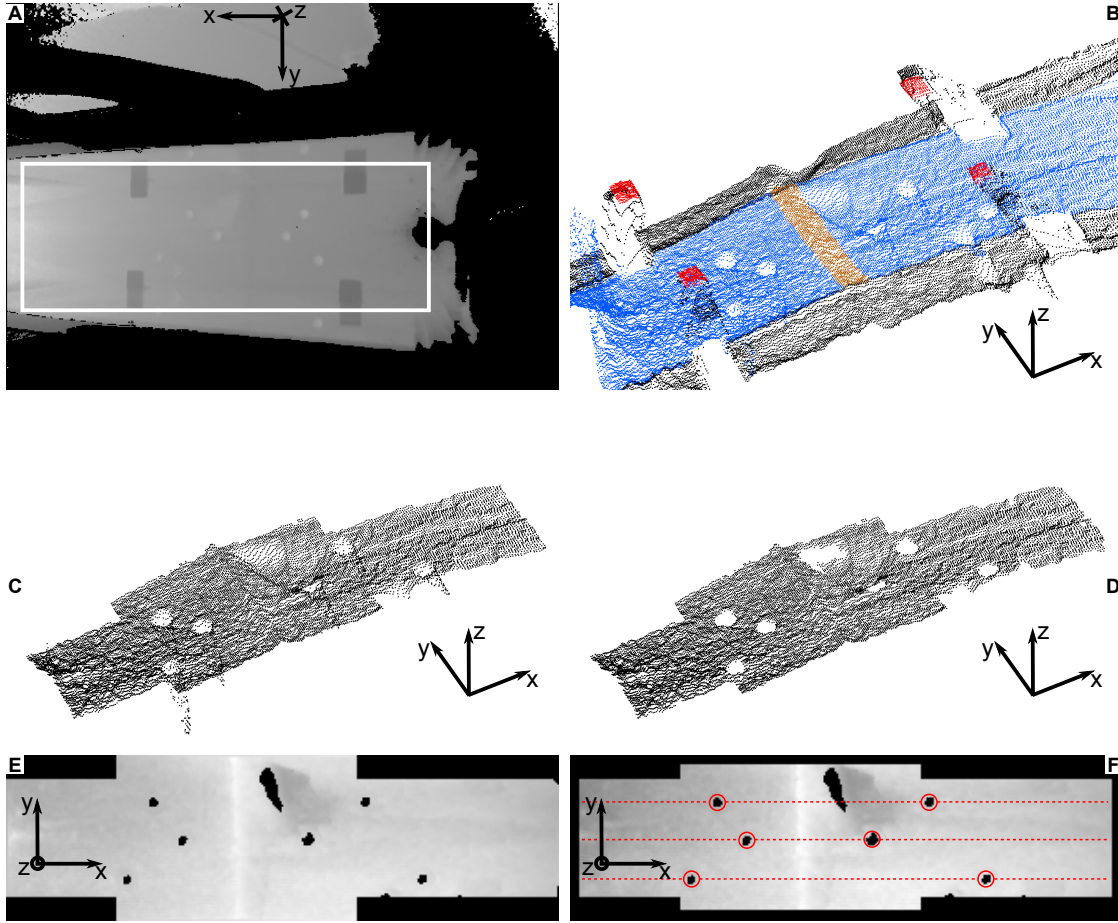
**Figure 3.3.:** Processing steps of the Kinect data. The coordinate system in each sub-figure shows the same real-life directions: $x$ is the streamwise direction, $y$ is the cross-stream direction and z is the vertical. (A): Raw Kinect depth image. The four darker rectangles are the targets, the lighter circles are SMP holes. The black circular shape on the right is the reflection blind spot. The other black areas are too close to the sensor to be resolved. (B): Point cloud of the raw depth image inside of the white rectangle in (A). The targets are red, the snow surface is blue and an almost buried artificial obstacle is colored brown. (C): Point cloud cropped to contain only the snow surface and the obstacle. The four corners are cut away to remove the targets. (D): Filtered point cloud. Isolated points are removed. The SMP holes are now more clearly visible. There is also a measurement shadow just downstream of the obstacle. (E): Processed depth image. The SMP holes and the measurement shadow appear as black areas, as do the cut off corners. The obstacle is visible as a light, vertical line. (F): Processed and corrected depth image. The edges are cut away during the correction. The effect of the correction is most visible on the left. The red circles indicate the manually determined SMP positions. The dashed, red lines show the three lines on which all SMPs are acquired and where the Kinect profiles are calculated.

discarded at each edge (Fig. 3.3F). The smoothed images were used to fit a second-order correction for each remaining pixel. These corrections fit the nine measured heights of the flat surface to the corresponding true heights and were then applied to the processed depth images. Averaged over every pixel, the second-order correction for the depth $D$ is $D_{new} = 2.51 \cdot 10^{-4} D_{old}^2 + 0.90 D_{old} - 20.15$. The fit is very good for every pixel. The adjusted $R^2$ is always higher than 0.999 and the Root Mean Squared Error is 0.6 mm on average and 1.8 mm for the worst pixel. The constant offset may seem like a large correction. It is due to the different coordinate systems used for the Kinect and to measure the real heights of the flat surface. The order of magnitude of this offset has no consequence because the Kinect is only used to measure depth changes.

The positions of the SMP measurements are determined manually in the processed and corrected depth images (Fig. 3.3F). The SMP holes were clearly visible in most cases. The snow depth evolution can then be calculated at each SMP position. The depths within a radius of six pixels of the SMP position were averaged and a moving window filter with a width of 10 seconds was applied afterwards.

The processed and corrected depth images were also used to calculate snow depth profiles in the streamwise direction. Profiles were calculated at the three cross-stream positions that were also used for all SMPs (Fig. 3.3F). The profiles were averaged over eight pixels in the cross-stream direction. The absolute depth measured by the Kinect depends on the position in the depth image. This is probably due to the Kinect's lens and is especially accentuated towards the edges of the field of view. This means that a flat surface in reality does not appear flat in the depth image. Therefore, relative snow depth profiles were calculated by subtracting the initial profiles. For experiments with an artificial obstacle in the main test section, the obstacle was not removed in the relative profiles. Fig. 3.7 in the results section includes some examples of relative snow depth profiles.

### 3.2.4. Kinect accuracy assessment

During the Kinect characterization, two measurements were made at each height of the flat surface. The first measurements were used to fit the corrections. The second measurements were used to assess the accuracy of the Kinect with regard to snow depth changes. We use "height" and "height changes" here because the characterization was done without snow. Height refers to the distance between the floor and the flat surface. The accuracy was assessed on a 3x16 grid of positions in the main test section that were usually used for SMP measurements. As for the SMPs, the depths were averaged within a radius of six pixels of these positions. For every position, absolute and relative errors were then calculated. The errors were large at the three positions at the upstream edge of the field of view. This could be due to the reflection blind spot which is located there. These positions are therefore neglected here and no Kinect data from these positions is used in the results. The errors in the remaining 45 positions were quite similar.

Fig. 3.4A shows the mean absolute errors as a function of the height change and the lower of the two heights and Fig. 3.4B shows the mean absolute relative errors. The means were calculated using the remaining 45 positions. For the mean absolute errors,
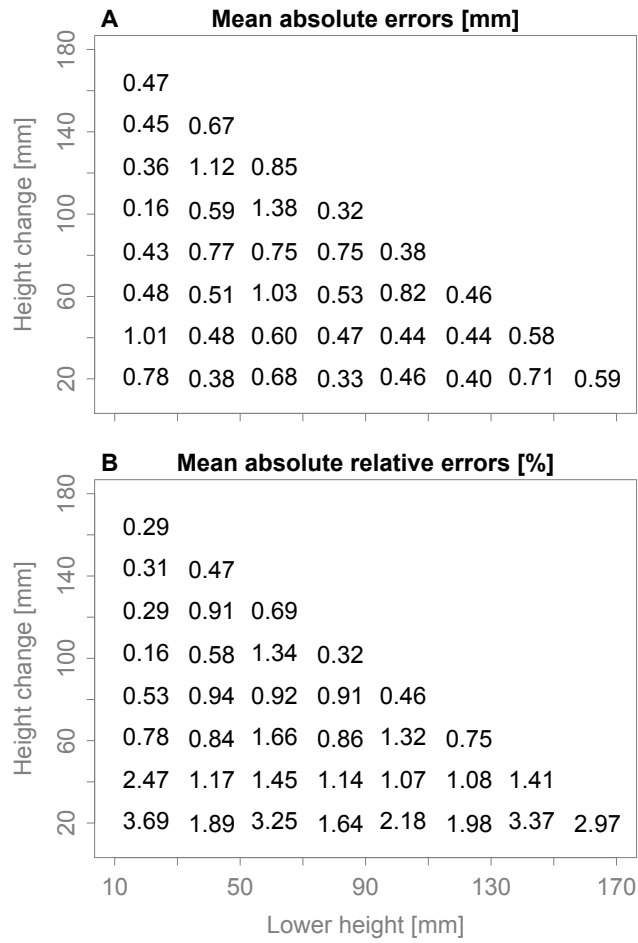
**Figure 3.4:** Mean absolute errors (A) and mean absolute relative errors (B) as functions of height change and the height of the bottom surface. Each number is the mean of the errors at the 45 remaining positions.

there is no significant trend with either height or height change. As a result, the mean absolute relative errors decrease with increasing height change. The overall averages of the mean absolute errors are 0.60 mm and 1.28%. The overall maximum absolute errors for any combination of position, height and height change are 2.58 mm and 9.69%.

### 3.2.5. Dataset and analyses

A total of 1054 SMPs were acquired during 38 experiments in the winters 2015/16 and 2016/17. 688 SMPs were taken after wind periods with drifting snow. For 335 of those measurements, snow depth data from the Kinect is available. The following results are mostly based on this last group of SMPs. Only 27 measurements from the first winter, i.e. SMPs without Kinect data, are used here. For these measurements we know from the log and by manual observation whether they were acquired after erosion or deposition, for example. This information is not available for most SMPs from the first winter and these data can therefore not be used here. The Kinect and SMP data, as well as the postprocessing scripts, are publicly available on Envidat (Sommer et al., 2017c; Sommer et al., 2017b).

In the next section, boxplots are used to compare groups of SMPs (e.g. erosion or deposition) and the Kruskal-Wallis test (Kruskal and Wallis, 1952) is used to determine whether they differ significantly. This is a non-parametric test and can therefore be used even if the data are not normally distributed or if the sample size is small. Scatterplots and correlation coefficients are used to show relationships between variables.

## 3.3. Results

### 3.3.1. Erosion and deposition

Fig. 3.5 compares SMPs that were taken at positions where snow was either eroded or deposited. The boxplots show the overall SMP hardness change between the initial and the current measurements. No measurable hardening occurs when snow is eroded. The median SMP hardness change of the "Erosion" group is 3 mN and the standard deviation is 2 mN. In the "Deposition" group, there are SMP hardness changes between 0 and 860 mN and the median of the group is 100 mN. A Kruskal-Wallis test confirms that the two groups are different at a significance level of $\alpha < 0.001$.
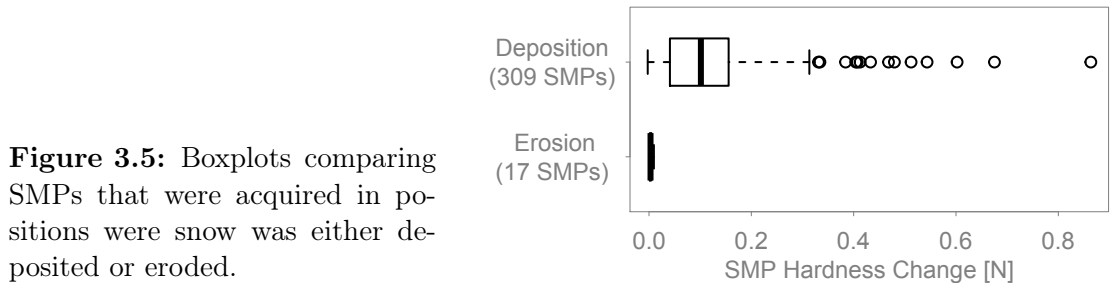


**Figure 3.5:** Boxplots comparing SMPs that were acquired in positions were snow was either deposited or eroded.

### 3.3.2. Obstacle experiments

Fig. 3.6 shows the boxplots comparing SMPs acquired on the windward or leeward side of the obstacle. The experiments with obstacle were split in two groups based on whether saltation started spontaneously or not. During experiments at warm temperatures and/or deliberate low wind speed, drifting snow did not start spontaneously and saltation could only be achieved and sustained by sieving snow into the wind tunnel (see Fig. 1 in Sommer et al. (2017a)). Furthermore, only SMPs that were acquired after a single wind period with drifting snow are shown in Fig. 3.6. Both the windward and leeward side of the obstacle were usually filled up during the first wind period with drifting snow. The obstacle as such was therefore not effective anymore during subsequent drifting snow events and the corresponding SMPs cannot be analyzed with regard to wind-exposed and wind-sheltered deposition.
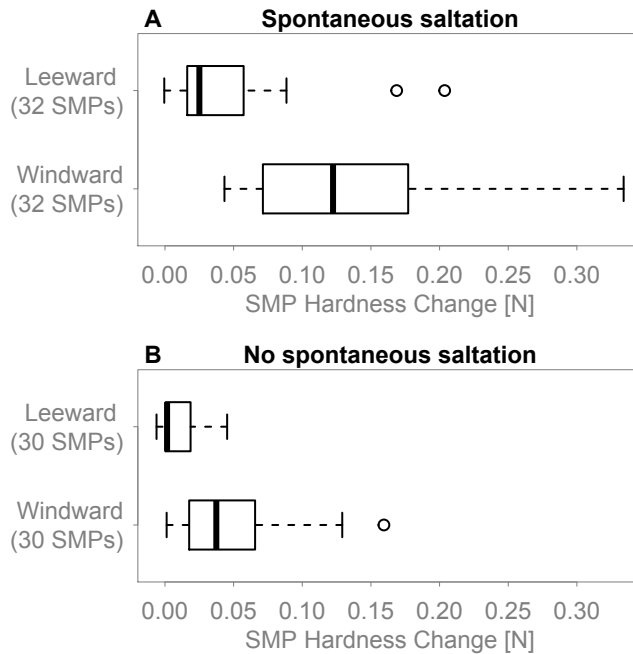


**Figure 3.6:** Boxplots comparing SMPs that were acquired either on the windward or the leeward side of the obstacle during experiments where (A) saltation started spontaneously or (B) saltation could only be achieved by sieving snow into the wind tunnel.

During the experiments with spontaneous saltation shown in Fig. 3.6A, the median hardness change of the SMPs on the leeward side of the obstacle was 25 mN. The median of the "Windward" group is 120 mN. For the experiments with no spontaneous saltation (Fig. 3.6B) the median SMP hardness change is 2 mN for the "Leeward" group and 37 mN for the "Windward" group. In both cases, the Kruskal-Wallis test confirms at a significance level of $\alpha < 0.001$ that the SMP hardness change on the windward side is higher than on the leeward side. The hardness increase with spontaneous drifting is higher than without spontaneous drifting in leeward and windward locations. In fact, the "Leeward" group in Fig. 3.6A shows comparable hardness changes as the "Windward" group in Fig. 3.6B. If the experiments with and without spontaneous saltation are not separated, the difference between the windward and the leeward side is less clearly visible

in the boxplots but a Kruskal-Wallis test still confirms that the SMP hardness increases more on the windward side at a significance level of $\alpha < 0.001$.

### 3.3.3. Wind exposure

The classification of SMPs in groups either windward or leeward of the obstacle is a very crude representation of wind-exposed and wind-sheltered deposition. For example, how wind-sheltered a position on the leeward side is depends on the distance to the obstacle and also on time as the surface evolves. As mentioned before, the leeward side becomes less wind-sheltered as snow is being deposited. We used the relative Kinect snow depth profiles to calculate the wind exposure parameter Sx (Winstral and Marks, 2002) for each SMP position as a function of time. Sx is the maximum upwind slope, i.e. the slope between the point of interest and the shelter-giving point which maximizes the upward angle. Positive Sx values mean the point of interest is wind-sheltered while wind-exposed points have negative Sx. We used a maximum search distance of 200 mm and also introduced a minimum distance of 5 mm to limit the influence of nearby features. 5 mm is the diameter of the SMP measuring tip. Fig. 3.7 shows some examples of shelter-giving points.



**Figure 3.7:** Relative Kinect snow depth profiles and arrows showing some examples of shelter-giving points. The circles show the SMP positions. The wind is from left to right. (A): Initial conditions of an experiment with an obstacle and two highly wind-sheltered SMP positions. (B): Same experiment as in (A) but after deposition of snow around the obstacle. The same SMP positions are now not wind-sheltered anymore. The dashed line outlines the obstacle. (C): Two examples of wind-exposed SMP positions during an experiment without an obstacle.
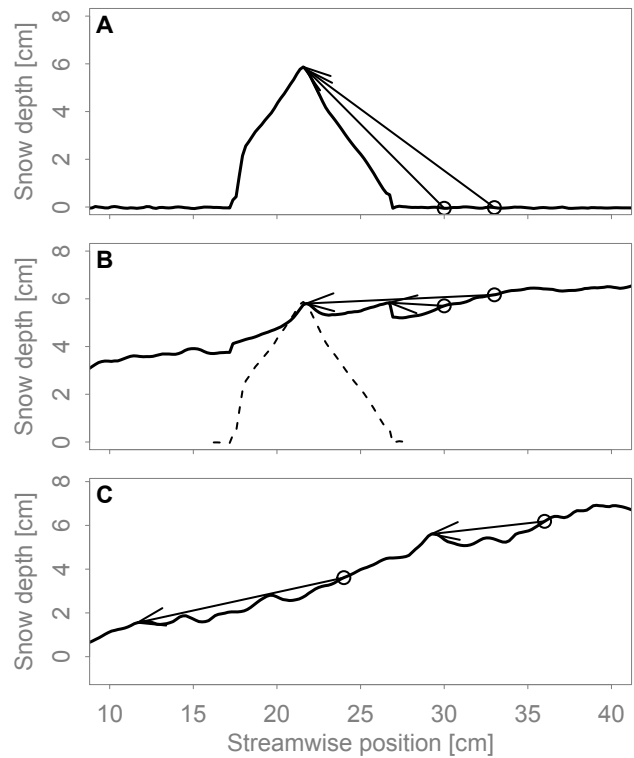
To analyze the effect of wind exposure or sheltering on wind-packing in more detail we want to correlate Sx with the penetration resistance or force measured by the SMP. While Sx is a function of time, the force is a function of penetration depth. Therefore we

need to map depth to time and vice-versa or, in other words, we need to know at what time each snow layer was deposited. The mapping for a given SMP is calculated on the basis of the Kinect snow depth data at this SMP position (Fig. 3.8A). Only time periods with a monotonically increasing snow depth are kept. If there was erosion during the wind period, the mapping splits the wind period in several deposition periods. A moving window filter with a width of 1 mm and 50% overlap is then applied to the mapping. However, there is no averaging across gaps between deposition periods longer than 10 s and there must be at least 30 SMP sample points in each window. Filter windows that do not meet these requirements were removed. Furthermore, filter windows within 4.3 mm of the snow surface were also removed. 4.3 mm is the height of the conic part of the SMP measuring tip. Only starting at this depth can the measuring tip be considered to be completely in the snow. For each remaining filter window, the Sx and force values within it are averaged (Fig. 3.8A,B and C and the red line between them). These averages are then plotted against each other in a scatterplot (Fig. 3.8D).

Fig. 3.9 shows a scatterplot of Sx against the SMP force with data from 87 SMPs. Settling can make it difficult to match the Kinect snow depth data to the SMP force profile. However, it is relatively straightforward for SMPs where saltation occurred only during one of the preceding wind periods. These 87 SMPs acquired during experiments both with and without the obstacle are used here. The overall correlation coefficient of the 4534 Sx and force pairs is -0.63. Practically no hardening occurs for Sx above 0.3. For Sx below 0.2, almost any force appears to be possible but the highest forces have mostly negative Sx. There are about ten points with Sx≈0.2 and forces between 0.17 N and 0.23 N that seem to contradict this. These points are all from a single SMP measurement. It is unclear whether this SMP measurement is reliable or if there was a problem with the mapping, for example. The influence of the moving filter width, which is 1 mm in Fig. 3.9, was tested. As the width is increased, the number of points decreases but the shape of the point cloud stays the same and the correlation coefficient actually increases. For a filter width of 20 mm, there are 1596 points and the correlation coefficient is -0.7.

### 3.3.4. Deposition rate

The Kinect data can also be used to calculate the deposition (and erosion) rate at the SMP positions. The snow depth data is too noisy to use a numeric derivative. Instead, the average slope in a 15 s moving window was calculated. The same mapping (Fig. 3.8A) is then used to correlate the SMP force to the deposition rate. Fig. 3.10 shows the corresponding scatterplot. Based on Fig. 3.9, only points with Sx<0.2 are shown here. The correlation coefficient between the 2983 point pairs is -0.40. All points with a hardness above 0.15 N have a deposition rate below about 0.2 mm s$^{-1}$ and all points with a deposition rate above about 0.6 mm s$^{-1}$ have a hardness below 0.1 N.

A multilinear regression between the SMP force and Sx, deposition rate and their interaction results in an adjusted R$^2$ of 0.47. All three terms in the model are highly significant. Sx alone explains 40% of the variability.
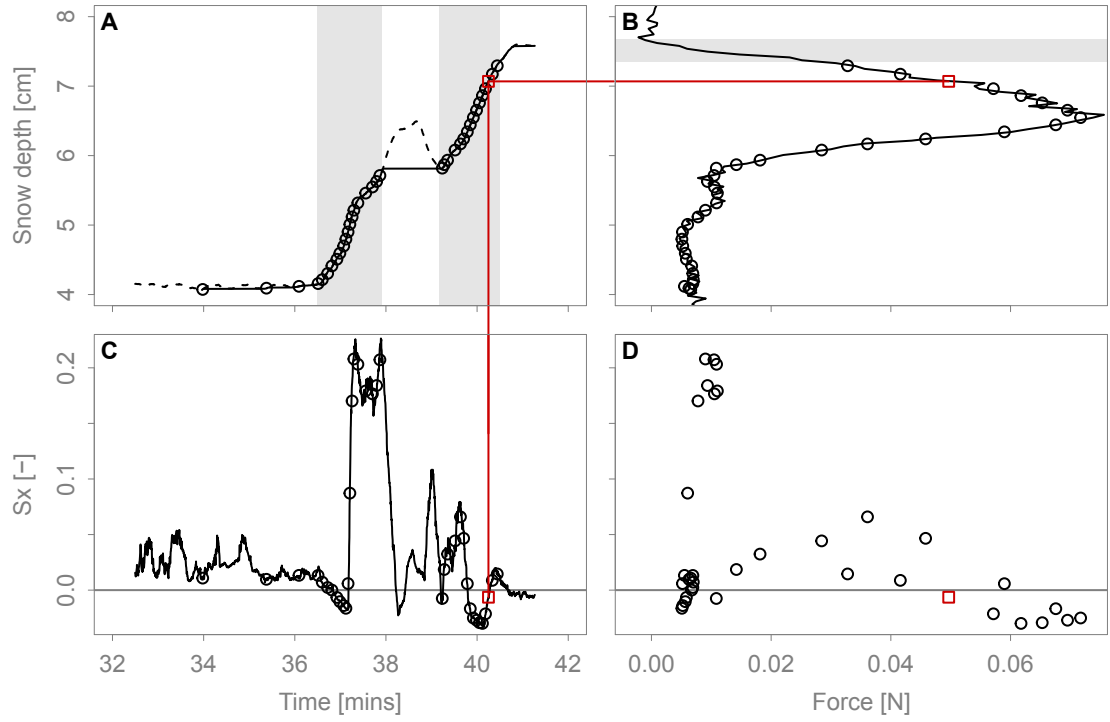
**Figure 3.8.:** Correlating the SMP force with Sx. (A): Depth-time mapping. The dashed line is the underlying snow depth data. It can be seen how the mapping splits the wind period in distinct deposition periods. The two main deposition periods are highlighted. The circles show the remaining points after the moving window filter is applied to the mapping. (B): SMP force profile. The neglected part of the profile close to the snow surface is highlighted (C): Sx as a function of time. (D): Scatterplot of Sx against force. The red line across the sub-plots shows for one filter window how the mapping in (A) connects force (B) with Sx (C). The corresponding filter window is shown as a red square in all four sub-plots.
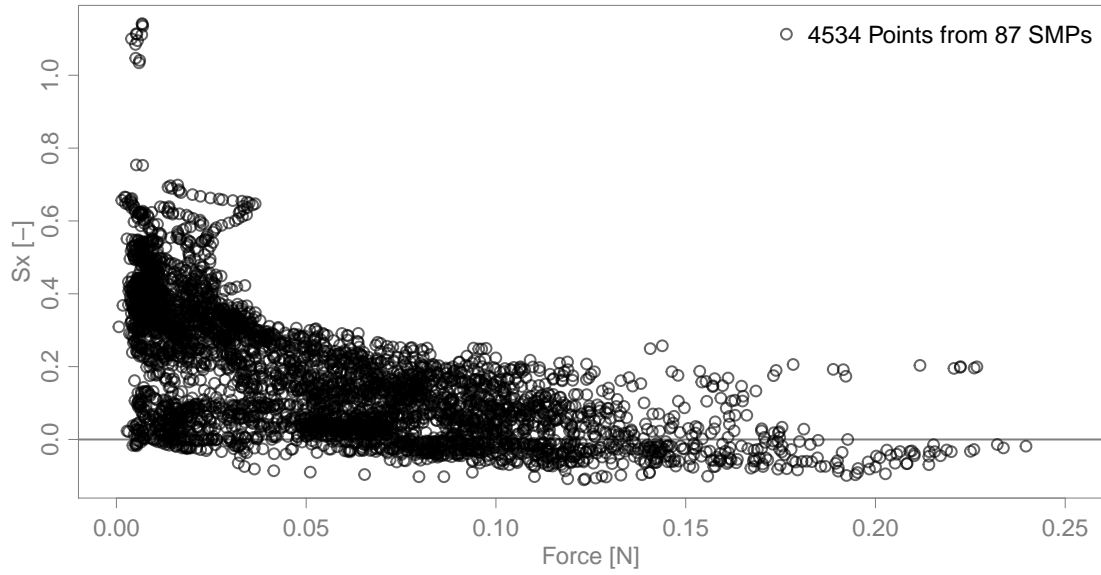
**Figure 3.9.:** Scatterplot of Sx against the SMP force showing the effect of wind exposure on wind-packing. The plot is the same as Fig. 3.8D but shows 4534 points from 87 SMPs.
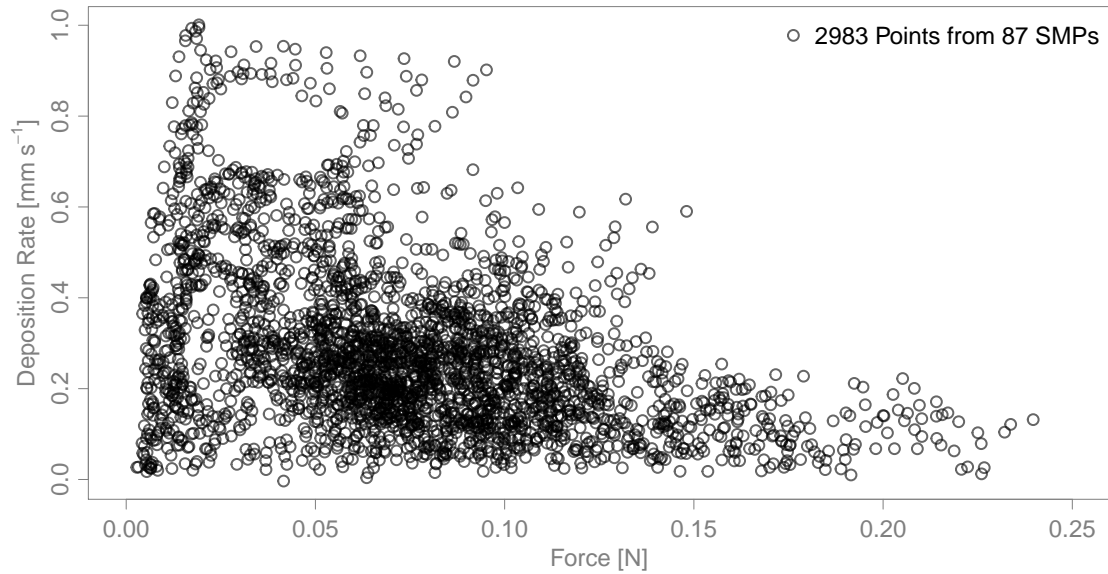


**Figure 3.10.:** Scatterplot of deposition rate against the SMP force. The plot shows the 2983 points with Sx<0.2 from the same 87 SMPs as in Fig. 3.9.

## 3.4. Discussion

The raw Kinect data requires complex processing to become useful but after the different corrections, snow depth changes could be measured with an accuracy of less than 1 mm in

most positions in the main test section (Fig. 3.4). Therefore, the Kinect is well adapted to quantify erosion and deposition in the wind tunnel. Even so, some problems remain. Settling makes it difficult to match SMP force profiles to the Kinect snow depth data if there was more than one wind period with drifting snow before the SMP was acquired. These SMPs had to be neglected in the current study. In many experiments, there was only one short wind period with drifting snow at the beginning of the experiment. Often, the wind was cut off as soon as the depositions in the test section buried the artificial obstacle and the subsequent measurement periods were either without drifting snow or even without wind. In these cases, the decrease of the snow depth measured by the Kinect after the first wind period is the settling and it can be corrected with a simple offset because the settling during the short period with drifting snow can be neglected. If saltation continues in subsequent wind periods, it is unclear how much of the snow depth change is due to erosion, deposition or settling. Maybe a simple model could be used to "reverse" the settling in these cases or the settling could be measured independently of the Kinect. It can be assumed that settling is mostly caused by the compaction of the undisturbed snow below the wind crust because the crust is usually a lot denser. Therefore, the depth evolution of the interface between the wind crust and the undisturbed snow would be a good indicator of settling except if an existing wind crust is completely eroded again.

During our experiments, no hardening occurred when snow was being eroded (Fig. 3.5). There are only 17 SMPs in the "Erosion" group. Most likely, more measurements were made after erosion but this plot only contains those for which we were absolutely sure that there was only erosion before the SMP was acquired. The distribution of these 17 measurements is very narrow and the conclusion that saltation can only form wind crusts if no snow is eroded can therefore be made. Nevertheless, we cannot generally conclude that erosion never leads to hardening of the remaining snow. The 17 SMPs in Fig. 3.5 measured the effect of erosion on new snow. The effect of erosion may be different on older, already wind-influenced snow. We acquired many SMPs were a wind crust was first deposited and then partly eroded again. These measurements could theoretically be used to study the effect of erosion on old snow. However, it is very difficult to differentiate between the effects of the initial deposition and the subsequent erosion. The SMPs before and after erosion were necessarily acquired at different positions. The spatial variability in our wind tunnel is too high to attribute hardness changes between those SMPs to erosion. Hardness changes between SMPs are only meaningful if the snow cover was homogeneous before the change occurred. We can test the effect of erosion on new snow because the initial snow cover is homogeneous. We would therefore need an equally homogeneous old snow cover. Maybe a slab of dense, homogeneous snow could be prepared in the cold lab and then be placed in the wind tunnel's test section or old snow could be sieved into the wind tunnel. In our opinion, the main factor determining whether erosion has a hardening effect on the remaining snow is the erosion rate. In the limiting case where saltation causes neither deposition nor erosion, i.e. the two are in equilibrium, it can be expected that the continuous impacts of particles at the surface will eventually harden the snow. Then, if snow is eroded only slowly, it is very likely that

the remaining snow is still being hardened because most particles only impact on the surface without removing any snow. The main reason why erosion had no effect on new snow is probably because the snow was eroded too quickly. For older snow consisting of smaller, already wind-influenced particles, erosion may be slower and could have a hardening effect on the remaining snow. It is likely that the effect increases as the angle of impact becomes more perpendicular. This could be how the extremely hard windward edges of zastrugi are formed. The formation of zastrugi has been described in detail by e.g Doumani (1967), Filhol and Sturm (2015) and Goodwin (1990). The potential hardening effect of erosion is not discussed, however.

We only observed wind crusts after snow had been deposited but not all depositions were hard (Fig. 3.5). An important factor determining the hardness of a deposition of wind-blown snow is whether the snow was deposited in a wind-exposed or wind-sheltered area. Our results show that the snow is hardened more on the windward side than on the leeward side of an obstacle (Fig. 3.6). However, the hardening on the windward side during experiments without spontaneous drifting (Fig. 3.6B) is comparable to the hardening on the leeward side during experiments were saltation occurred spontaneously (Fig. 3.6A). This suggests that environmental conditions such as wind speed, air temperature and the properties of the snow cover have an effect on wind crust formation as well. Furthermore, windward and leeward of an obstacle is a rather poor classification because the wind exposure of a given position can change dramatically as snow is being deposited and eroded at and upwind of this position. The combination of Kinect and SMP data enables us to correlate the SMP force at a given penetration depth with the wind exposure parameter Sx at the corresponding time. This scatterplot of Sx against force (Fig. 3.9) gives a more complete picture of the influence of wind exposure on wind-packing than the windward/leeward boxplots in Fig. 3.6. There appears to be a transition at Sx≈0.25. No significant hardening occurs at Sx>0.25 and below this value, any amount of hardening seems possible. The regime shift at Sx≈0.25 is valid in the wind tunnel and it is unclear whether the same value is relevant in real terrain at the catchment scale. In such a case, digital elevation models typically have a resolution between one and several tens of meters and the elevation differences are much higher than in the wind tunnel. The settings to calculate Sx have to be adapted to the larger scale and this could lead to different values.

The variability in wind-exposed areas can be partly explained by the deposition rate (Fig. 3.10). Deposition in wind-exposed areas only leads to significant hardening if the snow is deposited slowly enough. Rapidly deposited snow remains relatively soft. This could be observed on the windward side of the obstacle where snow was often deposited very quickly at the beginning of experiments. It appears that there is not enough time to harden the snow if it is deposited too quickly. However, there are also many points with a low deposition rate and a low SMP force. Slow deposition in a wind-exposed area is still not a sufficient condition to form a hard wind crust.

The parameters Sx and deposition rate explain roughly half of the observed variability of wind crust hardnesses. The remaining variability is difficult to explain with our data. There are small positive correlations between the SMP force and the density and tem-

perature of the fresh snow. This shows that the initial conditions have an effect on the resulting wind crust. However, adding these two parameters to the multilinear regression increases the adjusted $R^2$ by only four percentage points to 51%. We attempted to add meteorological parameters such as wind speed, air temperature and air humidity to the linear model. No clear and robust trends could be found between the SMP force and those parameters. The main reason for that is probably the narrow range of meteorological conditions in the wind tunnel during the experiments. Another parameter that could be important is the saltation intensity or the drifting mass flux. So far, this was not measured in the wind tunnel but this could maybe be done with a particle counter. We would expect a positive correlation between the saltation intensity and the hardness. This could explain the differences in SMP hardness change between the experiments with and without spontaneous saltation (Fig. 3.6). Another parameter that was not discussed so far is time. As described in section 3.2, the durations of wind periods varied a lot. However, at the time scale of hours there was no relationship between the hardness of snow and the duration of experiments.

Up to recently, no quantitative studies on wind-packing were available and which physical processes are at work was a matter of speculation (e.g. Alley, 1988; Benson, 1967; Kotlyakov, 1966; Schytt, 1958; Seligman, 1936). Sommer et al. (2017a) could show that saltation is necessary. This excludes some of the proposed processes and means that fragmentation of snow crystals in the saltation layer and subsequent sintering could be the dominating process. In this study, we now saw that the wind exposure during deposition is important and observed wind crusts after only a few minutes of wind. This suggests that the impact of snow particles during deposition could be another important hardening process. Sintering, on the other hand, appears less important since we did not observe increasing hardnesses with increasing experiment duration. However, it is important to keep the relevant time scales in mind. While the fragmentation happens as the snow particles are still mobile and the hardening due to the impact momentum happens at the moment of deposition, sintering begins only afterwards. At the time scale of hours, it could be that the hardening due to sintering is masked by the hardening due to deposition. It is possible that at a time scale of days, the hardness would continue to increase due to sintering of the previously deposited snow.

Even if no quantitative statements can be made about the importance of the different processes based on our results, they could help to improve snow cover models such as Snowpack or Crocus (Groot Zwaaftink et al., 2013; Vionnet et al., 2012) or earth system models (Kampenhout et al., 2017). Such models contain simple parameterizations to account for the hardening due to wind. With our results, it is not possible to replace the parametric model with a physical model of wind-packing but the necessary conditions that we found could be implemented.

Wind slabs deposited onto leeward slopes are a major avalanche danger (e.g. Schweizer et al., 2003). Our result, that snow deposited in wind-sheltered areas remains soft, does not contradict that. The observed, small hardness increase is enough to form a cohesive layer. The existence of such a cohesive slab is the main condition for the formation of a slab avalanche. The hardness of the overlying slab influences fracture initiation and

propagation in the weak layer and therefore how easily an avalanche can be triggered. In fact, as the hardness of the slab increases, it becomes more difficult to initiate a fracture but once initiated, it propagates more easily (Herwijnen and Jamieson, 2007). Our results suggest that soft wind slabs are prevalent shortly after drifting-snow events and that hard wind slabs may become more relevant as sintering hardens the deposited slab.

## 3.5. Conclusions

In this study, we looked at the effect of saltation on wind-packing through the combination of SMP and Kinect data. Several necessary conditions for the formation of a wind crust could be identified. There has to be deposition of snow in a wind-exposed area and the rate of deposition has to be low. However, these conditions are not sufficient and about half of the observed hardness variability cannot be explained. Furthermore, the results do not allow quantitative statements about which physical processes are at work or how saltation affects old snow. More experimental work is necessary to answer these questions. Nevertheless, the fact that about half of the variability could be explained may allow for a rudimentary parametrization in larger-scale models.

## Disclosure/Conflict-of-Interest Statement

The authors declare that the research was conducted in the absence of any commercial or financial relationships that could be construed as a potential conflict of interest.

## Author Contributions

CS did most of the research and wrote the manuscript. ML and CF conceived and supervised the project, provided guidance, helped with the analysis and revised the manuscript.

## Acknowledgments

# 4. Investigation of a wind-packing event in Queen Maud Land, Antarctica

## Authors

Christian G. Sommer[1,2], Nander Wever[1,2], Charles Fierz[1], Michael Lehning[1,2]
[1]WSL Institute for Snow and Avalanche Research SLF, Davos, Switzerland
[2]CRYOS, School of Architecture, Civil and Environmental Engineering, EPFL, Lausanne, Switzerland

## Publication

## Abstract

Surface snow in polar and mountainous regions is often mobile and this mobility influences surface mass balance and isotopic composition before final deposition, which is poorly understood thus far. In December 2016 and January 2017, during a field campaign in Queen Maud Land, Antarctica, a snowfall and subsequent drifting snow events were recorded by meteorological and drifting snow stations. Associated small-scale topography changes and snow hardness changes were measured by terrestrial laser scanning and with a SnowMicroPen. The polar field measurements show that drifting snow is necessary for wind-packing and thereby confirm previous findings from wind tunnel experiments. Furthermore, it is quantitatively demonstrated how the reorganization of fresh snow into barchan dunes during subsequent drifting snow events is accompanied by significant increases in surface hardness at all locations on the dune. These results form an important step in understanding how drifting snow links precipitation to deposition via snow hardening.

## 4.1. Introduction

Wind-packing of snow is the process through which wind hardens snow and forms wind crusts and slabs at the surface. Fierz et al. (2009) describe a wind crust as a hard, thin, irregular layer and a wind slab as a thicker, dense layer on leeward slopes. Wind-packing and its results have been described qualitatively in many studies especially in Antarctic literature (e.g. Benson, 1967; Endo and Fujiwara, 1973; Kotlyakov, 1966; Schytt, 1958; Seligman, 1936). The hardening of the snow is also related to the formation of surface features such as dunes and zastrugi as described in Filhol and Sturm (2015). Wind-packing in Antarctica is relevant because of its influence on the surface mass balance. In fact, snow is often only permanently deposited through wind hardening. Without it, the snow remains mobile and may be redeposited elsewhere (Groot Zwaaftink et al., 2013). Snow may then also be immobilized by other processes such as metamorphism or melting and refreezing.

Recently, wind tunnel experiments were conducted to study wind-packing in more detail (Sommer et al., 2017a; Sommer et al., 2018a). It was found that no wind crust or slab forms without drifting snow, that erosion had no hardening effect on fresh snow and that deposition only led to hardening in wind-exposed areas. A Microsoft Kinect sensor (Mankoff and Russo, 2013) was used to quantify erosion and deposition. Two parameters derived from this data, the wind exposure parameter Sx (Winstral and Marks, 2002) and the deposition rate, could explain almost half of the observed variability of snow hardness. Sx is defined as the upwind slope angle between the point of interest and the shelter-giving point, which is the point that maximizes this upward angle. Sx describes how sheltered or exposed a position is based on the upwind terrain. The hardness of snow was measured with a SnowMicroPen (SMP), a precise, constant-speed penetrometer (Schneebeli and Johnson, 1998; Proksch et al., 2015).

In December 2016 and January 2017 we were able to capture a snowfall and subsequent drifting snow events in Antarctica. The observed period resembled the previous wind tunnel experiments in that the sequence of events was the same: a snowfall without much wind, a period with wind but without a significant amount of drifting snow and finally a strong drifting snow event. Comparable measurements to those in the wind tunnel were performed. The Antarctic event is presented in this paper and we show how the observations compare to the wind tunnel results. An event as described below has not yet been observed in such detail. To our knowledge, simultaneous SMP and terrestrial laser scanning measurements of a barchan dune have never been performed. The results are expected to give new insight into how snow accumulation may happen in polar environments.

## 4.2. Data and Methods

The event was observed close to the Princess Elisabeth Station, which is located about 220 km inland in Queen Maud Land at an elevation of 1392 m above sea level (71°57' S and 23°20' E). Pattyn et al. (2010) studied the glacio-meteorological conditions in

the vicinity of the station. They observed mean monthly temperatures between about -25 and -8°C. The coreless winters are rather mild. The predominant direction of the katabatic winds is from the east. Mountains protect the site from very strong winds. The mean 2 m wind speed at the station is 6 m s$^{-1}$. The station is located in a low mass balance area. To the east of the site, the surface mass balance was slightly positive and to the west it was slightly negative. Snow depth changes derived from stake length measurements varied between -0.05 and 0.25 m a$^{-1}$ (Pattyn et al., 2010).

The period of interest for this experiment was from 18 December 2016 to 13 January 2017. During that time, meteorological data is provided by two identical drifting snow stations. Each station is equipped with two Young wind monitors (HD, Alpine Version, model 05108-45), a Campbell Scientific (CS) CSAT3B sonic anemometer, a CS SR50A ultrasonic snow depth sensor, a CS CS215 temperature and relative humidity probe, an Apogee Instruments SI-111 infrared radiometer to measure the snow surface temperature and a Niigata Electric Snow Particle Counter (SPC, model SPC-95, Sato et al. (1993)) measuring the number and size of drifting particles. The stations are each powered by a solar panel and a small wind turbine. The SPC data is available with a temporal resolution of one second. The mass flux measured by the two SPCs was averaged, filtered with a moving window to create one-minute data and then integrated to compute the cumulative mass flux. The measurement heights of the two SPC sensors varied between 13 and 24 cm above the snow surface during the observed period. The sensors may therefore have been above what Nemoto and Nishimura (2004) call the transition height between saltation and suspension. The actual drifting snow mass flux can therefore be expected to be significantly higher than what is measured by the SPCs. Nevertheless, if the measured mass flux is zero, there is most likely no significant snow transport. As Nemoto and Nishimura (2004) showed, the mass flux follows a height profile and does not suddenly drop to zero above a so-called saltation layer. Here and in the following, "drifting snow" always refers to snow transport by saltation.

The measurements of air temperature, relative humidity, snow depth and snow surface temperature have a temporal resolution of 10 minutes. This data was also averaged between the two stations. The CSAT and Young anemometer data has a temporal resolution of 10 Hz and one minute respectively. Due to data logger problems, there are gaps up to several days long in the time series of the different wind speed sensors. Therefore, all the CSAT and Young data was combined into a single wind speed time series with a temporal resolution of one minute. The six wind speed sensors were installed at heights above the surface between 1.1 and 3.6 m. The wind speeds measured by the Young anemometers at two different heights at each station were used to estimate the surface roughness under the assumption of a logarithmic wind profile. The resulting median surface roughness length of 7.5 mm was used to adjust all wind speeds to a height above the surface of 2 m, again assuming a logarithmic wind profile. The snow depth measured at the stations varied by less than 15 cm during the period of interest. These small variations were neglected for the wind speed adjustment. The adjusted 2 m wind speeds were then averaged.

Digital Surface Models (DSM) of the terrain around the two stations were acquired

on nine days with a Riegl VZ-6000 Terrestrial Laser Scanner (TLS). This scanner has a maximum range of 6 km and works in the near infrared, making it specifically adapted to scan snow and ice surfaces. The intrinsic accuracy and precision are 15 mm and 10 mm respectively (Riegl, 2017). The angular measurement resolution is better than 0.0005°. The minimum operating temperature is given as -20°C (Riegl, 2017). The minimum air temperature during the investigated period was -15°C. The scanner was positioned about 5 m above the surface on a tripod on top of a container. This elevated position helped to increase the field of view and to decrease the incidence angle, which is the angle between the laser beam and the surface normal. Even so, the incidence angle was very high and this led to many measurement shadows, especially at higher ranges. In this case, the maximum useful range was about 250 m. The range of scanned azimuth angles was about 230° leading to a scanned area of about 125000 $m^2$. At 250 m, the horizontal resolution of the point clouds is about 20 cm. The different scans were registered (adjusted) to each other using 14 reflectors as tie points. The absolute position of these reflectors was determined with differential GPS and the scans could therefore be transformed into global coordinates. The UTM system (zone 34 south) was used as the global coordinate system and the position of the differential GPS base station was used as the origin. To increase the precision of the registration, the scans were first registered between each other before transforming these project coordinates into the global coordinates. In each scan, between 8 and 11 of the 14 reflectors were found and the standard deviation between these tie points is 1.5 cm averaged over all scans. The highest standard deviation is below 2 cm. The transformation into global coordinates is a little less precise with a standard deviation of below 5 cm. The standard deviation between tie points of different scans is normally a good indicator of the precision of calculated snow depth changes based on these scans. In this case, however, we observed some patterns in some of the scans that are most likely due to very small changes in the inclination of the scanner during a scan. Fig. 4.1 shows the difference between the two scans where the strongest patterns appear. These two scans were acquired on 6 January and 11 January 2017 and since there was virtually no drifting snow in that period (see also Fig. 4.4), the difference between them should be close to zero. As can be seen, the patterns have the shape of sectors and become stronger with increasing range. The patterns have a magnitude of 10 cm or ± 5 cm at a range of 250 m. This corresponds to a change in inclination of about 0.02°. Theoretically it would be possible to correct such inclination changes since roll and pitch angles of the scanner are continuously measured during a scan. However, the noise in this data was often on the order of about 0.1° and sometimes as high as 0.5°. These inclination measurements can therefore not be used to correct the patterns in our scans. An inclination change on the order of 0.02° is very small and normally not a problem. In our case, however, even such small inclination changes lead to significant patterns and therefore a decrease of the accuracy. This is due to the very high incidence angles inherent in scanning a flat surface with a TLS. Fig 4.2 shows an overview of the study site, showing the locations of the drifting snow stations in the scanned area. One station is at the origin of the used coordinate system, the other station is about 350 m away.
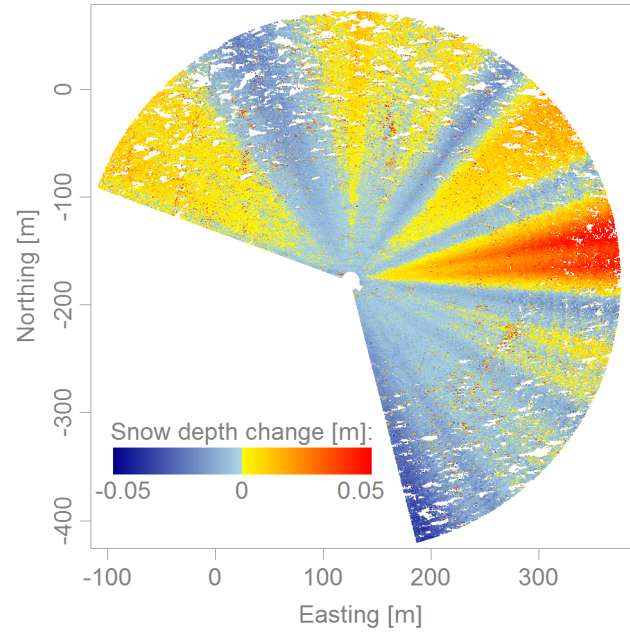
**Figure 4.1:** Difference between the scans acquired on 6 January and 11 January 2017. Patterns in the shape of sectors with a magnitude of up to 10 cm are visible. These patterns are caused by small inclination changes of the scanner.

454 SMP profiles were acquired on 11 different days over a period of 24 days. The same processing as in Sommer et al. (2017a) was applied to them. In short, each profile is reduced to a characteristic number which is the 90% quantile of the force in the topmost centimeter of the snowpack. This variable, henceforth named SMP hardness, is well suited to detect hardness changes at the surface. The positions of all SMP measurements was acquired by the SMP's internal GPS but the accuracy of this positioning seems to be on the order of several meters. 350 of the SMPs were acquired in transects or rectangles that were marked with bamboo poles and the SMP positions relative to the poles were determined with a measuring tape. The bamboo poles are visible in the TLS scans, allowing for an accurate positioning of these SMP measurements with respect to the DSMs. For these SMPs, the DSMs can therefore be used to calculate snow depth changes and Sx values. 104 other SMPs were made to assess the microstructure of the snow, follow the snow settling and support other measurements. They cannot be accurately positioned in the DSMs, due to the low GPS accuracy and the absence of other positioning methods. In the following, they are taken into account where possible. All SMP measurements were performed in the area between the drifting snow stations. Fig. 4.2 shows a rectangle within which all SMP measurements were taken. Fig. 4.3 shows a detail of this area with symbols marking all SMP positions. In this area, the TLS point clouds have a horizontal resolution of 5 cm or better due to the lower range. A 5 cm octree filter was applied to the scans to even out the resolution at this value and the resulting point clouds were used to calculate snow depth changes and Sx at the SMP positions. As mentioned above, the uncertainty of the registration was about 1.5 cm. To this we have to add the uncertainty due to the radial patterns shown in Fig. 4.1. Based on Fig. 4.1, we assume a maximum inclination change of 0.02°. All (accurately known)
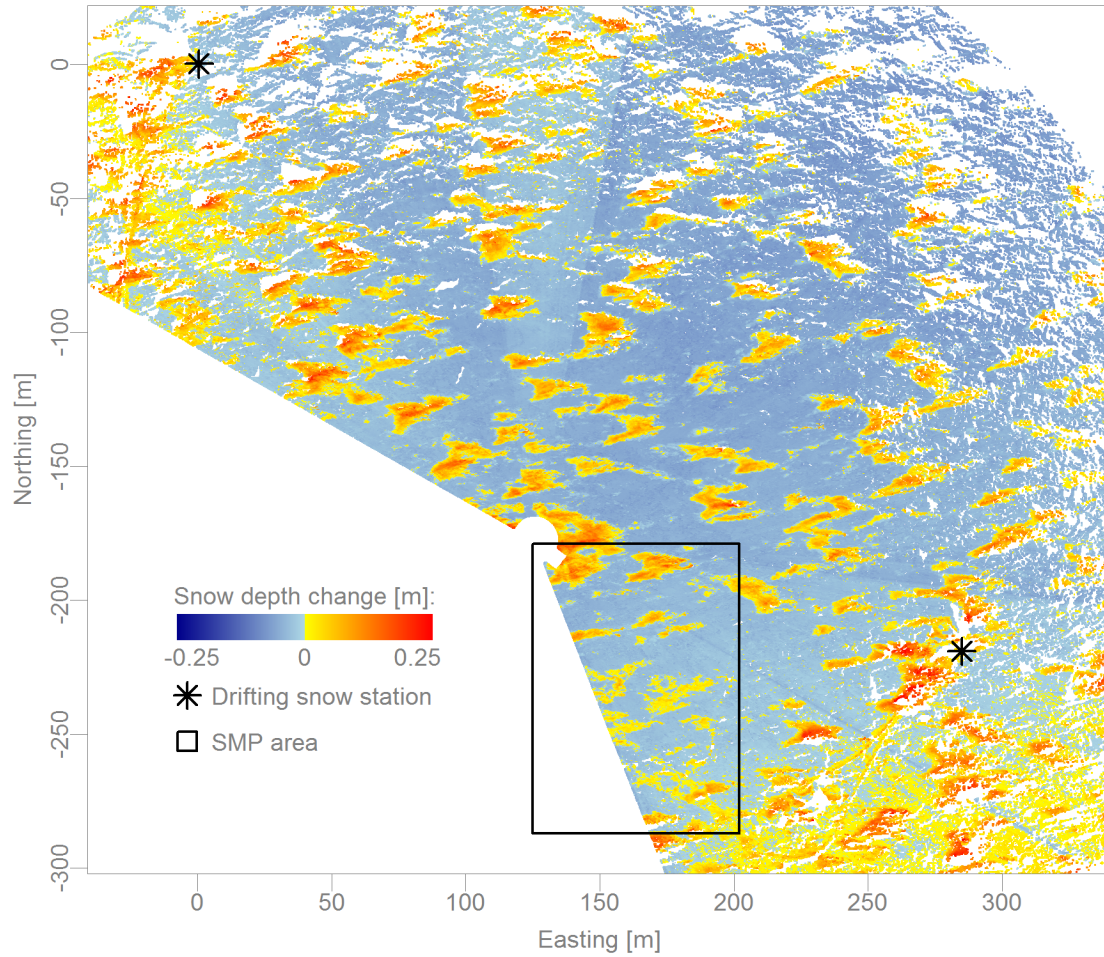
**Figure 4.2.:** Overview of the study area. The asterisks show the location of the drifting snow stations. All SMP measurements were acquired inside the rectangle. A detailed view of this area is shown in Fig. 4.3. The colors show the snow depth changes between the scans acquired on 18 December 2016 and 11 January 2017. Barchan dunes are visible in the whole area.
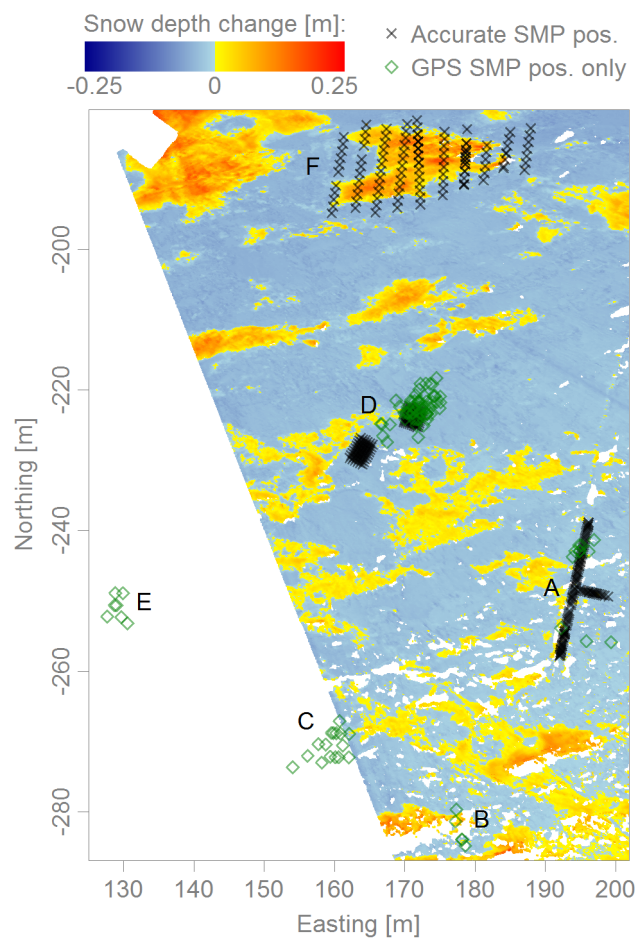
**Figure 4.3:** Detail of the area inside the rectangle in Fig. 4.2 showing all SMP positions. Black crosses show accurately known SMP positions determined with bamboo poles and measuring tape and green diamonds show the less accurately known SMP positions where only the GPS position is available. The letters are used to mark the different groups of SMPs (compare to Fig. 4.4D). Group A is a T-shaped transect, group D consists of three rectangular grids and group F are ten transects in the area of a barchan dune.

SMP positions have a range below about 100 m. At this range, the vertical snow depth uncertainty due to the inclination uncertainty is $\pm$ 2 cm. For the calculated snow depth changes, the uncertainties of the registration and inclination are combined and we can therefore expect an accuracy of $\pm$ 3.5 cm or better.

## 4.3. Results

### 4.3.1. Overview of the investigated period

Figure 4.4 gives an overview over the meteorological conditions during the studied period. Figure 4.4A shows the averaged 2 m wind speed, Fig. 4.4B the air temperature and the snow surface temperature, Fig. 4.4C the cumulative drifting snow mass flux and the mass flux itself and Fig. 4.4D the SMP hardness, all as a function of time. Figure 4.4D also shows when TLS scans were acquired.

Between 18 December and the begin of the snowfall period (light red in Fig. 4.4), the wind speed was high, exceeding 8 m s$^{-1}$ during three periods. The SPC data shows that there was drifting snow during those three periods. The mass flux or drifting snow intensity was rather low but each of the three periods was several hours long leading to a significant overall cumulative mass flux increase of 5.5 kg m$^{-2}$. During the snowfall period and afterwards until 27 December, the wind speed was below about 6 m s$^{-1}$ and almost no drifting snow was observed. There were three very small drifting snow events on 24 and 25 December but the cumulative mass flux barely increased in that period. The first significant drifting snow event happened on 28 December. The wind speed was between 7 and 8 m s$^{-1}$ and the cumulative mass flux increased by 0.7 kg m$^{-2}$. The main drifting snow event (light blue in Fig. 4.4) took place on 30-31 December. The wind speed exceeded 10 m s$^{-1}$ and the cumulative mass flux increased by 28 kg m$^{-2}$ which is 40 times more than the increase during the small drifting snow event on 28 December. The mass flux shows three peaks with very intense drifting snow and calmer periods in between. There were a few more drifting snow events after the main one, most notable of which is the event on 2 January. The cumulative mass flux increased by 0.7 kg m$^{-2}$ during this event and it was therefore very similar to the event on 28 December. On 2 January, however, the drifting snow intensity was lower and the duration of the event longer. From 3 January onwards, there were only very small drifting snow events and the cumulative mass flux remained virtually constant. The wind speed after the main drifting snow event was often below about 6 m s$^{-1}$ but there were some peaks where the wind speed exceeded 7 m s$^{-1}$ and some periods where no wind speed data is available at all.

The air temperature often varied between about -15 and -4°C during the day, except between 23 and 26 December when daytime air temperatures exceeded 0°C (Fig. 4.4B). The snow surface temperature was mostly below -5°C and always below -2°C. During the nights, the snow surface temperature often strongly decreased due to radiative cooling to minimum temperatures of as low as -23°C. Notable exceptions to this are the snowfall period and the main drifting snow event where the snow surface temperature closely
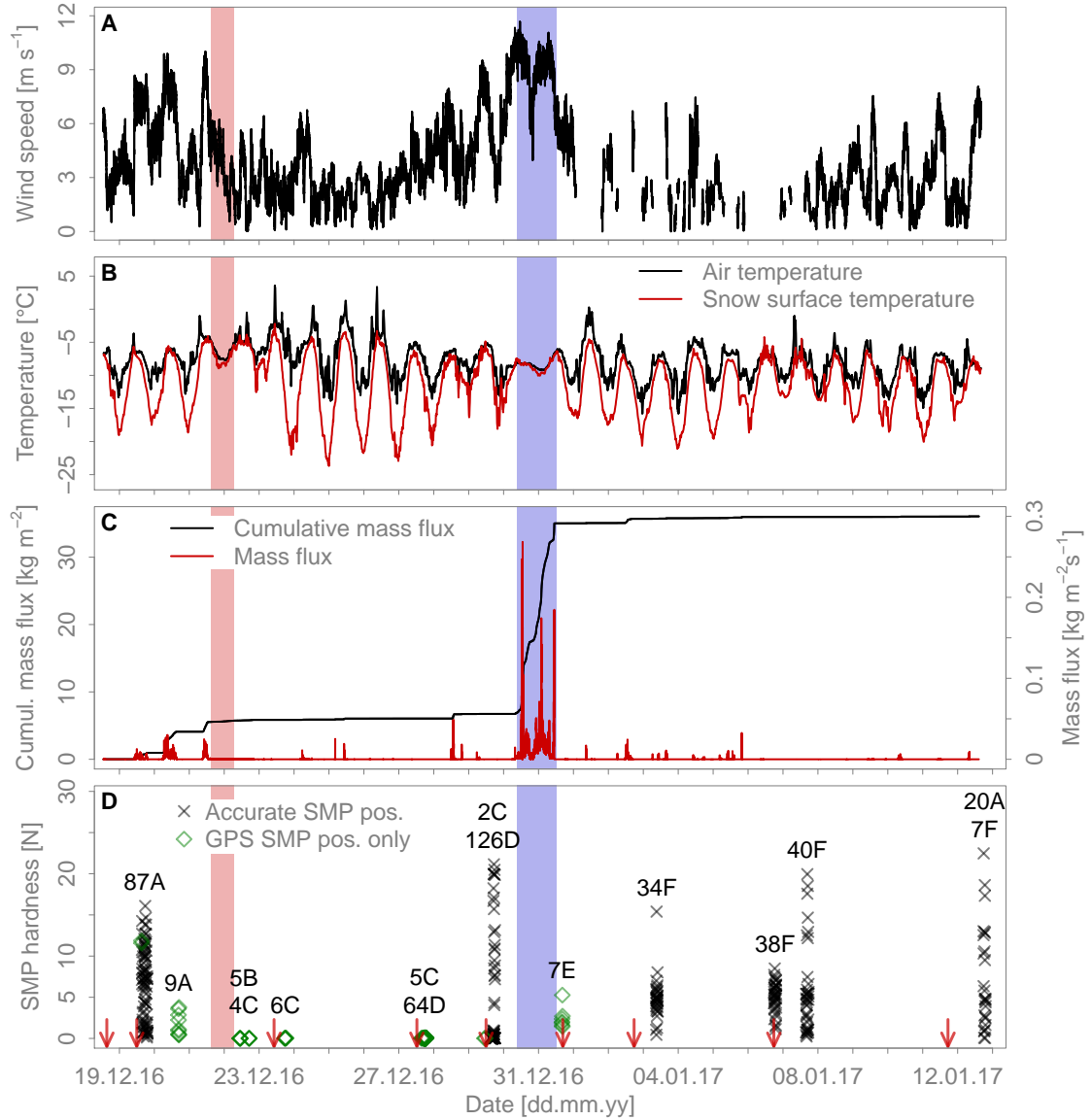
**Figure 4.4.:** Overview of the observed snowfall and drifting snow event. (A) shows the averaged 2 m wind speed, (B) the air temperature and the snow surface temperature, (C) the (cumulative) drifting snow mass flux and (D) the SMP hardness. Similarly to Fig. 4.3, SMPs with an accurately known position are shown with black crosses and SMPs where only the GPS position is available are shown with green diamonds. The codes (e.g. '87A') indicate how many SMPs were acquired on that day and in which group in Fig. 4.3 they are located. On several days, SMPs were acquired in two different groups. The snowfall period (light red) and the main drifting snow period (light blue) are highlighted. The vertical red arrows in (D) show when TLS scans were acquired.

followed the air temperature.

Two TLS scans were acquired before the snowfall period, three scans were performed between the snowfall period and the main drifting snow event and four more scans were acquired after the main drifting snow event (Fig. 4.4D). The DSM of 18 December is used as a reference to calculate subsequent snow depth changes. The scan of 19 December has a lower resolution and was therefore not used. Snow depth change maps were calculated in the area containing the accurately known SMP positions (see Fig. 4.3). Unfortunately, there is no scan available just before the snowfall event. We therefore do not know how the drifting snow events on 19-21 December changed the surface. This complicates the interpretation of calculated snow depth change maps. For snow depth changes relative to 18 December it is difficult to know whether the changes occurred before, during or after the snowfall period. Comparing the scans of 18 December and 23 December results in an average snow depth increase of 6.6 cm. The logbook notes about 10 cm of fresh snow on 22 December and the drifting snow stations measured a snow depth change of about 9 and 10 cm. This could indicate that, on average, some snow was eroded during the drifting snow events before the snowfall. However, it is more likely that this difference is mainly due to the settling of the new snow. The values from the logbook and the drifting snow stations represent the situation directly after the snowfall period on 22 December. Due to some continuing light snowfall, which disturbs the laser pulses, a TLS scan could not be performed until 23 December. In 24 hours, the settling of low-density new snow can be considerable. This is supported by density measurements on these two days. The average density over the full new snow depth was measured three times on 22 December. The obtained values were 54, 60 and 65 kg m$^{-3}$, leading to a mean of 60 kg m$^{-3}$. On 23 December, the mean of five measurements of the average density increased to 72 kg m$^{-3}$. On 23 December, five density measurements each were furthermore performed close to the surface and close to the bottom of the new snow. At the surface the mean density was 67 kg m$^{-3}$ and at the bottom it was 121 kg m$^{-3}$. The three scans acquired between the snowfall period and the main drifting snow event are all very similar. The differences between these scans are all within $\pm$ 2 cm and therefore within the uncertainty limit. The four scans acquired after the main drifting snow event are, for the most part, also similar between themselves. They are, however, significantly different from the scans acquired before the main drifting snow event and clearly show the formation of barchan dunes uniformly distributed in the study area. The maps in Figs. 4.2 and 4.3 show the difference between the scans of 18 December and 11 January as an example. Thanks to the scans on 29 and 31 December we can be certain that the barchans formed during the main drifting snow event.

The 454 SMPs were acquired on 11 different days. On most days, the hardness at the surface varies between very soft with SMP hardnesses close to 0 N and very hard with SMP hardnesses above 15 N (Fig. 4.4D). Seen over the whole period, there is therefore no clear overall hardening or softening trend. The time evolution of the SMP hardness is relatively constant. The notable exceptions to this are of course the SMPs acquired after the snowfall period between 22 and 27 December, which all have very soft snow at the surface. On 20 and 31 December the range of measured SMP hardness is also small.

This could be due to the small sample size on these days. Even after the main drifting snow event, there are many SMPs with very soft snow at the surface. This shows that drifting in itself is not a sufficient condition to form a wind crust.

To analyze the effect of wind on the hardness of snow, we only consider snow that was deposited during or after the snowfall period. Depositions that formed during drifting snow events after the snowfall period can be expected to consist mostly of fresh snow due to the large supply of this driftable snow. For such depositions, it is then possible to calculate a SMP hardness change since the hardness of the fresh snow is known and homogeneous. For this reference SMP hardness, we use the average SMP hardness of the SMPs acquired on 22 December (Fig. 4.4D). This average is 0.01 N. The standard deviation of these SMPs is 2.8 mN. The difficulty lies in determining which SMP locations lie in a newly formed deposition. At the accurately known SMP positions, snow depth changes can be calculated. But, the uncertainty of $\pm$ 3.5 cm must be kept in mind here. Furthermore, due to the drifting snow events that occurred between the reference scan was acquired on 18 December and the begin of the snowfall period, it is still difficult to determine if a deposition formed before or after the snowfall period. An exception to this are the barchan dunes for which it is clear that they formed during the main drifting snow event. For the inaccurately known SMP positions, snow depth changes cannot be calculated and it is theoretically impossible to know if there is new or old snow at the surface. For the SMPs acquired between 22 and 27 December, we assume that there is new snow at the surface because the hardness is very low and very homogeneous with a mean hardness of 29 mN and a standard deviation of 18 mN for all 84 measurements (Fig. 4.4D).

SMPs where snow was eroded are difficult to analyze. Even at SMP positions where, due to the TLS scans, it is clear that snow was eroded, a SMP hardness change cannot be reliably calculated. This is because it is very difficult to know how hard the snow was at a specific location before the erosion took place. As can be seen in Fig. 4.4D, the variability of the SMP hardness can be very high. A previous SMP measurement that was acquired close-by does also not guarantee a similar hardness. For these reasons, we do not analyze SMPs at locations with erosion in the following.

At first glance, the small drifting snow event on 28 December appears to have had a very big influence on the hardness. There was only soft snow on 27 December and on 29 December the hardness reaches 21 N (Fig. 4.4D). At all accurately known SMP positions there is at least 3.5 cm more snow than on 18 December. As pointed out before, however, it remains unclear whether that snow was deposited before or after the snowfall period. 105 out of the 128 SMPs acquired on 29 December show a hardness below 1 N. The other 23 SMPs have a hardness above 4 N. Fig. 4.5 shows one of the rectangular SMP grids of group D (see Fig. 4.3). The 23 measurements with a SMP hardness above 4 N are shown as full circles. 20 of these points are located in the far right corner of the rectangle. The surface is visibly different in that triangle compared to the rest of the rectangle and erosion features are visible upstream of it. By visual inspection, it was observed at the time that recent erosion had exposed the old snow surface in some areas. In these places, the surface snow consisted of relatively coarse grains, similar to the snow surface
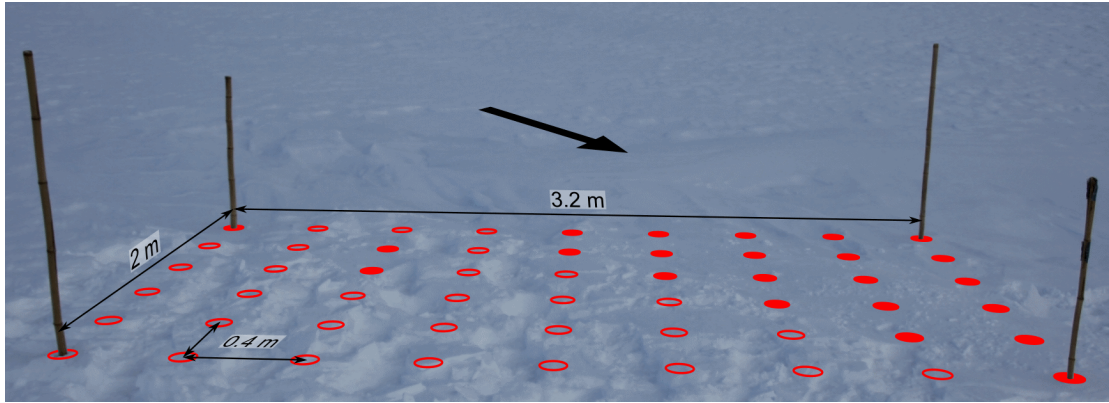
**Figure 4.5.:** View of one of the rectangular SMP plots in group D in Fig. 4.3 where measurements were performed on 29 December. The red circles indicate the regular grid with a spacing of 40 cm where SMP measurements were performed. Empty circles stand for a SMP hardness below 1 N and full circles for a SMP hardness above 4 N. All remaining 74 SMPs acquired on that day show a SMP hardness below 1 N. The arrow shows the approximate wind direction based on the erosion features visible behind the rectangle.

before the snowfall period. The most likely explanation is that a deposition formed in this area during the drifting snow events on 19-21 December and that the new snow there was eroded during the drifting snow event on 28 December. Based on the visual observations, we therefore consider the 20 SMPs in the triangle to have old snow at the surface. Consequently, they will not be considered in the following. The remaining 3 SMPs with a hardness above 4 N are kept.

SMPs were acquired on five days after the main drifting snow event (Fig. 4.4D). The positions of the SMPs acquired on 31 December are not precisely known and they are therefore not further analyzed. On 3, 6 and 7 January the SMPs were acquired in group F in the area of a barchan dune. On 12 January, 7 more measurements in group F were performed and 20 in group A. At all 20 positions in group A, the snow depth change between 18 December and 11 January is within the uncertainty range. In the following, we will therefore concentrate on the SMPs in group F around the barchan dune. We know that the barchan dune formed after the snowfall period, specifically during the main drifting snow event and for many of these SMP positions, the snow depth change is significant. In fact, the SMPs in group F were acquired closest to the TLS scan position at a maximum range of 63 m. For this group, the uncertainty due to the inclination changes can therefore be assumed to be only ± 1.25 cm. Consequently, we consider all SMPs in group F with a snow depth change above 2.75 cm to have new snow at the surface. To calculate the snow depth changes, the DSM from 2 January was used for the SMPs from 3 January, the DSM from 6 January for the SMPs from 6-7 January and the DSM from 11 January for the SMPs from 12 January.

## 4.3.2. Time evolution of the hardness

**Figure 4.6:** Time evolution of the SMP hardness for all SMPs with snow at the surface that was deposited during or after the snowfall period. The numbers below each boxplot indicate for each day how many SMPs were acquired in such deposition areas. The numbers in parentheses indicate how many SMPs were acquired in total on each day. The boxes show the first and third quartiles and the length of the whiskers is 1.5 times the interquartile range at most. The SMPs acquired after the main drifting snow event are color-coded based on when they were acquired. These colors are used again in Figs. 4.10, 4.11 and 4.12.
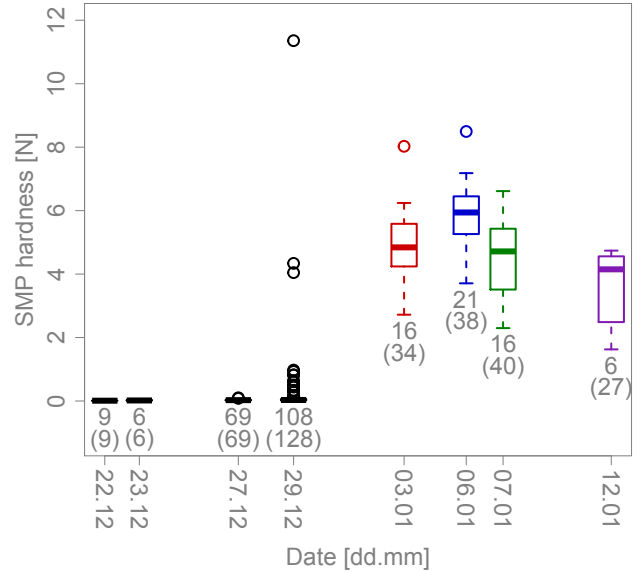


Fig. 4.6 shows the SMP hardness in boxplots as a function of the measurement day and how many SMPs remain when only those with newly deposited snow at the surface are considered. In the time span between the snowfall period and the main drifting snow event, all SMPs are kept except for the 20 SMPs on 29 December where the old snow surface was exposed (Fig. 4.5). After the main drifting snow event, 59 SMPs from group F remain. The hardness of the snow remained very low between 22 and 27 December. Between 27 and 29 December, the hardness increased to up to 1 N at some points (not considering the three extreme outliers). Most SMPs, however, still have a very low hardness on 29 December. The median SMP hardness increased from 27 mN on 27 December to 32 mN on 29 December. All SMPs acquired after the main drifting snow event are significantly harder. There are some differences in the hardness distributions of the four measurement days after the main drifting snow event. The SMP hardness tends to be higher on 6 January than on 3 or 7 January. We use the Kruskal-Wallis test (Kruskal and Wallis, 1952) to determine if groups of SMPs differ significantly. This is a non-parametric test that determines if groups of data points belong to the same distribution. It can be used even if the data is not normally distributed or if the sample size is small. Kruskal-Wallis tests result in a p-value of 0.005 between 3 and 6 January and of 0.002 between 6 and 7 January indicating that these groups of SMPs differ significantly. The distributions on 3 and 7 January are very similar (p-value of 0.55). The SMPs on 12 January tend to be softer than those acquired on the other days but a sample size of six is very low. In the period from 3 January to 12 January, therefore, the hardness did not

increase further overall. If anything, it appears to have decreased a little but the sample sizes are probably too small for any emerging trends to be robust.

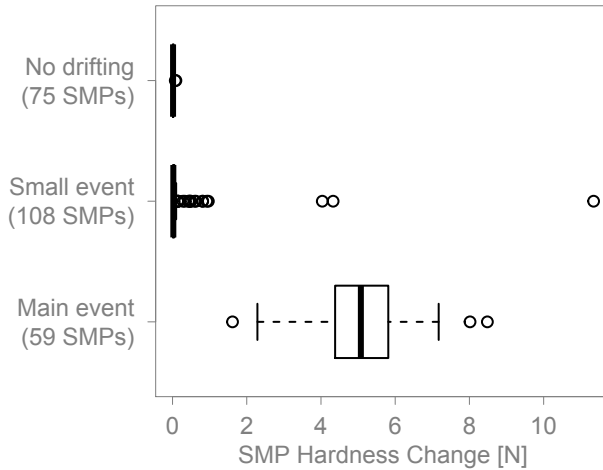### 4.3.3. Cumulative mass flux vs. SMP hardness change



**Figure 4.7:** Boxplots comparing the SMP hardness change for three groups of SMPs based on the amount of drifting that occurred previously. "No drifting" is defined by a cumulative mass flux below $0.25$ kg m$^{-2}$, "Small event" by a cumulative mass flux of $0.94$ kg m$^{-2}$ and "Main event" by a cumulative mass flux above $29.9$ kg m$^{-2}$. The boxes show the first and third quartiles and the length of the whiskers is $1.5$ times the interquartile range at most.

In Sommer et al. (2017a), groups of SMPs acquired after wind periods with or without drifting snow were compared and it was shown that no crust formed without drifting. Here, the cumulative mass flux is used as a measure of how much drifting occurred and it is used to group the SMPs into three categories. As a starting time for this cumulative mass flux, we use 22 December at 17:20. This is when the last SMP on 22 December was measured. As mentioned before, these SMPs are used as a reference to calculate SMP hardness change. The first group of SMPs ("No drifting") is defined by a cumulative mass flux below $0.25$ kg m$^{-2}$ at the time of the SMP acquisition, the second group ("Small event") by a cumulative mass flux of $0.94$ kg m$^{-2}$ and the third group ("Main event") by a cumulative mass flux above $29.9$ kg m$^{-2}$. The three groups are compared in Fig. 4.7. This plot shows the same SMPs as Fig. 4.6, i.e. only those with freshly deposited snow at the surface. The SMP hardness increased by up to $0.09$ N in the "No drifting" group but the median SMP hardness change is only $0.01$ N. The snow at the surface remained very soft. For the SMPs that were acquired after some drifting had occurred, the median SMP hardness change of $0.02$ N is low as well. However, 17 SMPs in this group are classified as outliers and have hardness increases up to $0.96$ N. Furthermore, there are three extreme outliers with hardness changes above $4$ N. The Kruskal-Wallis test comparing the "No drifting" and "Small event" groups confirms that they are different with a p-value of $0.003$ ($0.007$ if the three extreme outliers are not considered). The "Small event" group shows that drifting snow does not always create a hard wind crust. The SMPs acquired after an important amount of drifting occurred have SMP hardness increases between $1.62$ and $8.48$ N with a median of $4.89$ N.
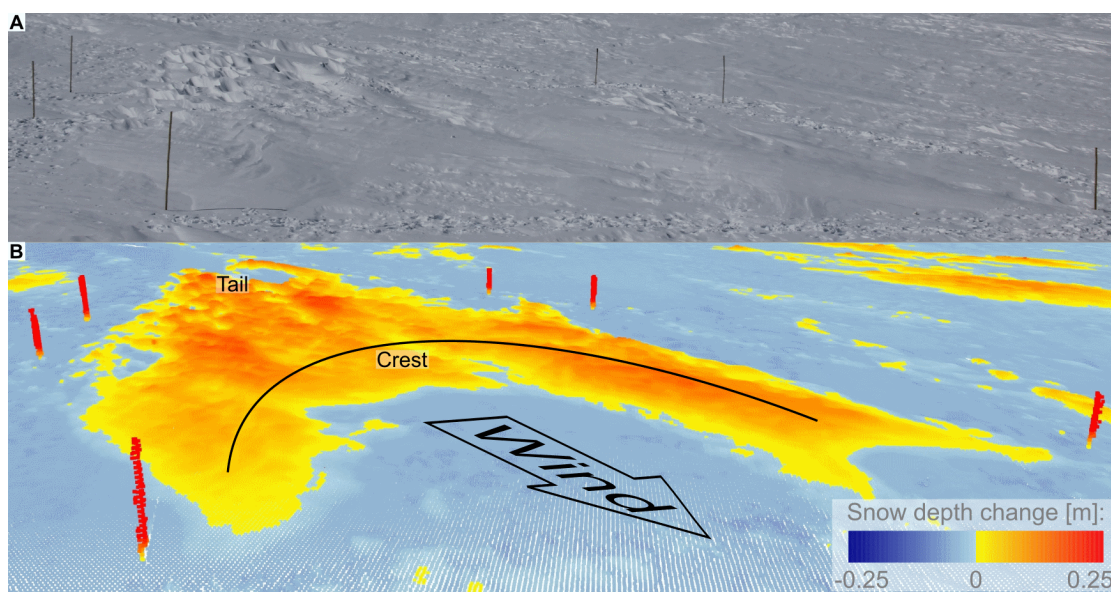
### 4.3.4. Barchan dune formation



**Figure 4.8.:** (A): View of a barchan dune from the scan position on 3 January. The bamboo poles mark the position of the three SMP transects in group F measured on that day. Note the zastrugi at the tail of the dune. (B) shows the snow depth changes between 18 December and 6 January from the same direction but at a little steeper angle. The arrow shows the direction in which the wind was blowing. The same nomenclature as in Filhol and Sturm (2015) is used here: The upwind end of the dune is called "tail" and the downstream end is called "crest". The dune is about 25 m long and 11 m wide.

Figure 4.8A shows a perspective view from the scan position on the container of the barchan dune where the SMPs in group F were acquired. Figure 4.8B shows the snow depth change between 18 December and 6 January from the same direction. The bamboo poles marking the SMP transects are clearly visible in both parts of the figure. It can be seen in Fig. 4.8A that zastrugi formed in the tail area (upstream end, see Fig. 4.8B) of the dune. Zastrugi are erosional surface features (e.g. Filhol and Sturm, 2015) meaning that the dune has already been partly eroded again. The dune is about 25 m long, 11 m wide and 15-20 cm high. With these dimensions, this dune is rather large in the horizontal and average in the vertical compared to values reported in the literature (Filhol and Sturm, 2015). It is clear from Fig. 4.8A how shallow the typical barchan dune is and that such a feature may not even be detectable by eye without differential snow depth measurements.

The dune formed during the main drifting snow event and was already partly eroded again during the same period. After the main drifting snow event, the dune was stationary. Fig. 4.9 shows the dune on the four scan days after the main drifting snow event and it can be seen that the position of the dune did not change anymore. Some snow
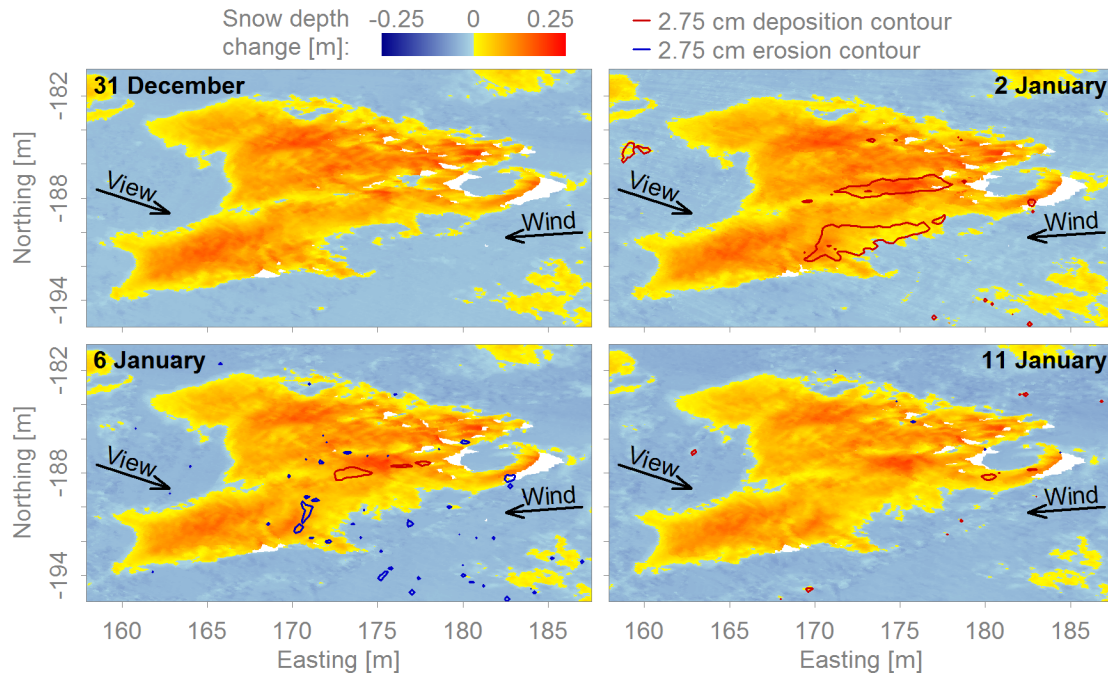
**Figure 4.9.:** Snow depth changes in the area of the dune between 18 December and each scan day after the main drifting snow event. The contour lines show where significant deposition or erosion took place since the previous scan day. The dune was stationary but there was some local deposition and erosion of snow. The arrows show the predominating wind direction during the main drifting snow event and the approximate view direction in Fig. 4.8.

was deposited on the dune between 31 December and 2 January. The contour lines in the plots show in which areas a significant amount of snow was deposited or eroded since the previous scan day. The contours were calculated based on the interpolation of the snow depth changes on a 20 cm grid. This leads to smoother contours compared to those calculated based on the original 5 cm data. Between 2 and 6 January there was some erosion and deposition but only in a few small areas. Between 6 and 11 January, there were virtually no changes. The white areas are measurement shadows caused mainly by the zastrugi in the tail area of the dune (Fig. 4.8).

### 4.3.5. Hardness variability on the barchan dune

Fig. 4.10 shows an overview of the SMPs in group F together with the snow depth changes between 18 December and 11 January. Group F consists of ten transects of SMPs that were acquired on 3, 6 and 7 January. Seven more SMPs were acquired on 12 January. These measurements as well as seven SMPs from 7 January were repeat measurements that were acquired close to clearly identifiable measurement locations from previous days. As mentioned above, the uncertainty range for the SMPs in group F is $\pm$ 2.75 cm. Circles mark the positions of SMPs where a significant amount of snow was deposited. The other SMP positions are marked with triangles. The size of the circles in Fig. 4.10 shows the SMP hardness change as a function of the position on the dune. The distribution seems to be mostly random but the snow tends to be slightly softer at the tail than further downstream on the dune. This can be seen more clearly in Fig. 4.11, which presents a scatterplot of SMP hardness change against the distance to the tail of the dune. The distance is measured in the main wind direction from the most upwind circle shown in Fig. 4.10. This reference SMP position is marked with a 'x' in Fig. 4.10. The main wind direction was estimated to be 86° based on the dune's orientation. The absolute values of the wind direction measurements of the drifting snow stations were not consistent between the different sensors but the data shows that the wind direction was quite constant during the main drifting snow event. The variations were within 20° and even within 10° during most of the event. The orientation of the dunes is therefore a reliable indicator of the main wind direction. To test the relationship between variables, we use Pearson's product-moment correlation, which is a measure of the linear correlation and Spearman's rank correlation as an non-parametric indicator of monotonic relationship. In the following, values related to Spearman's correlation are given in parentheses after the values related to Pearson's correlation. The correlation coefficient between the SMP hardness change and the distance to the tail is 0.40 (0.48). The correlation is significant with a p-value of 0.002 (0.0001). A linear regression results in a slope of 0.1 N m$^{-1}$. There appears, therefore, to be a positive trend between the SMP hardness change and the distance to the tail. This should not be overestimated, however, since the correlation coefficients are low and as can be seen in Figs. 4.10 or 4.11, the variability is high.

The repeat measurements are marked with asterisks (*) and show that the local variability can be high. These measurements were performed close to existing SMP holes and some of them have a remarkably different SMP hardness than their predecessors.
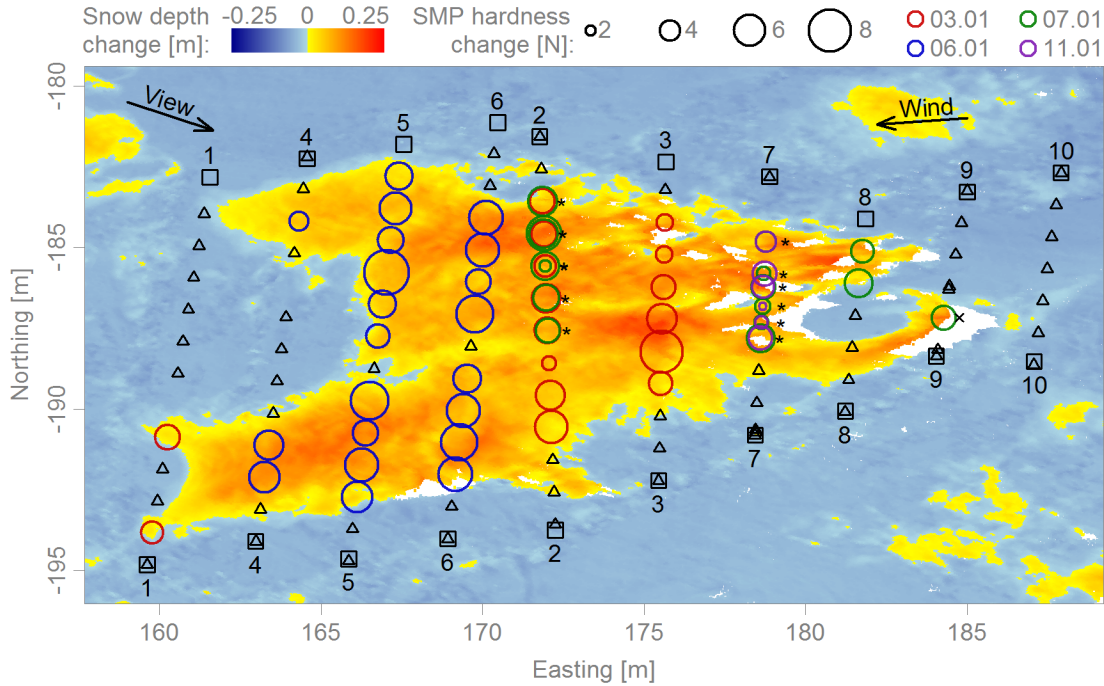
**Figure 4.10.:** Top view of the dune showing the snow depth change between 18 December and 11 January. The circles (○) show the positions of SMPs with at least 2.75 cm of freshly deposited snow at the surface. The diameter of the circles is proportional to the hardness increase. The colors indicate on which day the SMPs were acquired. Asterisks (*) mark positions were repeat measurements were performed. Squares (□) mark the positions of the bamboo poles. Triangles (△) show the positions of SMPs acquired in TLS measurement shadows or in areas of erosion or less than 2.75 cm of deposition. The SMP position at the tail marked with a 'x' is used as the reference to calculate the distance in Fig. 4.11. The arrows show the predominating wind direction during the main drifting snow event and the approximate view direction in Fig. 4.8. The numbers next to the bamboo pole markers show in which sequence the transects were acquired. Transects 1-3 were measured on 3 January, transects 4-6 on 6 January and transects 7-10 on 7 January. The repeat measurements in transect 2 were acquired on 7 January, those in transect 7 were taken on 12 January.

**Figure 4.11:** Scatterplot of SMP hardness change against the distance to the dune's tail. The reference for the distance measurement is the SMP position at the tail marked with a 'x' in Fig. 4.10. The colors indicate on which day the SMPs were acquired. Pearson's correlation coefficient is 0.40 with a p-value of 0.002. The dashed line shows the linear regression with a slope of 0.1 N m$^{-1}$ and an intercept of 3.8 N.
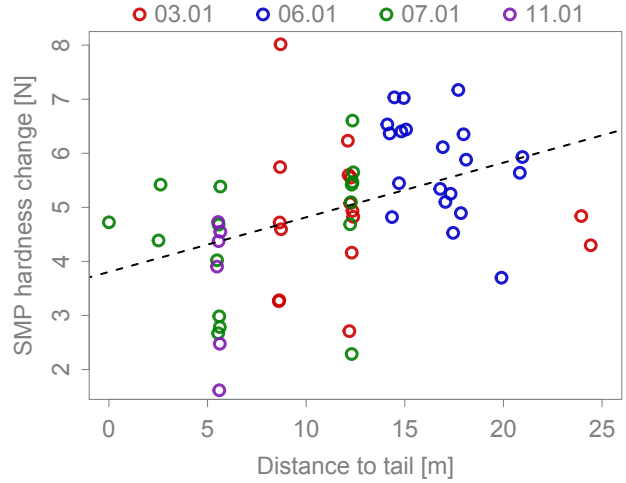


For others, on the other hand, similar SMP hardnesses were measured on different days. For all repeat SMPs, four days elapsed between the two measurements. The variability could therefore be due to temporal effects. However, in Fig. 4.6, it could be seen that there is no robust hardening or softening trend with time. The differences between the measurement days in Fig. 4.6 could in fact be explained by the spatial variability seen in Figs. 4.10 and 4.11. The SMPs acquired on 6 January, which are harder than those acquired on the other days, were all taken in the area of the crest on the dune. With the exception of two SMPs from 3 January, the SMPs acquired on the other days, when the SMP hardness tended to be softer, where acquired closer to the tail.

## 4.3.6. Wind exposure parameter Sx vs. SMP hardness change

Sommer et al. (2018a) showed that deposition of snow only led to hardening in wind-exposed areas. As explained in the introduction, the parameter Sx was calculated based on the Kinect data and was used to describe wind exposure and wind-sheltering. In Antarctica, the available DSMs can be used for a similar but restricted analysis. To calculate Sx, the DSM from 2 January was used for the SMPs from 3 January, the DSM from 6 January for the SMPs from 6-7 January and the DSM from 11 January for the SMPs from 12 January. The calculation of Sx depends on four settings: The main wind direction, the width of the sector that is considered around this main direction and the minimum and maximum search distances. As explained above, the main wind direction was estimated to be 86° based on the dune's orientation. A range of values was used for the other three settings to analyze their sensitivity on the result. We used sector widths of 5°, 10° and 20°, minimum search distances of 0, 0.1 and 0.2 m and maximum search distances of 0.5, 1, 2 and 5 m. For some SMP positions and some of these 36 combinations of settings, the resulting search sectors contained less than four TLS points. No Sx value was calculated for these SMP positions. For the three setting combinations with a sector width of 5° and a maximum search distance of 0.5 m, Sx could not be calculated at more than 7 SMP positions and these settings where therefore not considered.
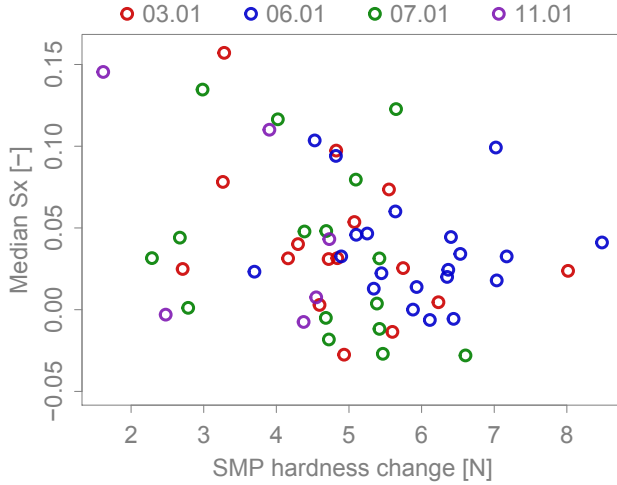
**Figure 4.12:** Scatterplot of Sx against the SMP hardness change. For each SMP, the median of all valid Sx values based on the different Sx settings was calculated. The colors indicate on which day the SMPs were acquired. There is no clear trend. Pearson's correlation coefficient is -0.29 and the corresponding p-value is 0.024. Without the three points in the top left corner, the correlation is significantly lower.

For the remaining 33 setting combinations, correlation coefficients and linear regressions were calculated. The correlation coefficients vary between -0.35 and -0.19 (-0.35 and -0.16). Only 19 (4) of them are significant with a p-value below 0.05 and only 3 (1) p-values are below 0.01. The slope of the linear regressions varies between -0.015 N$^{-1}$ and -0.007 N$^{-1}$. There is therefore no significant trend between the SMP hardness change and Sx, as also illustrated by the scatterplot between Sx and the SMP hardness changes in Fig. 4.12. This plot was constructed by taking the median of all valid Sx values for each SMP position. This results in a representative view of the different Sx settings. For these median values, the correlation coefficient is -0.29 (-0.25) with a corresponding p-value of 0.024 (0.059). The slope of the linear regression is -0.009 N$^{-1}$. Without the three points in the top left corner, the correlation coefficient drops to -0.09 (-0.14), the slope to -0.003 N$^{-1}$ and the p-value increases to 0.50 (0.29).

## 4.4. Discussion and conclusion

The observed period and the performed measurements were similar to how experiments in the wind tunnel were conducted. A snowfall without much wind led to a smooth snow surface with a homogeneous hardness. This was followed by a period with wind but without significant drifting snow events and finally, a strong drifting snow event took place, where snow was eroded and redeposited. This sequence of events was often simulated in the wind tunnel. In Antarctica, a 10 cm snowfall without much wind is rarely observed and we were fortunate to capture this event. The initial snow conditions in Antarctica and in the wind tunnel were remarkably similar. The initial hardness was 0.01 N in Antarctica. In the wind tunnel it was 0.024 N averaged over all 148 measurements (Sommer et al., 2017a). In Antarctica, the 18 density measurements of the new snow varied between 39 and 116 kg m$^{-3}$. There was one measurement with a density of 159 kg m$^{-3}$. The average was 82 kg m$^{-3}$. In the wind tunnel, 107 density measurements of new snow were performed in total. They ranged from 30 to 124 kg

m$^{-3}$ and the average was 75 kg m$^{-3}$ (Sommer et al., 2017a). The SMP and TLS data was analyzed similarly to the SMP and Kinect data acquired in recently published wind tunnel experiments. The comparison of the results provides a valuable validation of the wind tunnel experiments.

In the wind tunnel, Sommer et al. (2017a) first compared SMPs that were acquired after wind periods with or without drifting snow and found that drifting snow is a necessary but not sufficient condition for the formation of a wind crust. In Antarctica, we observed the same result (Fig. 4.7). For the SMPs with a corresponding cumulative mass flux close to zero, the SMP hardness did not increase considerably. In the group of SMPs acquired after the small drifting snow event the hardness increased by up to 1 N, if three extreme outliers are neglected. This is the range of hardness increases that was observed in the wind tunnel. Many SMPs, however, still had very soft snow at the surface. This shows that drifting snow does not always lead to the formation of a hard wind crust. All SMPs acquired after the main drifting snow event that were analyzed in detail, showed a significant hardness increase. However, Fig. 4.4D shows that even after this event, there were SMP positions with soft snow at the surface. The SMP hardness increases after the main drifting snow event are significantly higher than anything achieved in the wind tunnel. This is most likely due to higher wind speeds and more intense drifting in Antarctica. This leads to more frequent and more powerful impacts of snow particles on the surface causing more compaction and hardening. There is no logarithmic boundary layer in the wind tunnel and the mass flux was not measured. The conditions can therefore not be compared directly. However, the free stream wind speed in the wind tunnel was measured about 30 cm above the snow surface and rarely exceeded 6 m s$^{-1}$.

Kuznetsov (1960) measured the hardness of a mobile barchan dune and observed that the crest was softer than the tail. Filhol and Sturm (2015) explain this result with the different age of the snow at the tail and crest. Simply speaking, a barchan dune moves because snow is eroded from its tail and deposited behind the crest. The snow at the crest was therefore deposited only recently, while the tail consists of older snow. According to Filhol and Sturm (2015), the older snow in the tail area is harder because it has been affected by sintering for longer than the younger, and therefore, softer crest. Our measurements, on the other hand, suggest that the tail area is slightly softer than the crest (Figs. 4.10 and 4.11). It must be kept in mind that the scatter was high and that the trend, even though statistically significant, was not very strong. Furthermore, only one dune was surveyed. Nevertheless, this result at least shows that the measurements performed by Kuznetsov (1960) and the explanation provided by Filhol and Sturm (2015) are not generally true. It suggests that time is not the dominating factor explaining hardness and sintering is not the dominating process causing it. In this particular case, the SMPs in the tail area were acquired between one and five days after the SMPs at the crest. This means that the age difference between tail and crest was even higher in this case that it normally is. If sintering were the main hardening process, this measurement setup should have resulted in a much harder tail compared to the crest. But even with the increased age difference, the SMPs in the tail area were softer. The previous wind tunnel experiments also suggested that time and sintering are not the dominating processes in

wind-packing (Sommer et al., 2018a). Often, a wind crust was observed after only a few minutes of wind and at the time scale of hours, the hardness did not increase with the experiment duration. It was suggested that the impact of particles at the moment of deposition could be a more important hardening process than sintering.

In the wind tunnel, 40% of the observed hardness variability could be explained by the wind exposure parameter Sx (Sommer et al., 2018a). We therefore attempted to also use this parameter to explain the hardness variability observed on the barchan dune. As shown in Fig. 4.12 this did not work. There is no significant correlation between the calculated Sx values and the SMP hardness change. In the wind tunnel, the Kinect data that was used to calculate Sx was available with a frame rate of 3.6 Hz. This allowed to measure Sx continuously during deposition events. This made it possible to correlate the Sx value at the moment of deposition with the SMP hardness at the corresponding depth in the SMP force profile. The evolution of the snow depth at the SMP position was used to map depth to time. In Antarctica, such a detailed analysis was not possible. The scans provide snapshots of Sx values after deposition events. Unlike in the wind tunnel, a time evolution of Sx during deposition events cannot be calculated. However, the values calculated based on the scans were expected to reflect the wind exposure situation at the end of the deposition period. The SMP hardness change, which measures the hardness of the snow close to the surface, was expected to reflect the hardness situation at the same point in time. This assumption was based on the fact that some snow was deposited on the dune after the main drifting snow event (Fig. 4.9). The low correlation between Sx and the SMP hardness change, however, suggests that the assumption of simultaneousness of the measured hardness and the calculated Sx values is not correct. In particular, based on the description of barchan dune formation by Filhol and Sturm (2015), the snow at the surface was not necessarily deposited there at the end of the deposition period, especially upstream of the crest. To explain this hardness, we would need Sx values at the moment in time, when this snow was deposited. Unfortunately, with the available data, it is impossible to determine when a certain layer of snow was deposited and how the wind exposure situation was at that moment. The most likely reason for the low correlation is therefore that the SMP hardness change was correlated to the wrong Sx values. The various uncertainties in the Antarctic data could be another, but probably less important reason for the low correlation. The position of the SMP measurements, the digital surface model and the wind direction are all less precisely known than in the wind tunnel. We are not suggesting that wind exposure is not an important factor for wind-packing in Antarctica and hypothesize that if simultaneous measurements of the hardness and Sx were available, a significant correlation would emerge as it did in the wind tunnel.

Other than the wind exposure, we think that the wind speed and drifting intensity are important factors to explain the measured variability of the hardness. It can be seen in Fig. 4.4 that both the wind speed and the mass flux varied considerably during the main drifting snow event. To be able to calculate a meaningful correlation, however, we would again need to know when exactly the dune was formed. Based only on the TLS scans, this is not known precisely enough. We think that to explain the hardness, the

wind exposure, wind speed and drifting intensity at the moment of deposition are more important than the age of the deposition. It is possible however, that if these parameters are very uniform during a dune formation event, that the effect of time and sintering becomes visible. Such a uniform dune formation event could explain the results observed by Kuznetsov (1960).

The results from Antarctica confirm that drifting snow is necessary for wind-packing. The results also showed that time and sintering are probably not the dominating hardening processes but the measured hardness variability could not be adequately explained with the available data. This analysis furthermore documents quantitatively how fresh snow gets reorganized in a drifting snow event in Antarctica. The measured change in associated hardness can help to improve existing models of snow deposition (Groot Zwaaftink et al., 2013; Libois et al., 2014).

## Data availability

The data is publicly available on Envidat (Wever et al., 2018).

## Author contributions

ML and NW designed the project and collected the data in Antarctica. CS and NW processed the data. CS analyzed the data and wrote the Manuscript. NW, ML and CF helped with the analysis and revised the manuscript.

## Competing interests

The authors declare that there are no competing interests present.

## Acknowledgments

# 5. Conclusion

In this thesis, we investigated the formation of wind crusts in the wind tunnel and in the field. First, a new wind tunnel had to be developed and built from scratch. What was at first a ring-shaped channel became obround through the addition of two straight sections. The idea behind the closed-circuit configuration and the smooth turns was to simulate an infinite fetch. Gathering new snow on wooden trays and lowering the bottomless wind tunnel into this snow cover worked extremely well and allowed us to perform experiments with natural and practically undisturbed snow. A model-aircraft propeller created the airflow. This unfortunately led to a non-uniform flow in the wind tunnel. This mainly manifested itself in inhomogeneous erosion and deposition patterns at a large scale. Some sections of the wind tunnel were usually strongly eroded and the snow was redeposited in other sections, e.g. below the propeller. In the main test section, however, the flow was quite uniform and the patterns of erosion and deposition were largely random, meaning they were not consistent between different experiments. The small size of the wind tunnel and the strongly curved channel also meant that a logarithmic boundary layer could not develop. This makes it very difficult to compare the wind speed measured in the wind tunnel to other studies or to field experiments. The absence of a well-controlled flow in the wind tunnel limits its applicability or comparability with field measurements but it was nevertheless possible to achieve the formation of wind crusts and thus to study the process of wind-packing.

According to Seligman (1936), a wind crust should form under the influence of a humid wind, even in the absence of drifting snow. The first experiments were designed to test this and included wind periods without drifting snow and with drifting snow. The SMP measurements clearly showed that no wind crust forms without drifting snow. Even with a bowl of liquid water inside the channel to increase the humidity, a crust could not be formed. The observed effects of wind without drifting snow were an increased rate of settling and compaction of the snow compared to no wind at all. This means that the hardness did increase slightly during these experiments but the increase was homogeneous over the complete depth of the snowpack and was not limited to a surface layer. Furthermore, the resulting snow hardness was still very low. This is definitely not how Seligman (1936) describes a wind crust. It must be said that Seligman (1936) does not really provide any evidence that wind without drifting snow can form a wind crust, he simply states it. It is therefore difficult to discuss why we find a different result.

The fact that we observed no significant hardening without drifting snow suggests that the proposed processes that are unrelated to drifting snow, namely ventilation leading to an increased vapor flux as well as vapor condensation in the surface layer from the air and/or snow, are not predominant for wind packing. On the other hand, we cannot definitely dismiss these processes. Neither pressure variations at the snow surface nor

the air flow in the snowpack nor latent heat fluxes were measured. Furthermore the wind did have an effect on the snow. The increased rate of settling and compaction could be due to ventilation, but could also be attributed to the turbulent heat flux in the wind tunnel. What our measurements show is that the effect of these processes is small at most. The obtained results provide experimental justification for the parametric wind-packing routines in Crocus and Snowpack. Both models only increase the snow density and change the microstructural parameters if the wind speed exceeds the drifting snow threshold (Brun et al., 1997; Groot Zwaaftink et al., 2013).

Not all drifting snow events led to the formation of a wind crust and the variability of the snow hardness after wind periods with drifting snow was correspondingly high. The next experiments were designed to investigate and explain this variability. Since erosion and deposition appeared to be important, a Microsoft Kinect sensor was added to the wind tunnel to be able to quantify the random snow depth changes in the main test section. The combination of the SMP and Kinect data showed that wind crusts only form when snow is deposited. If snow is being eroded or if the snow depth stays constant, there was no significant increase of the snow hardness. In the case of new snow, this was explained by the fact that the snow was simply eroded too quickly. During the more recent experiment with old snow (see appendix C), the erosion of the snow was very slow or even negligible. We had speculated earlier that there might be further hardening of the snow in such a scenario. The SMPs acquired during this experiment, however, suggest that the effect of drifting snow without deposition is negligible. We did not observe any significant change of the snow hardness.

When snow was deposited during a drifting snow event, the resulting wind crust hardness was still highly variable. With the Kinect data it was possible to explain 47% of this variability. The wind exposure parameter Sx was the most important variable and explained about 40% of the variability. The snow was harder in wind-exposed areas with a low Sx value. Adding the deposition rate to the model increased its explanatory power by seven percentage points. The snow was harder when it was deposited slowly. The influence of the accumulation rate was mentioned in several studies (Craven and Allison, 1998; Kotlyakov, 1966) and they observed that the density decreased with increasing accumulation rate. We observed the same trend, but it must be kept in mind that the accumulation rate in these studies was measured at a time scale of years while the deposition rate in the wind tunnel is calculated at a time scale of seconds. It is therefore not necessarily the same effect or process that is observed in each case. The wind exposure is not mentioned explicitly as an influencing parameter in the literature, but when describing the difference between wind crust and wind slab it appears implicitly. Seligman (1936) and Fierz et al. (2009) both describe wind crust as being harder than wind slab and state that the first forms on windward slopes while the latter is often found on leeward slopes.

The proposed processes associated with drifting snow are mechanical fragmentation followed by sintering, ventilation leading to the deposition of fragmented particles in the snow and packing due to the impact forces of drifting particles. The processes unrelated to drifting snow could theoretically also play a role during wind periods with drifting

but it is unlikely that their effect is significantly larger in these conditions. Our results indicate that drifting snow has no significant hardening effect on an existing layer of snow. This result holds whether new or old snow was eroded quickly or slowly or the snow depth remained constant during the drifting snow event. This suggests that the impact forces of drifting particles are not strong enough to be relevant for wind-packing. However, this statement has to be put into perspective because the wind speeds in the wind tunnel are relatively low and the duration of the experiments was usually only on the order of hours. Furthermore, if no snow is deposited, the majority of the saltating particles rebound on the snow surface and their momentum is therefore only partly transferred to the snow surface. When a saltating particle is deposited, on the other hand, the complete momentum is available for fragmentation and packing of the snow. The packing by impact forces might therefore still be a relevant process during the formation of wind crusts. The absence of an effect of drifting snow on an existing snow layer also suggests that ventilation is also not an important process during wind periods with drifting snow. But again, this is merely an implication and there are no direct measurements to prove that. This leaves the process of mechanical fragmentation of snow grains in the saltation layer, followed by close packing of the small particles during deposition and sintering. This is the only proposed process that can happen only when snow is deposited and our measurements suggest that this is probably the main physical process behind wind-packing. The process of packing the snow due to impact forces of the saltating particles at the moment of deposition is of course a part of this and the relative effects of these processes are difficult to keep apart. The results show that a deposition of wind-blown snow already had a significant hardness only a few minutes after it formed. At the time scale of hours, there was furthermore no significant relationship between the hardness and the experiment duration. This supports the idea that impact forces at the moment of deposition are important and that the hardening is not just due to sintering.

As mentioned above, wind-packing in Crocus and Snowpack takes place when the wind speed exceeds the drifting snow threshold. In both models, the existing surface layer is compacted with a decreasing effect with depth. In Snowpack, the effect decreases linearly down to the maximum affected depth of 7 cm (Groot Zwaaftink et al., 2013) and in Crocus the effect decreases exponentially with depth until a non-transportable layer of snow is found (Vionnet et al., 2012). These implementations are clearly very different from our observations. Not every drifting snow event led to hardening and there was no effect on the existing surface layer. In a 1D model, it is of course not possible to take into account the spatial variability of erosion and deposition or the influence of wind exposure. Such models must therefore implement an "average effect" of the wind on the snow. In that sense, a decreasing effect with increasing depth below the surface is not a far-fetched way of implementing wind-packing. How well the used parameterizations represent the "average effect" of wind packing, however, is very difficult to test. It can probably not be done with our data. First, the variability is extremely high and second, we usually only measured the resulting hardness while the models modify the strain rate or the density and microstructural parameters. There is a statistical model that derives density and SSA from SMP penetration force signals (Proksch et al., 2015) but

for the other variables, the relationship between them and the hardness is unknown. We can therefore not evaluate or improve the implementation of wind-packing in 1D models with our results. In surface processes models such as Alpine3D (Lehning et al., 2006), the observations about the influence of erosion, deposition and wind exposure could be implemented.

The field campaign in Antarctica provided a possibility to compare the wind tunnel results to measurements performed in natural conditions. This was only partly successful, however. The necessity of drifting snow for wind-packing to occur could be confirmed. On the other hand, no significant relationship between the hardness and the wind exposure parameter Sx could be found. We explained this with the fact that the data used to calculate Sx was available only at a much lower temporal resolution than in the wind tunnel. Sx could therefore not be calculated at the relevant point in time. The strong correlation in the wind tunnel suggests that this relevant point in time is the moment of deposition. To successfully correlate the hardness to Sx, we therefore need to know at what time each layer of snow was deposited and what the wind exposure situation was at that time. This necessitates snow depth measurements in 2D with a high temporal resolution.

The wind tunnel results suggested that the main physical processes in wind-packing are mechanical fragmentation, followed by packing due to the impact forces at the moment of deposition and sintering. The latter two processes were difficult to discern but the absence of a time dependence at the time scale of hours is evidence that sintering might not be the dominating hardening process. In Antarctica, the hardness changes were observed at a time scale of days and there was still no evident relationship between the hardness and time. Furthermore, there was no relationship between the hardness and Sx most likely because Sx could not be calculated at the moment of deposition. These two observations again suggest that the deposition of snow and therefore the packing due to the impact forces occurring at that moment is probably a more important hardening process than sintering. However, it must be kept in mind that the observations made in Antarctica are only based on the analysis of one case study. The number of data points was relatively low and the variability was quite large.

The experiments performed in the wind tunnel and in Antarctica provided valuable quantitative information about wind-packing and new insights into the physics of this process. The collected data, especially the combination of SMP and Kinect measurements, allowed to answer some of the original research questions. It is now clearer which physical processes and parameters are important. However, with the available data, some of the answers remain rather speculative and some questions unanswered. The following chapter mentions some of these questions and provides some suggestions as to how they might be answered.

# 6. Outlook

Simply speaking, the remaining open questions are the same as those asked originally. Which physical processes are important for wind-packing and under what conditions does wind-packing take place?

We found several necessary conditions for wind-packing, namely saltation leading to slow deposition of snow in a wind-exposed area. However, these conditions are not sufficient, meaning we only answered the question under what conditions wind-packing does not occur. Finding sufficient conditions for wind-packing is related to explaining the observed hardness variability. With the available data, only half of it could be explained. If we find the correct parameters to explain the other half, we also fully answered the question of the conditions for wind-packing.

Some possibly relevant parameters were already investigated but for one reason or another, no strong or significant correlation between them and the hardness was found. These parameters are the wind speed, air temperature, air humidity and initial density and temperature of the snow. There is a weak correlation between the initial snow conditions and the hardness. The initial snow temperature and initial snow density could therefore be relevant and should be investigated further. No significant relationships were found for the other parameters. The wind speed and air temperature are still expected to be relevant due to their influence on processes involved with wind-packing. The wind speed influences the packing due to the impact forces at the moment of deposition and the air temperature influences sintering. The reason why no significant correlation was observed for these two parameters and why the correlation was weak for the initial snow conditions is probably that the range of observed values was too limited. More experiments with an increased range of values should therefore be performed. In case of the air humidity, the observed range of values was also small. The reason for this, however, is that the air humidity is always high during drifting snow events. And since drifting snow is necessary for wind-packing, the explanatory power of the air humidity is expected to be low. Two other parameters that were measured are the snow temperature and the snow surface temperature. These parameters were highly correlated with the air temperature during the experiments and were therefore not considered separately. It is possible, however, that one of these parameters might be slightly better suited to explain the hardness variability than the air temperature. The snow temperature during the experiment is not to be confused with the initial snow temperature measured before the experiment, which is a separate parameter.

Other possibly relevant parameters have not yet been investigated. In this category there is mainly the drifting snow mass flux. A higher mass flux can be caused by more drifting particles, larger drifting particles or both. The former leads to more frequent and the latter to stronger impacts at the surface. Especially the stronger impacts can

be expected to cause more compaction of the snow at the moment of deposition. More frequent impacts may be relevant when most particles rebound from the surface and could increase or speed up the hardening in such conditions. The easiest way to measure the drifting snow mass flux is probably with a particle counter, for example a SPC. As mentioned before, the initial snow conditions play a role. These conditions were characterized with the density and temperature of the initial snow. Additional parameters that could be investigated in this context are the atmospheric air temperature and wind speed during the snowfall. These parameters influence the microstructure or grain shape of the initial snow, for example if there are dendrites or if there are already small, broken up particles at the beginning of the experiment. Whether these parameters are more relevant than the initial snow density and temperature is unclear, however.

The example of the wind exposure parameter Sx showed that it is important to correlate the hardness of the snow to the conditions at the time of deposition of this snow. This is expected to be equally important for the other possibly relevant parameters. Snow depth measurements with a high spatial and temporal resolution appear, therefore, indispensable for any future experiments. The Microsoft Kinect provided such data with a high accuracy and reliability and at a low cost.

More experiments are probably necessary to find a significant relationship with the hardness or to be able to dismiss the relevance for any of the above mentioned possibly relevant parameters. The question is whether it will suffice to simply collect more data points and increase the range of values or if new methods or even a new experimental facility is needed. As mentioned before, the wind tunnel has some limitations. The main problem is that the flow is largely uncontrolled and unknown. Due to the small size of the channel, the strong curvature and the use of a single propeller as the source of the wind, no logarithmic boundary layer can develop and there are large-scale irregularities. To correctly interpret the influence of some of the possibly relevant parameters, more controlled conditions might be necessary. For example, the effect of the air temperature on the snow is strongly connected to the turbulent heat flux. Without a logarithmic wind profile it is very difficult to estimate this flux and therefore, how the air temperature affects the snow. Deposition of snow was found to be necessary for wind-packing. Deposition can be forced by placing an obstacle on the snow and this would therefore allow to perform such experiments in a wind tunnel with controlled and well-known flow conditions. Since the fragmentation of particles appears to be important, such a wind tunnel should have a closed-circuit configuration.

The second main question concerns the processes involved in wind-packing. We mainly investigated different conditions during the experiments and observed if a wind crust formed or not and how hard it was. Based on these observations, certain conclusions were made about the importance of the different processes. For example, no wind crust was observed without drifting snow, leading to the conclusion that the processes that happen without drifting are probably not important for wind-packing. Such indirect conclusions are not necessarily wrong, of course, but more direct measurements of the involved processes would render a clearer picture of the physics of wind-packing. This appears necessary to further improve the implementation of wind-packing in snow cover

models. Direct measurements of the involved processes are more difficult than only observing conditions and how they affect the snow. For example, to make quantitative statements about the importance of ventilation, pressure variations at the snow surface should be measured. Walter et al. (2014) performed such measurements with Irwin sensors during drifting events with sand. With snow, it would be even more difficult to keep the sensors flush with the surface. For such specialized and difficult measurements, the question arises again if these experiments could be performed in the existing wind tunnel or if better controlled flow conditions would be necessary. The latter would certainly help to make the experiments and the interpretation of the results easier.

In addition to such complex experiments, modeling might be another avenue along which the relative importance of different physical processes could be further investigated. For example, Comola et al. (2017) introduced a model capable of simulating the fragmentation of saltating particles and of reproducing measured particle size distributions. This model could be a starting point to model the packing due to the impact forces at the moment of deposition and sintering of mechanically fragmented particles.

A further limitation of the existing wind tunnel is that the maximum observed hardness was only about 1 N. Significantly harder wind crusts are observed in nature. In Antarctica, for example, hardnesses of up to 8 N were measured. How do such wind crusts form? Or how does a wind crust with a hardness of 1 N evolve into one with a much higher hardness? These questions can most likely not be answered with the current wind tunnel. Maybe all that is necessary are higher wind speeds and more intense drifting snow. It could also be, however, that there are processes going on in nature that we are missing completely in the wind tunnel. An example for such a process, even though it may be unrelated to wind-packing, is long wave radiation. It could therefore also be beneficial to perform more field experiments. Such experiments will not be easy but an important step has already been made by Crivelli et al. (2018), who successfully used the Microsoft Kinect to measure erosion and deposition of snow in the field. A drifting snow station provided meteorological data and drifting snow mass flux measurements. Adding a SnowMicroPen to this setup and measuring the hardness changes during drifting snow events would be very interesting and could be a next step in the investigation of wind-packing.

# Appendices

# A. Near-infrared photography and computer tomography

The specific surface area (SSA) of snow is an important microstructural parameter. It is defined as the ratio of the surface area of the ice to the volume of ice. New snow has therefore a high SSA since the small dendritic structures have a high surface area and a low ice volume. Metamorphism of snow usually leads to the destruction of these small features, more rounded grains and consequently a decrease of SSA. We also expect such a decrease in SSA during wind-packing and wanted to measure the SSA at the surface of the snow during the wind tunnel experiments to see how the microstructure changes. Domine et al. (2009) presented three examples when the SSA of snow can increase over time. They suggest that wind can increase the SSA of snow with a previously low SSA and that ventilation may deposit fragmented grains into the snow cover thereby increasing the SSA as well. Measuring the SSA regularly and calculating a rate of change could therefore also provide evidence for or against physical processes possibly involved with wind-packing.

The reflectance of snow at near-infrared (NIR) wavelengths ($\approx$ 900 nm) is highly dependent on SSA. Measuring this reflectance with NIR photography is therefore a way to indirectly measure SSA (Langlois et al., 2010; Matzl and Schneebeli, 2006; Tape et al., 2010). We used an Imaging Development Systems UI-5370CP industrial camera with a 4 megapixel CMOS sensor specifically adapted for use in the NIR domain. It is sensitive in the visible spectrum and to wavelengths up to about 1000 nm. NIR light was provided by two LEDs working at 940 nm. Fig. A.1 shows how the camera and the two LEDs are included in the cover of the main test section.

At the beginning of each wind tunnel experiment, a reference image of a flat surface was taken. Such a reference image is necessary to normalize the brightness of the SSA images (Fig. A.2). The camera's optics always generate a bright center and darker corners. All images in the near-infrared are taken in absence of ambient light. The holes in the wind tunnel's covers were all closed and the windows were covered with aluminum sheets (Fig. A.1). This guaranteed consistent lighting for all SSA measurements. For an SSA measurement, four reflectance standards were inserted through holes in the windows (Fig. A.1) and an image was taken with the LEDs on and one with the LEDs off. This "no lights" image was used to make sure that there is no stray light in the wind tunnel. After the normalization (Fig. A.2B), the reflectance standards, which have reflectances of 2.5, 25, 50 and 99%, are then used to fit a linear transformation between the pixel intensity and the reflectance. The linear fit was always good. Averaged over 50 linear regressions, $r^2$ was 0.999 and the standard error was 0.018. The optical model of Kokhanovsky and Zege (2004) is used to calculate SSA from the reflectance. The model contains a shape
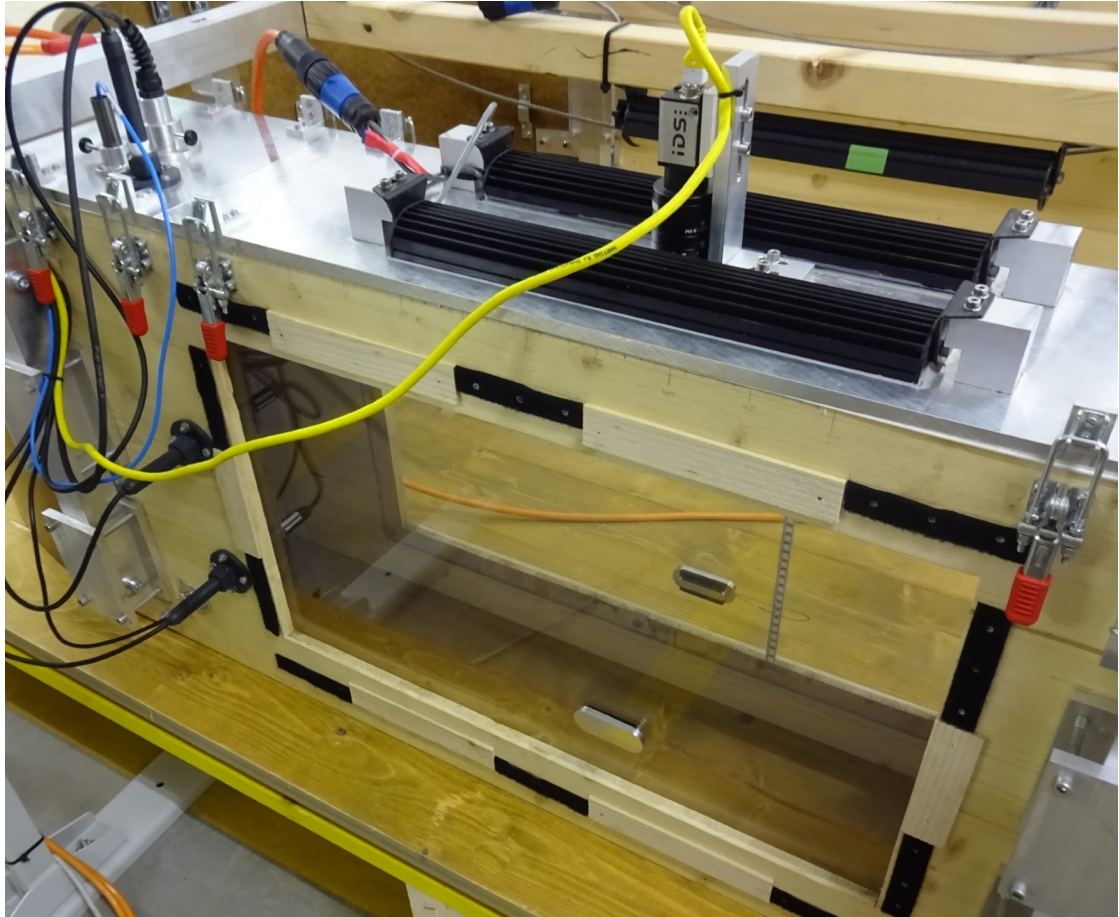
**Figure A.1.:** The near-infrared photography setup. The camera and the two NIR LEDs are incorporated in the cover above the main test section. During the photography, the windows are covered with aluminum sheets, which are attached using the Velcro visible around the windows. The aluminum plugs in the windows close the holes through which the reflectance standards are inserted for SSA measurements.
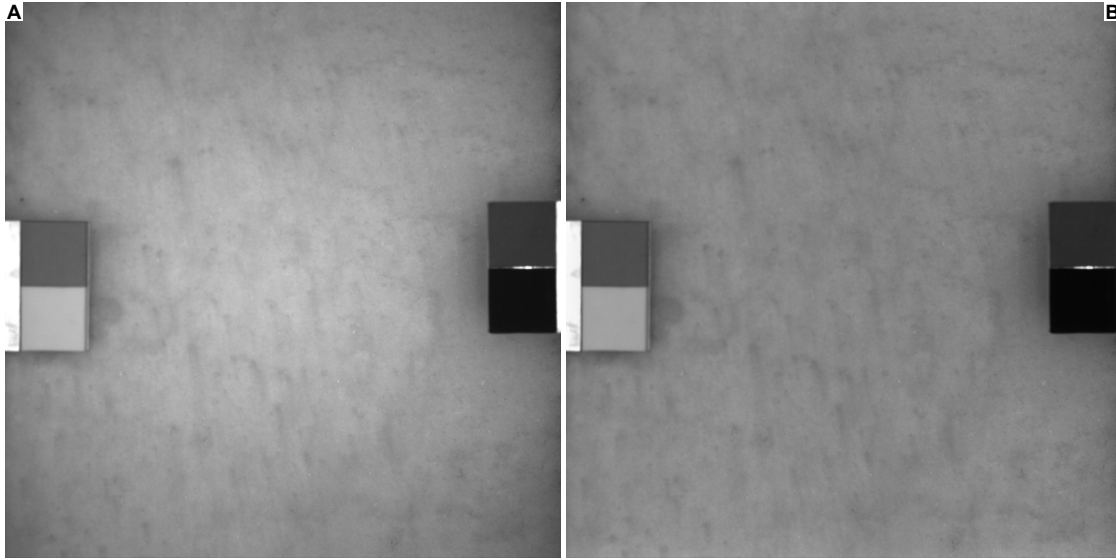
**Figure A.2.:** Example of an untreated (A) and normalized (B) SSA image showing the snow surface and the four reflectance standards. It can be seen how the normalization brightens the corners and darkens the center. The differences in brightness are equalized.

factor $b$ which has to be calibrated. Six snow samples from five photographed surfaces were measured in the computer tomograph (Scanco $\mu$-CT80) to obtain reference values of the SSA (e.g. Heggli et al., 2009; Kaempfer and Schneebeli, 2007; Schneebeli and Sokratov, 2004). These calibration measurements are shown in Fig. A.3. Horizontal error bars with a length of $\pm$ 0.018 show the standard error of the reflectance introduced by the linear transformation. As can be seen, this uncertainty is not negligible, especially since the range of measured values is quite limited. This figure also shows the optical model of Kokhanovsky and Zege (2004) for three values of the shape factor $b$. Picard et al. (2009) showed that $b$ varies between 3.62 and 4.53 for snow. The model predicts an exponential increase of SSA with increasing reflectance. The calibration measurements, however, show an almost constant SSA for all reflectance values. This means that each measurement leads to a completely different prediction for the shape factor $b$. Clearly, a calibration of $b$ is not possible like that. Even more importantly, for most reflectance measurements, the model predicts a much lower SSA than what was measured. Or, in other words, for most SSA measurements with the $\mu$-CT the reflectance measured with the NIR photography is a lot lower than what would be expected based on the model. The measurement of SSA with the $\mu$-CT is generally very reliable since the actual microstructure of snow is measured with this method. The SSA can therefore be calculated directly according to its definition. These measurements indicate that the NIR photography method employed in the wind tunnel underestimates the reflectance and therefore the SSA. It is unclear why this method, which was shown to be viable in e.g. Langlois et al. (2010), Matzl and Schneebeli (2006), and Tape et al. (2010) did not work in this case.
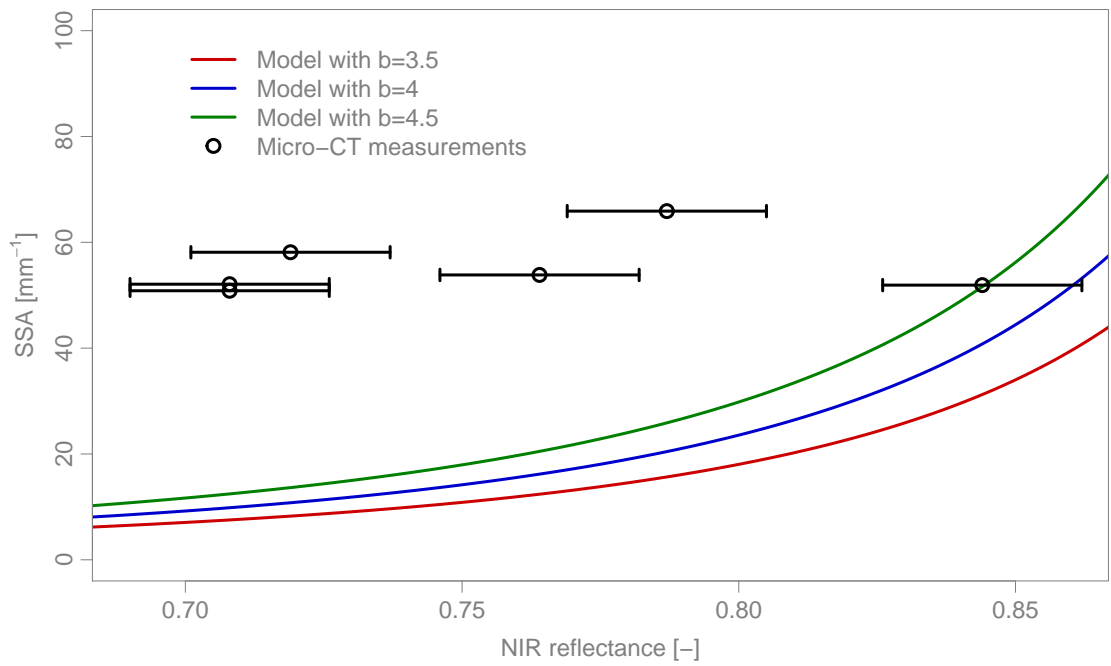
**Figure A.3.:** SSA calibration. The black circles show the calibration measurements. The error bars show the average standard error of 0.018 of the linear regressions between the pixel intensity and the reflectance. The lines show the SSA model for three values of the shape factor $b$.
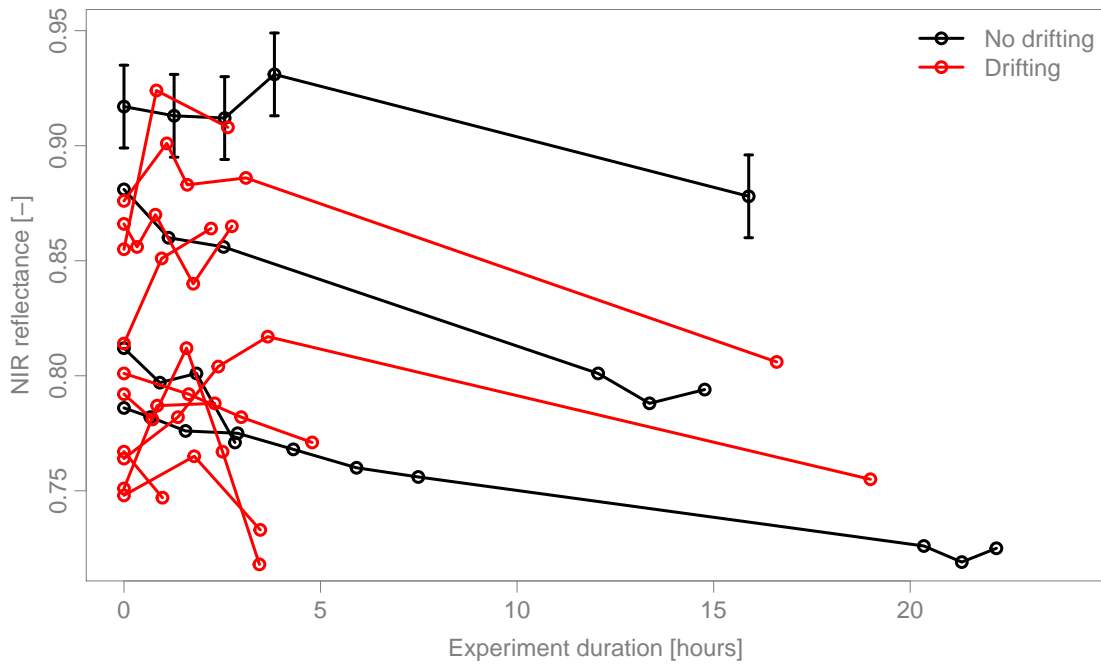
**Figure A.4.:** Evolution of the NIR reflectance during experiments with and without drifting snow. The error bars show the average standard error of 0.018 of the linear regressions between the pixel intensity and the reflectance. This error applies to all lines but the bars are not plotted everywhere to avoid cluttering.

The NIR photography results can, as a consequence, not be used to study the evolution of SSA at the surface of the snowpack in the wind tunnel. The evolution of the reflectance itself could however still give an indication of how the microstructure of the snow in the wind tunnel changes. Fig. A.4 shows the evolution of the reflectance during 14 experiments. The uncertainty introduced by the linear transformation between pixel intensity and reflectance is shown with vertical error bars with a length of $\pm$ the standard error of 0.018. Four of the experiments were conducted without drifting snow and ten with drifting snow. As can be seen, the reflectance sometimes increases and sometimes decreases, especially at the beginning of or during shorter experiments. Some of these variations are within the uncertainty limit but not all. It would have been expected that there is generally a decrease of the reflectance with time. This shows again that the NIR photography in the wind tunnel is probably not reliable and this measurement method was therefore discontinued after the first winter.

During winter 2016/2017, some samples with a thin wind crust were analyzed in the $\mu$-CT. This allowed to compare the SSA and the density of the snow in the freshly deposited crust with the values of the undisturbed snow below the crust. Fig. A.5 shows an example of a sample measured in the $\mu$-CT. This sample was scanned with a resolution of 10 $\mu$m At least three layers can be easily distinguished. At the bottom, there is snow that was not disturbed by the wind. Above it, are two unmistakable layers of deposited snow. The bottom two layers are relatively homogeneous, while the surface layer contains several sublayers. The SSA and the density was calculated for each of the three main layers in the areas shown by the white rectangles in Fig. A.5. The rectangle in the top layer was placed in the corner because the snow is most homogeneous there. The undisturbed snow in the bottom layer has a SSA of 59.1 mm$^{-1}$ and a density of 93 kg m$^{-3}$. This value is in the same range as the manual density measurements that were done at the beginning of the experiment with measured values ranging between 69 kg m$^{-3}$ and 97 kg m$^{-3}$ in different positions. The layer in the middle has a density of 177 kg m$^{-3}$ and a SSA of 56.8 mm$^{-1}$. In the surface layer the density is 370 kg m$^{-3}$ and the SSA is 50.5 mm$^{-1}$. These values suggest that wind-packing is associated with a decrease of the SSA and an increase in density. According to the Kinect data the layer in the middle was deposited during the first wind period at a wind speed of 5 m s$^{-1}$ and the surface layer was deposited during the last wind period at a wind speed of 6 m s$^{-1}$. The higher wind speed could explain the differences between the middle and the top layer. Another reason for the lower SSA and the higher density in the surface layer compared to the middle layer could be that the snow in the surface layer had been mechanically worked by the wind for a longer time. The snow in the middle layer was deposited early in the experiment and those particles were probably less broken up than those deposited in the surface layer.
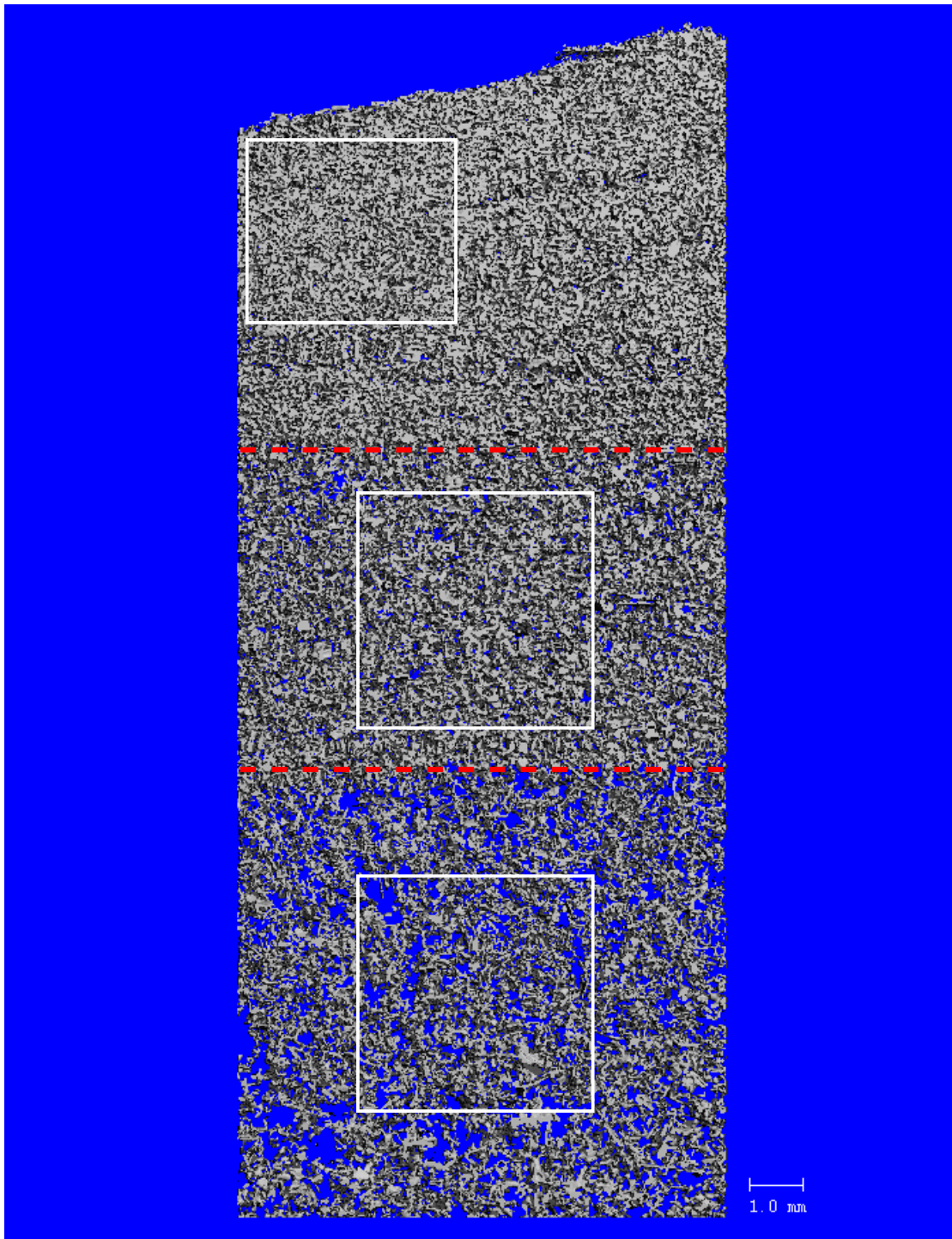
**Figure A.5.:** Slice of a $\mu$-CT sample of snow with a thin wind crust at the surface and undisturbed snow at the bottom. There is a third layer in between with an intermediate density. The dashed, red lines show the boundaries between the main layers. The three rectangles show where the density and SSA were calculated. The slice is 1 mm thick in the third dimension.

# B. Drifting snow detection

The UI-5370CP camera shown in Fig. A.1 was also used in the visible range to detect the absence or presence of drifting snow in the main test section. During the wind periods, a pair of images was acquired every ten seconds. The second image was acquired 0.5 seconds after the first. To increase the contrast in these images, the snow surface was illuminated with a green LED during the wind periods. To determine whether there was drifting snow or not, the correlation between each pair of images was calculated. It was expected that the correlation would be very high in the absence of drifting snow and that the correlation would decrease with increasing drifting mass flux.
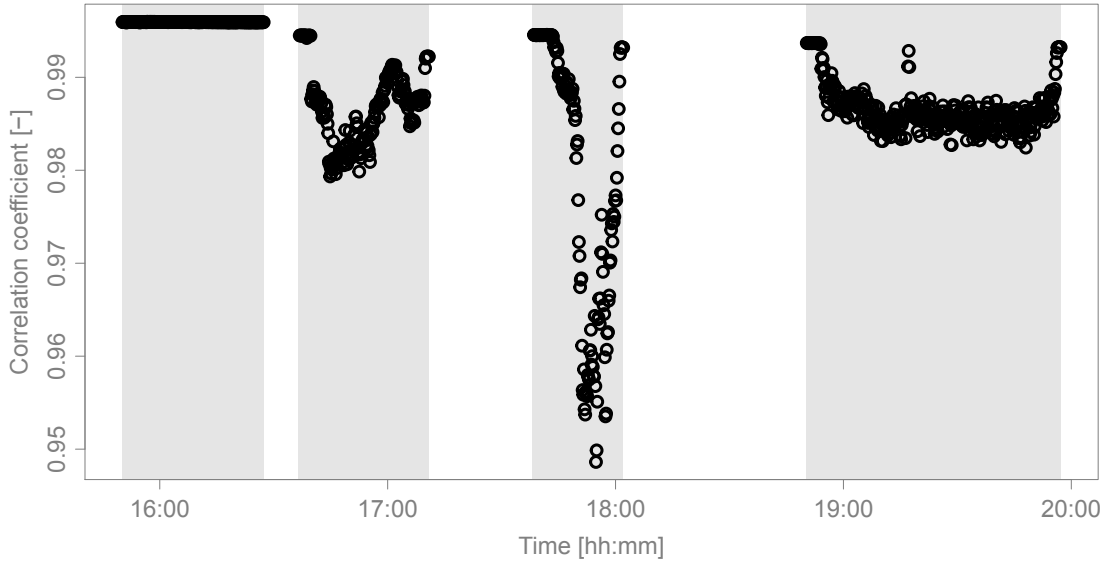


**Figure B.1.:** Example of the drifting snow correlation during an experiment with four wind periods. The four wind periods are highlighted. There was drifting snow during the second, third and fourth periods.

Fig. B.1 shows an example of an experiment where the detection of drifting snow by image correlation worked well. There was no drifting snow during the first wind period and the correlation was very high and very constant. During the other three periods, there was drifting snow and it can be seen that the correlation is lower and much more irregular. At the beginning and end of these three periods, the correlation is high and constant too. These short periods correspond to the start-up and shut-down phases of the wind tunnel where the wind speed was too low to cause drifting snow. Furthermore,

the third wind period exhibits much lower values of the drifting snow correlation than the second or fourth periods. This corresponds well with the fact that snow was sieved into the wind tunnel during the third period but not during the second and fourth periods. The sieving probably increased the drifting mass flux which explains the lower correlation.

Based on this example, the drifting snow detection using the correlation between images looks like a powerful method. However, it was not always reliable. The original idea was to differentiate between wind periods with or without drifting snow using a threshold value of the correlation coefficient. The absolute value of the correlation coefficient, however, varied between wind periods and between experiments. This means that the correlation coefficient during wind periods without drifting snow could be as low as 0.98 or as high as 0.995. The correlation coefficient during wind periods with drifting snow was often in the same range. Sometimes, the correlation coefficient even increased when drifting started. This makes the use of a threshold value as a criterion for drifting snow impossible. The other feature that most drifting snow periods exhibited is the irregularity or high variability of the correlation coefficient within the wind period. However, there were also wind periods without drifting snow that had a higher variability than the first wind period in Fig. B.1 and there were also wind periods with drifting snow where the correlation coefficient was almost constant. This was especially the case during wind periods with only very weak saltation. The variability of the correlation coefficient could therefore also not be used as a criterion for drifting snow. Interpreting the measured drifting snow correlation was usually easy if independent information about the presence or absence of drifting snow was available but it became difficult if this information was missing.

The acquisition of the image pairs was therefore discontinued after the first winter and if there was drifting snow or not was subsequently determined by frequent manual observations and recorded in the log file. The first image of each pair had also been used to create time lapse videos of the experiments. These videos were very helpful to reconstruct what had happened at the surface of the snowpack. The reason why these images were not acquired anymore after the first winter, was that the cover containing the camera assembly was replaced with a cover containing the Kinect assembly. The Kinect data was an adequate replacement for these images.

# C. Wind-packing of old snow

In section 3.4, we discussed how all experiments were conducted with fresh snow and how wind might have a different effect on old, already wind-influenced snow. In particular, we suggested that the slow erosion of old snow might lead to a hardness increase of the remaining old snow. The goal of some experiments in winter 2017/2018 was to test these hypotheses.

The first challenge was to have a layer of old snow with a homogeneous hardness in the main test section of the wind tunnel. The homogeneity is very important since each SMP measurement has to be performed in a different location. Measured hardness changes can therefore only be attributed to the wind if the hardness was homogeneous in the beginning.

Fig. C.1 shows the homogeneity of the initial snowpack in the main test section that was achieved with different methods. Group 1 is shown as a reference and consists of all 148 initial SMPs that were acquired in the winters 2015/2016 and 2016/2017 during the experiments with fresh snow. It can be seen that the fresh snow was always quite homogeneous. The standard deviation in this group is 7.3 mN. For each individual experiment the homogeneity was even higher. The standard deviation of the initial SMPs of one experiment was 1.9 mN on average. For groups 2, 3 and 4, the snow was sieved directly into the main test section using round sieves with a diameter of about 20 cm. For group 2, fresh snow was sieved using a sieve with a 2 mm wide mesh. This led to a quite homogeneous snowpack with a standard deviation of 10 mN. For group 3, the same sieve was used to sieve old snow that had fallen several days earlier. This lead to a harder snowpack and a much higher variability. The standard deviation in group 3 is 34 mN. Sieving the same snow using a sieve with a 1 mm wide mesh for group 4, lead to a little softer snowpack and a similar variability with a standard deviation of 32 mN. For group 5, we tried to increase the homogeneity by using a larger, rectangular sieve 20 cm wide and 50 cm long and by sieving into a cardboard frame instead of into the wind tunnel. Sieving into a 20 cm high cardboard frame instead of the 50 cm high wind tunnel allowed to achieve a more homogeneous snow height in the main test section. However, as the boxplot for group 5 shows, the hardness was not homogeneous at all. The standard deviation for group 5 is 48 mN. For group 6 finally, a block of old snow was cut out and placed into the main test section. The snow was several weeks old and very well bonded. It was therefore easy to cut out and carry around such a block of snow. The standard deviation for group 6 is 18 mN. The variability is therefore a lot lower than what was achieved with sieving old snow.

Fig. C.1 shows that cutting out a block of old snow is the best way to get a homogeneous layer of old snow in the wind tunnel. Sieving old snow resulted in a high variability regardless of the sieve and method. Sieving fresh snow, on the other hand, leads to a
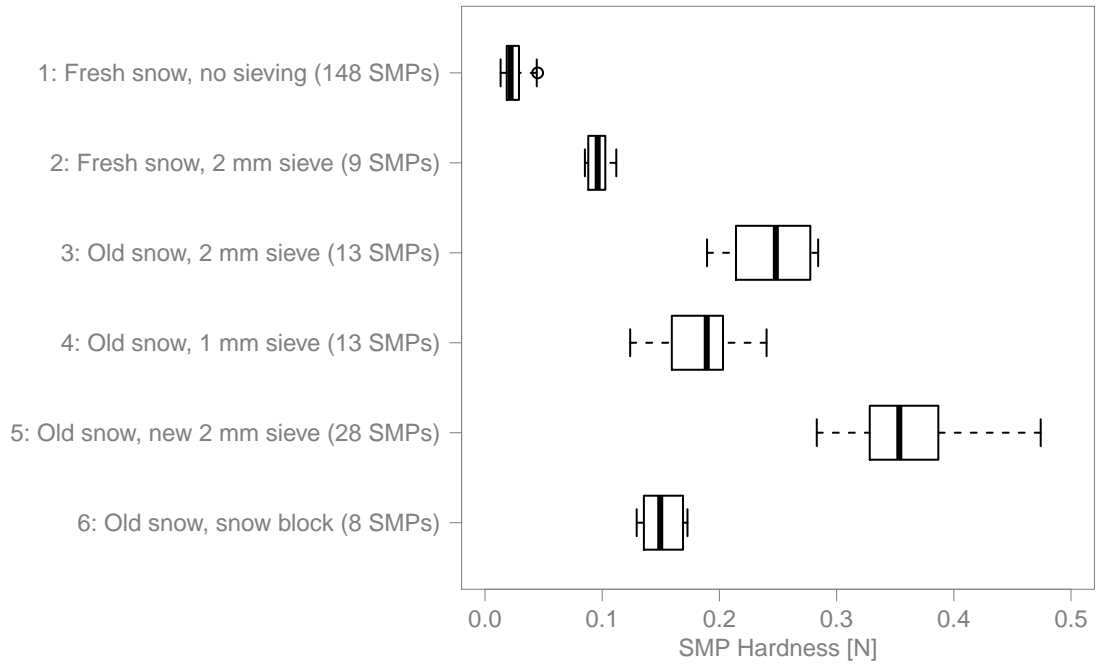
**Figure C.1.:** Homogeneity of the snow in the main test section for different types of snow and methods. Group 1 consists of all initial SMPs that were acquired during the fresh snow experiments in the first two winters and is shown as a reference. For group 2, fresh snow was sieved into the wind tunnel with a 2 mm sieve. For group 3, old snow was sieved with the same 2 mm sieve. For group 4, the same old snow was sieved with a 1 mm sieve. For group 5, old snow was sieved with a new, larger 2 mm sieve. For group 6, a block of old snow was cut out and placed in the main test section.

quite homogeneous snowpack which, however, remained quite soft.
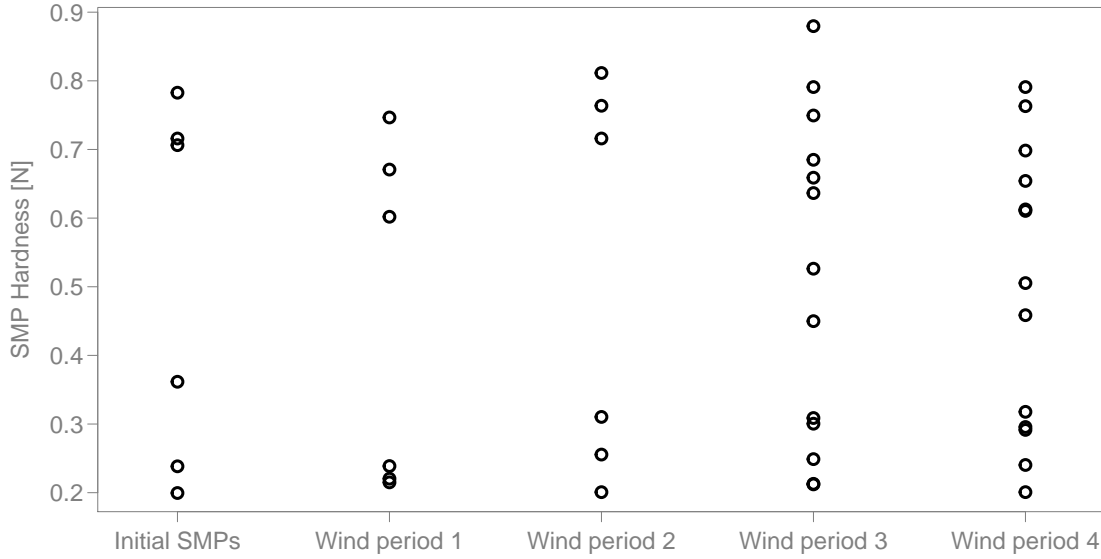


**Figure C.2.:** Evolution of the SMP hardness during an experiment with old snow. The first two wind periods were 30 min long and the last two wind periods were 1 hour long.

Fig. C.2 shows how the SMP hardness evolved during an experiment with old snow. Based on Fig. C.1, a block of old snow was cut out and placed in the main test section. A second block was placed upstream of it and was shaped as a ramp. The rest of the wind tunnel was not filled with snow initially. The initial SMPs in Fig. C.2 show that this snow block had a highly variable surface hardness. The standard deviation of 263 mN is an order of magnitude higher than what was observed during the last test. This high variability is the reason why individual data points instead of boxplots are shown in Fig. C.2. There is a group with a low SMP hardness and a group with a high SMP hardness (see also Fig. C.3). Maybe the top of the block was not cut exactly horizontal and different layers of snow were therefore at the surface within the main test section.

The experiment consisted of four wind periods with a wind speed of 6 m s$^{-1}$. The first two wind periods were 30 min long and the last two wind periods were one hour long. An earlier test with a cut out snow block showed that achieving saltation with such old and well sintered snow was impossible in our wind tunnel. The maximum wind speed of almost 9 m s$^{-1}$ was simply not enough to initiate drifting. During this experiment, saltation was therefore initiated by sieving snow into the wind tunnel. During the first two wind periods, we had to continue to sieve snow to sustain the drifting. During the last two wind periods, there was already enough loose snow sieved into the wind tunnel that drifting started spontaneously and was also sustained. The Kinect data showed that the block of snow was slowly eroded in most places. The overall erosion during the experiment was limited to several millimeters. In some places, the snow depth remained practically constant. SMP measurements were taken after each of the four wind periods.

Fig. C.2 shows that the wind and the drifting snow had no measurable effect on the hardness of the remaining snow. The range of the SMP hardness remained the same during the whole experiment. Theoretically, it is of course possible that the snow at a certain position had an initial hardness at the bottom of the observed range and that the wind increased this hardness towards the top of the observed range. Fig. C.3 shows that this is extremely unlikely. This figure shows the SMP hardness for all measurements during the experiment as a function of the position in the main test section. As can be seen, the upstream half of the main test section had harder snow at the surface while the snow in the downstream half was softer. This did not change over the course of the experiments. The soft snow remained soft and the initially hard snow did not become harder. In the middle of the test section some intermediate hardnesses were observed after the third and fourth periods. This is also clearly visible in Fig. C.2.
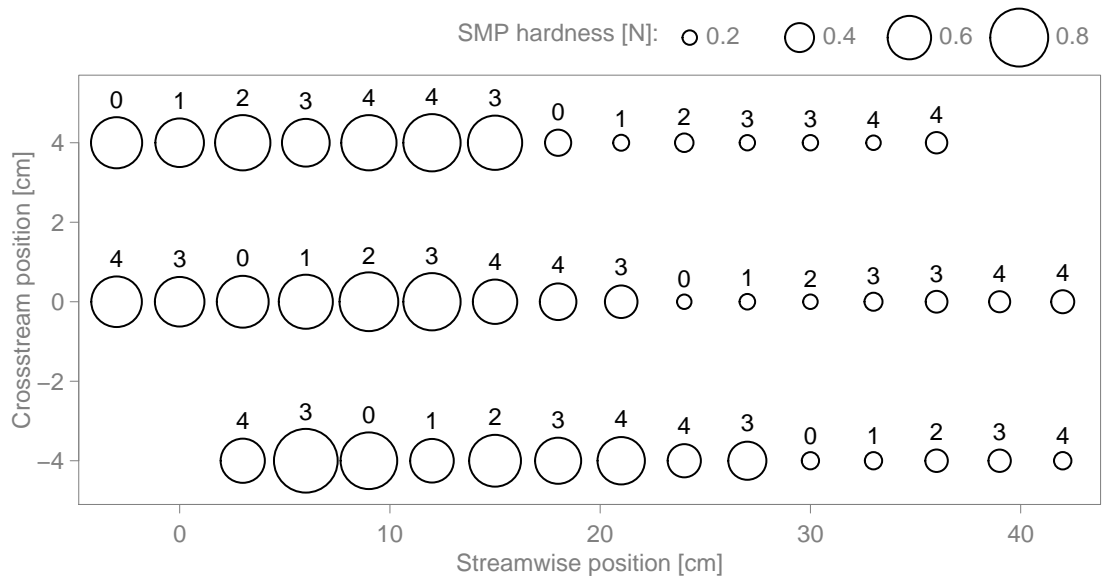


**Figure C.3.:** SMP hardness as a function of the position in the main test section acquired during an experiment with old snow. The numbers next to the circles show after which wind period that SMP was acquired. The initial SMPs are denoted with 0.

# D. Scatterplots between hardness and meteorological and snow conditions

In section 3.4 we discussed the influence of meteorological parameters such as wind speed, air temperature etc. and initial snow conditions on the hardness. This appendix shows the corresponding scatterplots between the snow hardness and these parameters. The plots are created based on the Kinect data similarly to Figs. 3.9 and 3.10. This means that the depth-time mapping is used to correlate the snow hardness to the measured parameters at the time of deposition of the corresponding layer.
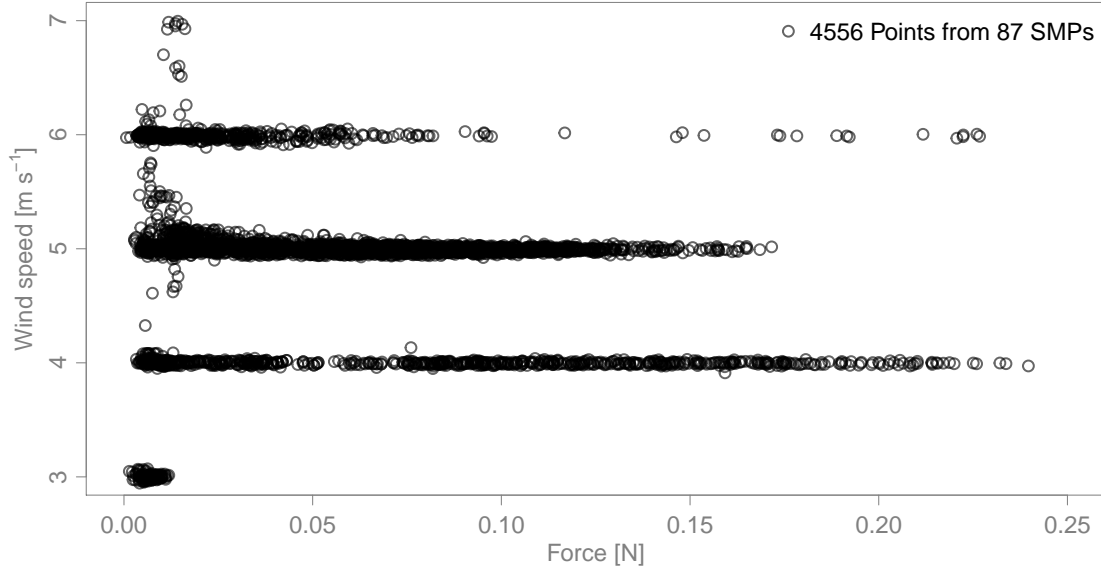


**Figure D.1.:** Scatterplot of the wind speed against the SMP force. The correlation between the two variables is -0.19 with a p-value $\sim 10^{-16}$.
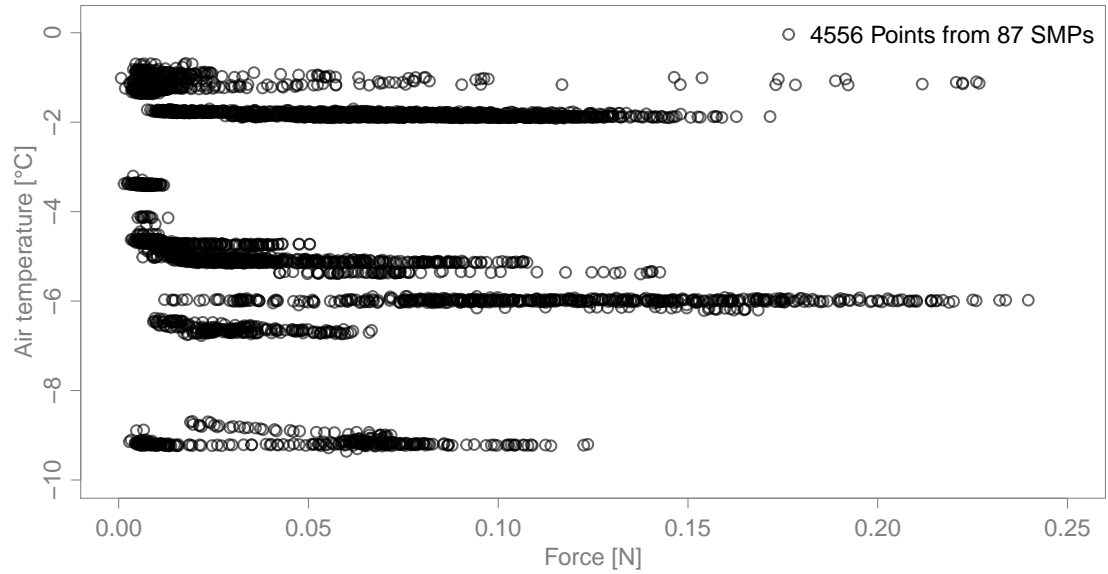
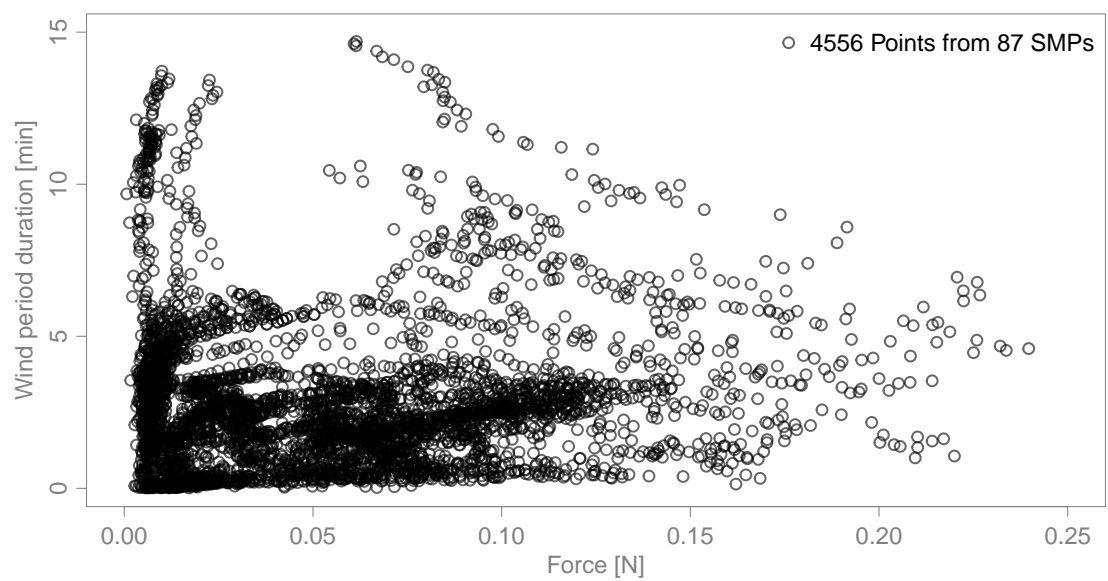**Figure D.2.:** Scatterplot of the air temperature against the SMP force. The correlation between the two variables is -0.05 with a p-value of 0.0009.
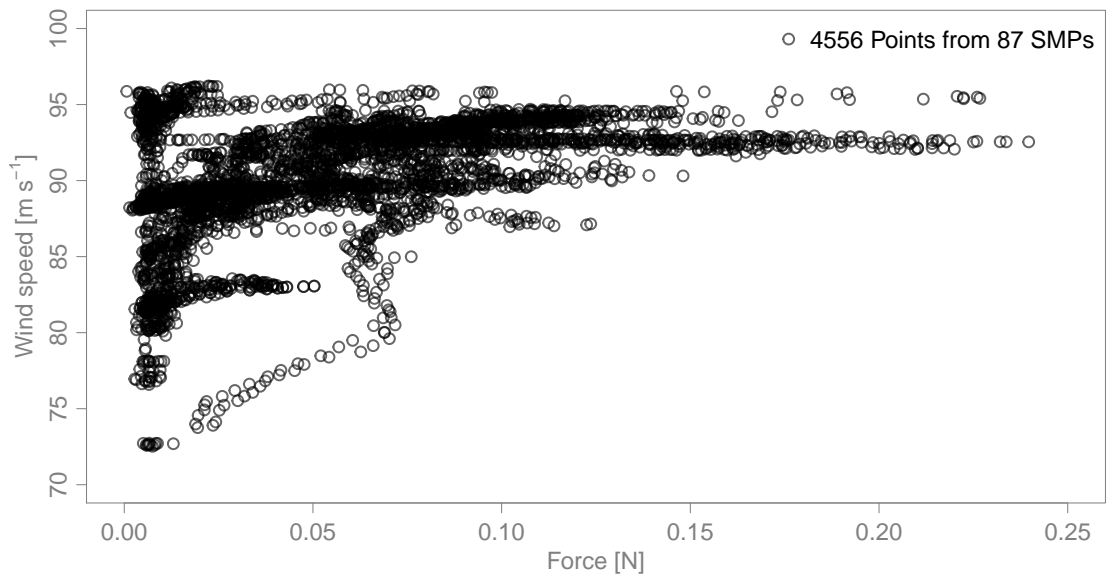


**Figure D.3.:** Scatterplot of the air humidity against the SMP force. The correlation between the two variables is 0.46 with a p-value $\sim 10^{-16}$.
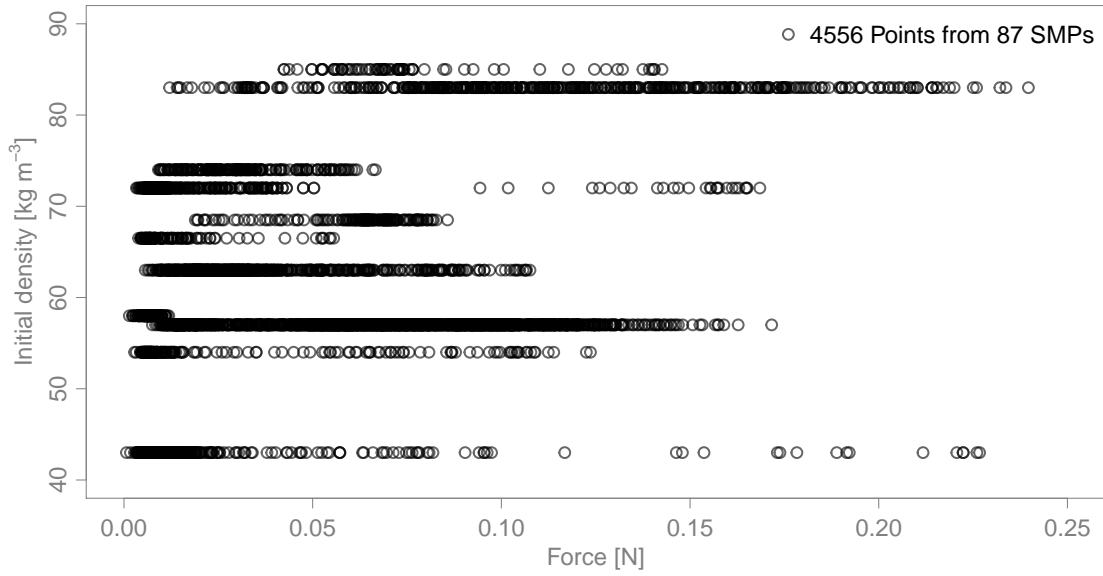
**Figure D.4.:** Scatterplot of the initial snow density against the SMP force. The correlation between the two variables is 0.32 with a p-value $\sim 10^{-16}$.
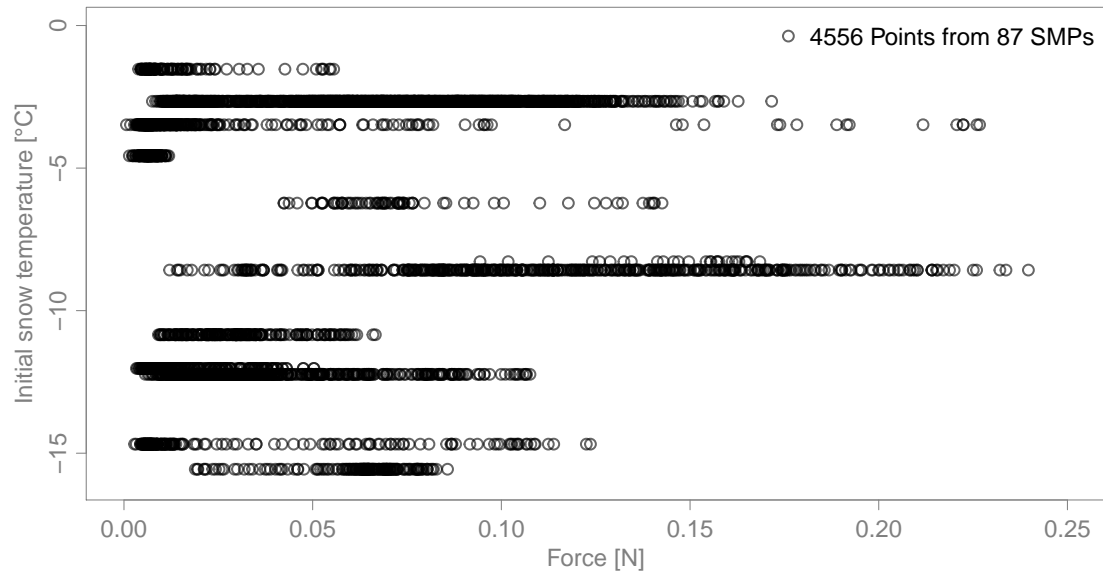


**Figure D.5.:** Scatterplot of the initial snow temperature against the SMP force. The correlation between the two variables is 0.15 with a p-value $\sim 10^{-16}$.

**Figure D.6.:** Scatterplot of the wind period duration against the SMP force. The correlation between the two variables is 0.04 with a p-value of 0.015.

# Bibliography

Adams, E. E., S. M. Jepsen, and B. Close (June 2008). "A bonding process between grains in mechanically disaggregated snow". In: *Annals of Glaciology* 48.1, pp. 6–12. DOI: 10.3189/172756408784700770.

Adkins, C. N. and R. H. Liebeck (Sept. 1994). "Design of optimum propellers". In: *Journal of Propulsion and Power* 10.5, pp. 676–682. DOI: 10.2514/3.23779.

Alley, R. B. (1988). "Concerning the deposition and diagenesis of strata in polar firn". In: *Journal of Glaciology* 34.118, pp. 283–290.

Armstrong, B. R. and E. Brun (2008). *Snow and Climate: Physical Processes, Surface Energy Exchange and Modeling*. Cambridge, UK: Cambridge University Press, p. 222.

Barnett, T. P., J. C. Adam, and D. P. Lettenmaier (Nov. 2005). "Potential impacts of a warming climate on water availability in snow-dominated regions". In: *Nature* 438.7066, pp. 303–309. DOI: 10.1038/nature04141.

Bartlett, S. J. and M. Lehning (Apr. 2011). "A theoretical assessment of heat transfer by ventilation in homogeneous snowpacks". In: *Water Resources Research* 47. DOI: 10.1029/2010WR010008.

Benson, C. S. (1967). "Polar Regions Snow Cover". In: *Proceedings of the Physics of Snow and Ice* 1.2, pp. 1039–1063.

Bleier, F. (1998). *Fan Handbook: Selection, Application, and Design*. New York: McGraw-Hill Education, p. 640.

Brun, E., E. Martin, and V. Spiridonov (1997). "Coupling a multi-layered snow model with a GCM". In: *Annals of Glaciology* 25, pp. 66–72.

Carolus, T. (2013). *Ventilatoren: Aerodynamischer Entwurf, Schallvorhersage, Konstruktion*. Wiesbaden: Vieweg+Teubner Verlag, p. 196. DOI: 10.1007/978-3-8348-2472-1.

Churchill, S. W. (1977). "Friction factor equation spans ali fluid flow regimes". In: *Chemical Engineering* 7, pp. 91–92.

Clifton, A., J.-D. Rüedi, and M. Lehning (Dec. 2006). "Snow saltation threshold measurements in a drifting-snow wind tunnel". In: *Journal of Glaciology* 52.179, pp. 585–596. DOI: 10.3189/172756506781828430.

Colbeck, S. C. (1991). "The layered character of snow covers". In: *Reviews of Geophysics* 29.1, p. 81. DOI: `10.1029/90RG02351`.

Comola, F., J. F. Kok, J. Gaume, E. Paterna, and M. Lehning (May 2017). "Fragmentation of wind-blown snow crystals". In: *Geophysical Research Letters* 44.9, pp. 4195–4203. DOI: `10.1002/2017GL073039`.

Cordier, O. (1953). "Ähnlichkeitsbedingungen für Strömungsmaschinen". In: *BWK Zeitschrift* 5.10, pp. 337–340.

Craven, M. and I. Allison (1998). "Firnification and the effects of wind-packing on Antarctic snow". In: *Annals of Glaciology* 27, pp. 239–245.

Crivelli, P., E. Paterna, S. Horender, and M. Lehning (Dec. 2016). "Quantifying Particle Numbers and Mass Flux in Drifting Snow". In: *Boundary-Layer Meteorology* 161.3, pp. 519–542. DOI: `10.1007/s10546-016-0170-9`.

Crivelli, P., E. Paterna, N. Wever, and M. Lehning (2018). "Small-scale spatiotemporal snow/erosion/deposition dynamics in a mountain field site, a wind tunnel and Antarctica". In: *Frontiers in Earth Science*, in preparation.

Domine, F., A.-S. Taillandier, A. Cabanes, T. a. Douglas, and M. Sturm (Mar. 2009). "Three examples where the specific surface area of snow increased over time". In: *The Cryosphere* 3.1, pp. 31–39. DOI: `10.5194/tc-3-31-2009`.

Doorschot, J., M. Lehning, and A. Vrouwe (2004). "Field measurements of snow drift and mass fluxes and comparison with model simulations". In: *Boundary-Layer Meteorology* 113, pp. 347–368.

Doumani, G. A. (1967). "Surface structures in snow". In: *Physics of Snow and Ice : proceedings* 1.2, pp. 1119–1136.

Endo, Y. and K. Fujiwara (1973). *Characteristics of the snow cover in East Antarctica along the route of the JARE South Pole Traverse and factors controlling such characteristics.* Tech. rep. Tokyo: National Institute of Polar Research, pp. 1–38.

Fang, C. and B. Sill (Oct. 1992). "Aerodynamic roughness length: Correlation with roughness elements". In: *Journal of Wind Engineering and Industrial Aerodynamics* 41.1-3, pp. 449–460. DOI: `10.1016/0167-6105(92)90444-F`.

Fierz, C., R. Armstrong, Y. Durand, P. Etchevers, E. Greene, D. McClung, K. Nishimura, P. Satyawali, and S. Sokratov (2009). *The international classification for seasonal snow on the ground.* IHP-VII Technical Documents in Hydrology No 83, IACS Contribution No 1. Paris: UNESCO-IHP.

Filhol, S. and M. Sturm (Sept. 2015). "Snow bedforms: A review, new data, and a formation model". In: *Journal of Geophysical Research: Earth Surface* 120.9, pp. 1645–1669. DOI: 10.1002/2015JF003529.

Glauert, H. (1935). "Airplane Propellers". English. In: *Aerodynamic Theory.* Ed. by W. F. Durand. Berlin: Julius Springer, pp. 169–360. DOI: 10.1007/978-3-642-91487-4_3.

Goodwin, I. D. (Sept. 1990). "Snow accumulation and surface topography in the katabatic zone of Eastern Wilkes Land, Antarctica". In: *Antarctic Science* 2.03, pp. 235–242. DOI: 10.1017/S0954102090000323.

Gow, A. J. (1965). *Snow studies in Antarctica.* Tech. rep. 177.

Groot Zwaaftink, C. D., A. Cagnati, A. Crepaz, C. Fierz, G. Macelloni, M. Valt, and M. Lehning (Feb. 2013). "Event-driven deposition of snow on the Antarctic Plateau: analyzing field measurements with SNOWPACK". In: *The Cryosphere* 7.1, pp. 333–347. DOI: 10.5194/tc-7-333-2013.

Guyomarc'h, G. and L. Mérindol (1998). "Validation of an application for forecasting blowing snow". In: *Annals of Glaciology* 26, pp. 138–143.

Hartnett, J. P., J. C. Y. Koh, and S. T. McComas (1962). "A Comparison of Predicted and Measured Friction Factors for Turbulent Flow Through Rectangular Ducts". In: *Journal of Heat Transfer* 84.1, p. 82. DOI: 10.1115/1.3684299.

Heggli, M., E. Frei, and M. Schneebeli (Sept. 2009). "Snow replica method for three-dimensional X-ray microtomographic imaging". In: *Journal of Glaciology* 55.192, pp. 631–639. DOI: 10.3189/002214309789470932.

Herwijnen, A. van and B. Jamieson (Nov. 2007). "Snowpack properties associated with fracture initiation and propagation resulting in skier-triggered dry snow slab avalanches". In: *Cold Regions Science and Technology* 50.1-3, pp. 13–22. DOI: 10.1016/j.coldregions.2007.02.004.

Jähne, B. (1980). "Zur Parametrisierung des Gasaustauschs mit Hilfe von Laborexperimenten". PhD thesis. Ruprecht-Karl-Universität Heidelberg.

Jones, D. (1983). *Snow stratigraphy observations in the katabatic wind region of eastern Wilkes Land, Antarctica.* Tech. rep.

Kaempfer, T. U. and M. Schneebeli (Dec. 2007). "Observation of isothermal metamorphism of new snow and interpretation as a sintering process". In: *Journal of Geophysical Research* 112.D24, p. D24101. DOI: 10.1029/2007JD009047.

Kampenhout, L. van, J. T. M. Lenaerts, W. H. Lipscomb, W. J. Sacks, D. M. Lawrence, A. G. Slater, and M. R. van den Broeke (Oct. 2017). "Improving the Representation of

Polar Snow and Firn in the Community Earth System Model". In: *Journal of Advances in Modeling Earth Systems*. DOI: `10.1002/2017MS000988`.

Kleinstreuer, C. (2010). *Modern Fluid Dynamics*. Vol. 87. Fluid Mechanics and Its Applications. Dordrecht: Springer Netherlands. DOI: `10.1007/978-1-4020-8670-0`.

Kokhanovsky, A. A. and E. P. Zege (Mar. 2004). "Scattering optics of snow". EN. In: *Applied Optics* 43.7, p. 1589. DOI: `10.1364/AO.43.001589`.

Kotlyakov, V. (1966). *The Snow Cover of the Antarctic and Its Role in the Present Day Glaciation of the Continent*. Jerusalem: IPST. DOI: `10.1016/S0039-128X(84)80034-3`.

Kozak, M. C., K. Elder, K. Birkeland, and P. Chapman (Nov. 2003). "Variability of snow layer hardness by aspect and prediction using meteorological factors". In: *Cold Regions Science and Technology* 37.3, pp. 357–371. DOI: `10.1016/S0165-232X(03)00076-4`.

Krall, K. E. (2013). "Laboratory Investigations of Air-Sea Gas Transfer under a Wide Range of Water Surface Conditions". PhD thesis. Ruperto-Carola University of Heidelberg.

Krishnappan, B. G. (June 1993). "Rotating Circular Flume". In: *Journal of Hydraulic Engineering* 119.6, pp. 758–767. DOI: `10.1061/(ASCE)0733-9429(1993)119:6(758)`.

Kruskal, W. H. and W. A. Wallis (1952). "Use of Ranks in One-Criterion Variance Analysis". In: *Journal of the American Statistical Association* 47.260, pp. 583–621.

Kuznetsov, M. A. (1960). "Barchan snow drift in the wind belt of east Antarctica". In: *Sov. Antarkt. Eksped* 10, pp. 175–179.

Lachat, E., H. Macher, M.-A. Mittet, T. Landes, and P. Grussenmeyer (Feb. 2015). "First Experiences with Kinect v2 Sensor for Close Range 3D Modelling". In: *ISPRS - International Archives of the Photogrammetry, Remote Sensing and Spatial Information Sciences* XL-5/W4.5W4, pp. 93–100. DOI: `10.5194/isprsarchives-XL-5-W4-93-2015`.

Langlois, A., A. Royer, B. Montpetit, G. Picard, L. Brucker, L. Arnaud, P. Harvey-Collard, M. Fily, and K. Goïta (Apr. 2010). "On the relationship between snow grain morphology and in-situ near infrared calibrated reflectance photographs". In: *Cold Regions Science and Technology* 61.1, pp. 34–42. DOI: `10.1016/j.coldregions.2010.01.004`.

Lehning, M., P. Bartelt, B. Brown, and C. Fierz (Nov. 2002). "A physical SNOWPACK model for the Swiss avalanche warning Part III: meteorolical forcing, thin layer formation and evaluation". In: *Cold Regions Science and Technology* 35.3, pp. 169–184. DOI: `10.1016/S0165-232X(02)00072-1`.

Lehning, M. et al. (2006). "ALPINE3D: a detailed model of mountain surface processes and its application to snow hydrology". In: *Hydrological Processes* 20.10, pp. 2111–2128. DOI: 10.1002/hyp.6204.

Libois, Q., G. Picard, L. Arnaud, S. Morin, and E. Brun (Oct. 2014). "Modeling the impact of snow drift on the decameter-scale variability of snow properties on the Antarctic Plateau". In: *Journal of Geophysical Research: Atmospheres* 119.20, pp. 11, 662–11, 681. DOI: 10.1002/2014JD022361.

Mankoff, K. D. and T. A. Russo (July 2013). "The Kinect: a low-cost, high-resolution, short-range 3D camera". In: *Earth Surface Processes and Landforms* 38.9, pp. 926–936. DOI: 10.1002/esp.3332.

Matzl, M. and M. Schneebeli (Dec. 2006). "Measuring specific surface area of snow by near-infrared photography". In: *Journal of Glaciology* 52.179, pp. 558–564. DOI: 10.3189/172756506781828412.

Mehta, R. D. and P. Bradshaw (1979). "Design Rules for Small Low Speed Wind Tunnels". In: *The Aeronautical Journal* 83.827, pp. 443–449.

Moody, L. F. (1944). "Friction Factors for Pipe Flow". In: *Transactions of the A.S.M.E.* 66.8, pp. 671–684.

Mori, Y. and W. Nakayama (1967). "Study on Forced Convective Heat Transfer in Curved Pipes : 2nd Report, Turbulent Region". In: *International Journal of Heat and Mass Transfer* 10, pp. 37–59.

Münnich, K. O., W. B. Clarke, K. H. Fischer, D. Flothmann, B. Kromer, W. Roether, U. Siegenthaler, Z. Top, and W. Weiss (1978). "Gas Exchange and Evaporation Studies in a Circular Wind Tunnel, Continuous Radon-222 Measurements at Sea, and Tritium/Helium-3 Measurements in a Lake". In: *Turbulent Fluxes Through the Sea Surface, Wave Dynamics, and Prediction.* Ed. by A. Favre and K. Hasselmann. New York: Plenum Press, pp. 151–166. DOI: 10.1007/978-1-4612-9806-9_11.

Naaim-Bouvet, F., M. Naaim, and J.-L. Michaux (2002). "Snow fences on slopes at high wind speed: physical modelling in the CSTB cold wind tunnel". In: *Natural Hazards and Earth System Science* 2.3/4, pp. 137–145. DOI: 10.5194/nhess-2-137-2002.

Nemoto, M. and K. Nishimura (2004). "Numerical simulation of snow saltation and suspension in a turbulent boundary layer". In: *Journal of Geophysical Research Atmospheres* 109.18, pp. 1–14. DOI: 10.1029/2004JD004657.

Pagliari, D. and L. Pinto (Oct. 2015). "Calibration of Kinect for Xbox One and Comparison between the Two Generations of Microsoft Sensors". In: *Sensors* 15.11, pp. 27569–27589. DOI: 10.3390/s151127569.

Paterna, E., P. Crivelli, and M. Lehning (May 2016). "Decoupling of mass flux and turbulent wind fluctuations in drifting snow". In: *Geophysical Research Letters* 43.9, pp. 4441–4447. DOI: 10.1002/2016GL068171.

Pattyn, F., K. Matsuoka, and J. Berte (Feb. 2010). "Glacio-meteorological conditions in the vicinity of the Belgian Princess Elisabeth Station, Antarctica". In: *Antarctic Science* 22.01, p. 79. DOI: 10.1017/S0954102009990344.

Picard, G., L. Arnaud, F. Domine, and M. Fily (Apr. 2009). "Determining snow specific surface area from near-infrared reflectance measurements: Numerical study of the influence of grain shape". In: *Cold Regions Science and Technology* 56.1, pp. 10–17. DOI: 10.1016/j.coldregions.2008.10.001.

Proksch, M., H. Löwe, and M. Schneebeli (Feb. 2015). "Density, specific surface area, and correlation length of snow measured by high-resolution penetrometry". In: *Journal of Geophysical Research: Earth Surface* 120.2, pp. 346–362. DOI: 10.1002/2014JF003266.

Riegl (2017). *RIEGL VZ-6000 Datasheet*. Horn, Austria: Riegl Laser Measurement Systems GmbH.

Rixen, C., M. Teich, C. Lardelli, D. Gallati, M. Pohl, M. Pütz, and P. Bebi (Aug. 2011). "Winter Tourism and Climate Change in the Alps: An Assessment of Resource Consumption, Snow Reliability, and Future Snowmaking Potential". In: *Mountain Research and Development* 31.3, pp. 229–236. DOI: 10.1659/MRD-JOURNAL-D-10-00112.1.

Robinson, D. A. and T. W. Estilow (2012). *NOAA Climate Data Record (CDR) of Northern Hemisphere (NH) Snow Cover Extent (SCE), Version 1*. NOAA National Centers for Environmental Information. DOI: 10.7289/V5N014G9.

Sato, T., T. Kimura, T. Ishimaru, and T. Maruyama (1993). "Field test of a new snow-particle counter (SPC) system". In: *Annals of Glaciology* 18, pp. 149–154.

Sato, T., K. Kosugi, S. Mochizuki, and M. Nemoto (Feb. 2008). "Wind speed dependences of fracture and accumulation of snowflakes on snow surface". In: *Cold Regions Science and Technology* 51.2-3, pp. 229–239. DOI: 10.1016/j.coldregions.2007.05.004.

Sato, T., K. Kosugi, and A. Sato (Jan. 2001). "Saltation-layer structure of drifting snow observed in wind tunnel". In: *Annals of Glaciology* 32.1, pp. 203–208. DOI: 10.3189/172756401781819184.

Schmucki, E., C. Marty, C. Fierz, and M. Lehning (Mar. 2014). "Evaluation of modelled snow depth and snow water equivalent at three contrasting sites in Switzerland using SNOWPACK simulations driven by different meteorological data input". In: *Cold Regions Science and Technology* 99, pp. 27–37. DOI: 10.1016/j.coldregions.2013.12.004.

Schmundt, D., T. Münsterer, H. Lauer, and B. Jähne (1995). "The circular wind/wave facilities at the University of Heidelberg". In: *Air-Water Gas Transfer*. Ed. by B. Jähne and E. C. Monahan. Hanau: AEON Verlag, pp. 505–516.

Schneebeli, M. and J. B. Johnson (1998). "A constant-speed penetrometer for high-resolution snow stratigraphy". In: *Annals of Glaciology* 26, pp. 107–111.

Schneebeli, M. and S. A. Sokratov (Dec. 2004). "Tomography of temperature gradient metamorphism of snow and associated changes in heat conductivity". In: *Hydrological Processes* 18.18, pp. 3655–3665. DOI: 10.1002/hyp.5800.

Schweizer, J., J. B. Jamieson, and M. Schneebeli (2003). "Snow avalanche formation". In: *Reviews of Geophysics* 41.4, p. 1016. DOI: 10.1029/2002RG000123.

Schytt, V. (1958). *Snow studies at Maudheim*. Oslo: Norsk Polarinstitutt.

Seligman, G. (1936). *Snow structure and ski fields: being an account of snow and ice forms met with in nature, and a study on avalanches and snowcraft*. London: Macmillan.

Smith, K. (2013). *Environmental Hazard. Assessing risk and reducing disaster*. Sixth edit. Abingdon: Routledge, p. 504.

Sokratov, S. a. and A. Sato (Jan. 2000). "Wind propagation to snow observed in laboratory". In: *Annals of Glaciology* 31.1, pp. 427–433. DOI: 10.3189/172756400781820020.

Sommer, C. G., M. Lehning, and C. Fierz (Dec. 2017a). "Wind tunnel experiments: saltation is necessary for wind-packing". In: *Journal of Glaciology* 63.242, pp. 950–958. DOI: 10.1017/jog.2017.53.

Sommer, C. G., M. Lehning, and C. Fierz (2017b). *Wind crust formation: Microsoft Kinect data*. WSL Institute for Snow and Avalanche Research SLF, Davos, Switzerland. DOI: 10.16904/22.

– (2017c). *Wind crust formation: SnowMicroPen data*. WSL Institute for Snow and Avalanche Research SLF, Davos, Switzerland. DOI: 10.16904/21.

– (Jan. 2018a). "Wind Tunnel Experiments: Influence of Erosion and Deposition on Wind-Packing of New Snow". In: *Frontiers in Earth Science* 6. DOI: 10.3389/feart.2018.00004.

Sommer, C. G., N. Wever, C. Fierz, and M. Lehning (2018b). "Investigation of a wind-packing event in Queen Maud Land, Antarctica". In: *The Cryosphere*, in review.

Sugiyama, S., H. Enomoto, S. Fujita, K. Fukui, F. Nakazawa, P. Holmlund, and S. Surdyk (June 2012). "Snow density along the route traversed by the Japanese-Swedish Antarctic Expedition 2007/08". In: *Journal of Glaciology* 58.209, pp. 529–539. DOI: 10.3189/2012JoG11J201.

Tabler, R. D. (1980). "Self-similarity of wind profiles in blowing snow allows outdoor modeling". In: *Journal of Glaciology* 26.94, pp. 421–434.

Tape, K. D., N. Rutter, H. P. Marshall, R. Essery, and M. Sturm (2010). "Instruments and methods recording microscale variations in snowpack layering using near-infrared photography". In: *Journal of Glaciology* 56.195, pp. 75–80. DOI: `10.3189/002214310791190938`.

Vionnet, V., E. Brun, S. Morin, A. Boone, S. Faroux, P. Le Moigne, E. Martin, and J.-M. Willemet (May 2012). "The detailed snowpack scheme Crocus and its implementation in SURFEX v7.2". In: *Geoscientific Model Development* 5.3, pp. 773–791. DOI: `10.5194/gmd-5-773-2012`.

Walter, B., S. Horender, C. Voegeli, and M. Lehning (Sept. 2014). "Experimental assessment of Owen's second hypothesis on surface shear stress induced by a fluid during sediment saltation". In: *Geophysical Research Letters* 41.17, pp. 6298–6305. DOI: `10.1002/2014GL061069`.

Ward-Smith, A. J. (1980). *Internal Fluid Flow: The Fluid Dynamics of Flow in Pipes and Ducts.* Oxford: Oxford University Press, p. 566.

Wever, N., M. Lehning, C. Sommer, and P. Crivelli (2018). *Expedition to Princess Elisabeth Antarctica Station, 2016/2017.* WSL Institute for Snow and Avalanche Research SLF, Davos, Switzerland. DOI: `10.16904/envidat.30`.

Winstral, A. and D. Marks (Dec. 2002). "Simulating wind fields and snow redistribution using terrain-based parameters to model snow accumulation and melt over a semi-arid mountain catchment". In: *Hydrological Processes* 16.18, pp. 3585–3603. DOI: `10.1002/hyp.1238`.

Wright, T. and P. Gerhart (2009). *Fluid machinery: application, selection, and design.* 2nd ed. Boca Raton: CRC Press, p. 437.

Yang, L., L. Zhang, H. Dong, A. Alelaiwi, and A. E. Saddik (Aug. 2015). "Evaluating and Improving the Depth Accuracy of Kinect for Windows v2". In: *IEEE Sensors Journal* 15.8, pp. 4275–4285. DOI: `10.1109/JSEN.2015.2416651`.

# Curriculum Vitae

Name: Christian Sommer

Date and place of birth: 04 August 1989, Wetzikon ZH, Switzerland

**Education:**

2014-2018:  PhD at École polytechnique fédérale de Lausanne (EPFL), Lausanne, Switzerland and the WSL Institute for Snow and Avalanche Research SLF, Davos, Switzerland

2009-2014:  Master of Science in Mechanical Engineering at École polytechnique fédérale de Lausanne (EPFL), Lausanne, Switzerland
Master thesis: "Variability of snow depth changes in a rock face"

2002-2009:  High School Solothurn

**Publications:**

- Sommer C.G., Lehning M. and Fierz C. (2018). Wind tunnel experiments: influence of erosion and deposition on wind-packing of new snow . Front. Earth Sci. 6:4. doi: 10.3389/feart.2018.00004

- Sommer C.G., Lehning M. and Fierz C. (2017). Wind tunnel experiments: Saltation is necessary for wind-packing. Journal of Glaciology, 63(242), 950-958. doi: 10.1017/jog.2017.53

- Sommer C.G., Lehning M. and Mott R. (2015). Snow in a Very Steep Rock Face: Accumulation and Redistribution During and After a Snowfall Event. Front. Earth Sci. 3:73. doi: 10.3389/feart.2015.00073